Stapp Car Crash Journal, Vol. 61 (November 2017), pp. 227-276

2017-09

Biofidelity Evaluation of the THOR and Hybrid III 50th Percentile Male Frontal Impact Anthropomorphic Test Devices

Daniel Parent, Matthew Craig, Kevin Moorhouse

National Highway Traffic Safety Administration

ABSTRACT – The objective of this study is to present a quantitative comparison of the biofidelity of the THOR and Hybrid III 50th percentile male ATDs. Quantitative biofidelity was assessed using NHTSA's Biofidelity Ranking System in a total of 21 test conditions, including impacts to the head, face, neck, upper thorax, lower oblique thorax, upper abdomen, lower abdomen, femur, knee, lower leg, and whole-body sled tests to evaluate upper body kinematics and thoracic response under frontal and frontal oblique restraint loading. Biofidelity Ranking System scores for THOR were better (lower) than Hybrid III in 5 of 7 body regions for internal biofidelity and 6 of 7 body regions for external biofidelity. Nomenclature is presented to categorize the quantitative results, which show overall good internal and external biofidelity of the THOR compared to the good (internal) and marginal (external) biofidelity of the Hybrid III. The results highlight the excellent internal and external biofidelity of the THOR thorax.

KEYWORDS – THOR, THOR-50M, biofidelity, ATD, BioRank, frontal oblique

INTRODUCTION

The National Highway Traffic Safety Administration (NHTSA) has been researching advanced frontal anthropometric test devices (ATDs) since the early 1980s (Haffner et al., 2001), with the primary objective of better representing the interaction of automotive occupants with modern and sophisticated restraint systems, such as force-limited three-point belts and air bags, which have become standard equipment. This research culminated in the development of the Test Device for Human Occupant Restraint (THOR) 50th percentile adult male ATD, first as the THOR Alpha (Haffner et al., 2001), later upgraded to the THOR-NT (Shams et al., 2005), later upgraded to the THOR Mod Kit (Ridella and Parent, 2011), which was subsequently converted from imperial to metric and defined as THOR-50M in a drawing package developed in September 2015 (NHTSA, 2015a) and an incremental update to that drawing package in August 2016 (NHTSA, 2016b).

Biomechanical response requirements have previously been defined and published for the THOR Alpha (GESAC, 2001) and THOR-NT (GESAC, 2005a), and were since updated as part of the Mod Kit design (Ridella and Parent, 2011). These requirements were based, for the most part, on existing post-mortem human surrogate (PMHS) data available in the literature. The intended application of these requirements was to both guide the design of the hardware and assess the response of the manufactured ATDs. As there have been both manufacturing changes and updates to the biomechanical response requirements since the biofidelity was last assessed (GESAC, 2005a), the objective of this study is to evaluate the biofidelity of the THOR as manufactured to the August 2016 drawing package (NHTSA, 2016b). To minimize subjectivity in the evaluation, biofidelity is quantified using the Biofidelity Ranking System, and in the process compared to the existing 50th percentile adult male frontal impact ATD used in regulation and consumer information testing, the Hybrid III (Part 572 Subpart E), referred to herein as the H3-50M.

Address correspondence to Daniel Parent, 1200 New Jersey Ave SE, Washington, DC 20590. Electronic mail: dan.parent@dot.gov

METHODS

ATDs

A brief history of the past decade of THOR 50th percentile adult male ATD development is necessary to provide a basis for the description of the ATD. The THOR-NT, which was built by GESAC, Inc., was based on the drawing package released in 2005 and corresponding biofidelity (GESAC, 2005a) and certification (GESAC, 2005b) requirements. After several years of research by NHTSA in collaboration with researchers in the automotive industry, academia, ATD manufacturers, and global users, a modification package (or Mod Kit) was developed with the intent to improve the biofidelity, durability, and usability of the THOR-NT (Ridella and Parent, 2011). This modification package was installed on all NHTSA-owned THOR-NT ATDs, which then became known as THOR Mod Kit ATDs. At the same time, the Mod Kit design updates were incorporated into the THOR-NT drawing package and the entire package was converted from imperial to metric, including a soft-conversion of units and replacement of fasteners with metric equivalents. This integrated drawing package was referred to as the THOR Metric (Parent et al., 2013). After the NHTSA-owned THOR-NT ATDs were upgraded to the Mod Kit design, subsequent THOR procurements were manufactured from scratch based on the THOR Metric drawing package. While there were minor differences between the THOR Mod Kit and the THOR Metric that may have resulted from fabrication by a different manufacturer, the performance specifications for both ATDs are based on the test conditions defined in the biomechanical response requirements (GESAC, 2005a) and certification requirements (GESAC, 2005b) of the THOR-NT with additional specifications added during development of the Mod Kit (Ridella and Parent, 2011).

Throughout several years of use of the THOR Mod Kit and THOR Metric ATDs in component, sled, and vehicle testing, several additional upgrades were implemented to the NHTSA fleet of THORs, which currently consists of 4 Mod Kit and 3 Metric THORs. Two examples are the SD-3 shoulder design, which was added to improve shoulder interaction with the shoulder belt, and the iliac wing, which was redesigned to improve durability in conditions involving high lap belt loads. These upgrades were retroactively implemented in the entire NHTSA fleet of THORs. These changes were also incorporated into the THOR Metric drawing package and published as the THOR-50M in September 2015 (NHTSA, 2015a). The drawing package was later updated in August 2016 (NHTSA, 2016a) to include the molded shoe discussed later in this paper. Throughout this document, references to the THOR-50M refer to a THOR that either matches exactly or is functionally equivalent to the August 2016 drawing package. Any exceptions expected to influence biofidelity will be discussed in relevant sections of this paper.

The objective of the current study is to quantify the biofidelity of the THOR-50M. A limitation of this biofidelity evaluation is that it was not always possible to conduct tests with a THOR-50M exactly consistent with the August 2016 drawing package (NHTSA, 2016a), as much of the testing described herein occurred before the drawing package was published. However, in any test conditions where the differences in design were expected to have an influence on response and the test apparatus was available, the tests were rerun with a THOR-50M matching the August 2016 drawing package. For example, any tests involving torso response were rerun with the SD-3 shoulder assembly installed to ensure biofidelity was not adversely affected. On the other hand, where changes were primarily intended to improve usability or durability and not expected to influence the biofidelity, previously-conducted tests were not reproduced. For example, after the upgrade of the iliac wing, biofidelity tests were not reproduced because the change to the iliac wing design added structural reinforcement to improve durability of a non-deformable part without altering the inertial properties of the pelvis.

For all but two of the test conditions, H3-50M data was identified or new tests were conducted. Unless otherwise noted, the H3-50Ms used in these tests were qualified and instrumented consistent with 49 CFR Part 572, Subpart E.

Data Sources

Where possible, ATD test data referred to in this report are available in the NHTSA Biomechanics Test Database (BioDB) available through the NHTSA website (NHTSA, 2017). References to each test include the test reference (TSTREF) and test number (TSTNO) when available, which can be used to download the relevant test data from the BioDB. If any of the PMHS data used to generate or reproduce PMHS corridors are available in the NHTSA BioDB, these tests are referenced by BioDB TSTNO and TSTREF as well. Otherwise, PMHS corridors were digitized from referenced publications for the purposes of quantitative comparison. Any data conditioning carried out to enable this comparison of ATD data to PMHS corridors is described in the relevant sections of this paper.

Biofidelity Ranking

The Biofidelity Ranking System ("BioRank" herein) calculation assesses the biofidelity of an ATD by comparing the dummy response to the mean cadaver response, as originally defined by Rhule et al. 2002. To account for the variability in individual cadaver responses, BioRank calculates a cumulative variance between the dummy response and the mean cadaver response (DCV) and normalizes this value by the cumulative variance between the mean cadaver response and the mean plus one standard deviation cadaver response (CCV). A BioRank value of 0.0 would indicate an ATD response identical to the corridor mean; a value of 1.0 would indicate an ATD response that is on average one standard deviation away from the corridor mean; and a value of 2.0 would indicate an ATD that is considered to respond as much like the corridor as another PMHS (Rhule et al., 2002).

The original version of BioRank implemented weighting of test conditions based on the number of subjects used to develop a given corridor and how well the test condition represented the environment of the intended application. This weighting was removed in a later update to BioRank (Rhule et al., 2009), in part due to the inherent subjectivity of the test condition weights.

As implemented herein, the BioRank calculation closely mirrors the system used in the biofidelity assessment of the WorldSID 50th ATD (Rhule et al., 2009), with the exception that phase optimization was applied on a case-by-case basis, depending on how well the individual test condition was controlled for impact time and whether phase optimization introduced artefactual error. For test conditions where phase optimization is applied, the rationale and implementation is discussed in the respective section. For each body region and ATD, two BioRank scores were calculated: one for External Biofidelity, or the extent to which the ATD represents a human surrogate to the vehicle or restraint system; and one for Internal Biofidelity, or the ability of the ATD to represent the human responses that relate to prediction of injury. External Biofidelity measures are generally those recorded at the test fixture level, such as pendulum force or belt force, whereas Internal Biofidelity measures are generally those recorded by the internal instrumentation of the ATD or by test equipment such as motion tracking that records subject deformation. Force-deflection and moment-rotation corridors are considered to be measures of External Biofidelity, as they represent the stiffness of the subject as seen by the vehicle or restraint system, and are calculated using deflection or rotation (typically measures of Internal Biofidelity) as the independent variable. Summary tables have been marked throughout to indicate whether measurements are considered Internal (INT) or External (EXT). Any measures marked as “Input” in the summary tables are informational and not included in the calculation of either internal or external biofidelity.

BioRank scores from each measurement within a test condition were averaged to obtain an External and Internal Test Condition BioRank (TCBR), and if a body region included more than one test condition the TCBR scores were averaged to obtain a Body Region BioRank (BRBR) score. The overall BRBR scores were in turn averaged to obtain an External and Internal Biofidelity Rank for each ATD.

Test conditions were selected based on relevance to frontal and frontal oblique crash test applications, availability of response corridors from PMHS and/or volunteer tests, and availability of THOR-50M and H3-50M data in the same condition. To obtain PMHS response corridors appropriate for the calculation of DCV and CCV, four different approaches were considered. A decision was made in each test condition based on the available information.

Approach A. Digitization or electronic acquisition of a response corridor presented in the literature. Where previously-published corridors were available and known to represent the mean plus/minus one standard deviation, these corridors were used as presented in the literature.

Approach B. Digitization or electronic acquisition of the individual responses presented in the literature. This approach necessitates recalculation of the response corridors, but the benefit is that the resulting corridor can be calculated in a manner appropriate for BioRank calculation. Where corridors were recalculated based on individual response data, the corridor development strategy employed in the original publication was followed as near as possible to recreate the published corridors. In this case, the calculated corridor was compared to the reference corridor from the literature to ensure qualitative agreement.

Approach C. Modeling of the impact condition as a mechanical system, such as a spring-mass-damper system, to infer response time-history information while allowing the differentiation of internal vs. external response. This approach is the most time-consuming, and was only carried out in the blunt thoracic impact condition.

Approach D. For conditions that did not allow for any of the above approaches (e.g. time-history or force-deflection responses were not available in the literature or in the NHTSA BioDB), BioRank was calculated using a single point measure such as the peak force or peak deflection.

The approach taken in each test condition is described in the relevant sections. If any additional data processing steps such as debiasing, filtering, and phase shifting were applied to the PMHS corridors or individual responses presented in the literature, these steps are noted in the relevant sections; otherwise, data processing steps can be found in the relevant references. Unless otherwise noted, ATD responses were zeroed and filtered according to the filter class recommendations in SAE J211-1 (SAE, 2007). The calculation range of BioRank was constrained to the time displayed on the respective plots for time-history calculations. For force-deflection or moment-rotation characteristics, the BioRank calculation was carried out up to the peak deflection/rotation of the corridor or the peak deflection/rotation of the ATD response, whichever occurred first.

In many of the test conditions described herein, the ATD tests were repeated multiple times. In these cases, only a single ATD test, selected randomly, was used in the calculation of BioRank based on the assumption that the test-to-test variation in ATD response is substantially smaller than the subject-to-subject variation represented by the PMHS response corridor.

For the purposes of this study, the Biofidelity Scale presented by Rhule et al. 2009 is adapted to include subjective nomenclature to facilitate classification (Table 1).

Table 1. Biofidelity Scale Nomenclature

BioRank (√R)	Description	Classification
√R ≤ 1	within one standard deviation of the mean PMHS response	Excellent
1 < √R ≤ 2	between one and two standard deviations of the mean PMHS response	Good
2 < √R ≤ 3	between two and three standard deviations of the mean PMHS response	Marginal
3 < √R	more than three standard deviations from the mean PMHS response	Poor

Though not explicitly stated throughout this report and not necessarily known for data presented in the literature, all standard deviations calculated herein are done so as population standard deviations, as the goal is to represent the variance in the responses of a finite number of subjects:

$$\sigma = \sqrt{\frac{1}{N}\sum_{i=1}^{N}(x_i - \mu)^2}$$

Figures

Throughout this report, data is presented graphically to demonstrate the comparison of ATD response to PMHS corridors. If not otherwise labeled, the naming convention follows that described in Figure 1.

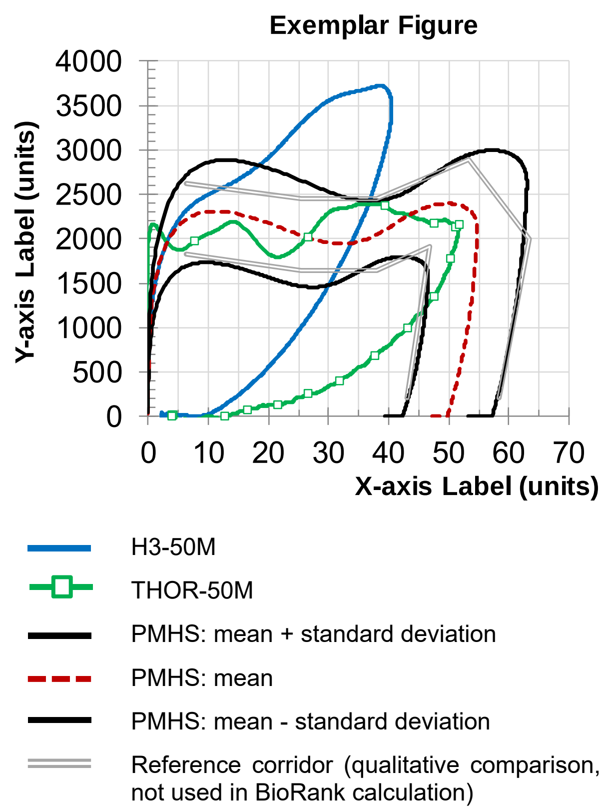

Figure 1. Example figure, showing line styles used throughout this report

Body Regions

A total of seven (7) body region groupings were used in this study: head, neck, thorax, abdomen, knee/thigh/hip (KTH), lower extremity (LX), and whole-body. Test conditions grouped into the first six body regions involve component tests which either isolate the body region of interest mechanically, or involve a localized impact to the whole body. Test conditions grouped into the whole-body category involve sled tests using the assembled ATD or intact PMHS. Each body region includes at least two test conditions, and each test condition includes one or more measurement. All body regions include at least one internal measurement and at least one external measurement.

Head

Four impact test conditions involving the head were assessed: isolated head drop, whole-body head impact, face rigid bar impact, and face rigid disk impact.

Table 2. Test Information: Head

	THOR-50M	H3-50M
Head Drop Test		
ATD Description	S/N 006 (Mod Kit)	
Data Source	b11155	b09704
Whole-body Head Impact		
ATD Description	S/N 006 (Mod Kit)	
Data Source	b11152	b09709
Face Rigid Bar Impact		
ATD Description	S/N 9799 (Metric)	
Data Source	b11344	b09732
Face Disk Bar Impact		
ATD Description	S/N 9799 (Metric)	
Data Source	b11345	b09725

Isolated Head Drop. The head drop biomechanical response requirement was based on a subset of the PMHS tests reported by Hodgson and Thomas (1971) which were tested in the flat plate loading condition. This test was carried out by dropping intact PMHS such that their heads impacted a stiff plate attached to a load cell. Drop heights ranged from nominally 250 to 750 millimeters, resulting in impact velocities from 2.2 to 3.9 meters per second. The average impact velocity was 2.71 meters per second, achieved with a drop from a height of 376 millimeters. Hubbard and McLeod (1974) specified an ATD performance requirement equal to the mean peak head resultant acceleration from this data set (250 g) with an allowable variation of 10% (plus/minus 25 g), which was used in the original THOR design requirements (GESAC, 2005a). The actual standard deviation of peak head resultant acceleration from the PMHS data set was much larger (63 g); while such a wide target would not prove useful in ATD design, it is used herein to calculate BioRank.

To evaluate ATD biofidelity, head drop tests were conducted using both the THOR-50M and H3-50M (Table 2). In each case, the head was dropped from a height of 376 millimeters, resulting in an impact velocity of 2.71 meters per second on a flat plate. The resultant head acceleration was recorded for each ATD. The THOR used in test b11155, THOR Mod Kit S/N 006, is assumed to be functionally equivalent to the THOR-50M as specified in the August 2016 drawing package (NHTSA, 2016a) as there were no significant design changes to the head since the Mod Kit version of the THOR. To quantify the biofidelity of the THOR-50M and H3-50M responses, a single-point BioRank was calculated as the difference between the peak head resultant acceleration of the ATD and the mean PMHS peak head resultant acceleration divided by the standard deviation.

Whole-body Head Impact. The whole-body head impact biomechanical response requirement was derived by Melvin et al. (1988) through an analysis of a combined data set of embalmed and unembalmed PMHS in various impact conditions. This analysis developed the head impact performance requirement for the Advanced Anthropomorphic Test Dummy (AATD), which was retained as the project evolved into the THOR. Under impact from a 23.4 kilogram impactor at 2.0 meters per second, the peak response requirement was determined to be 5,800 Newtons plus/minus 580 Newtons with a duration of 3.9 milliseconds. It is not clear, however, if the size of the corridor is related to the standard deviation of the combined sample, or actively selected to be 10% of the mean. For lack of additional information, it is assumed for the purposes of this analysis that published corridor represents plus/minus one standard deviation.

To evaluate ATD biofidelity, whole-body head impact tests were conducted using both the THOR-50M and H3-50M (Table 2). In each case, the ATD was impacted with a 23.4 kilogram impactor with a flat disk interface at a velocity of 2.0 meters per second. The impactor acceleration was recorded and multiplied by the impactor mass to determine impact force. The THOR used in test b11152, THOR Mod Kit S/N 006, is assumed to be functionally equivalent to the THOR-50M as specified in the August 2016 drawing package (NHTSA, 2016a) as there were no significant design changes to the head after the Mod Kit upgrade. To quantify the biofidelity of the THOR-50M and H3-50M responses, a single-point BioRank was calculated as the difference between the peak impact force in each ATD test and the mean PMHS peak impact force, divided by the standard deviation.

Face Rigid Bar Impact. The face rigid bar impact biomechanical response requirement was derived by Melvin and Shee (1989) based on the testing conducted by Nyquist et al. (1986). This test condition is a generalized representation of a face impact to a steering rim or similar stiff, narrow structure in a motor vehicle crash occupant environment. The requirement in this condition is presented as the impactor force time-history, and was calculated based on the response of 7 subjects in which only the nasal bones were fractured. This analysis developed the head impact performance requirement for the AATD, which was retained as the project evolved into the THOR. Under impact from a 32 kilogram impactor with a 25 millimeter diameter rigid bar impact surface at between 2.8 and 4.8 meters per second, the peak response requirement was determined to be 2,970 ± 720 Newtons with a rise time of 5.9 ± 1.1 milliseconds.

To evaluate ATD biofidelity, face rigid bar impact tests were conducted using both the THOR-50M and H3-50M (Table 2). In each case, the ATD was impacted by a 32 kilogram impactor with a 25 millimeter diameter rigid bar interface at a velocity of 3.6 meters per second, the average of the impact velocities in the tests used to develop the corridor. The impactor acceleration was recorded and multiplied by the impactor mass to determine impact force. The THOR used in test b11344, THOR-50M S/N 9799, meets the specifications of the THOR-50M August 2016 drawing package (NHTSA, 2016a).

To quantify the biofidelity of the THOR-50M and H3-50M responses, BioRank was calculated over the time domain of the response corridor. Before BioRank was calculated, the ATD responses were phase-shifted such that the peak force occurred in the temporal center of the defined peak duration (5.9 milliseconds), to be consistent with the method of generation of the PMHS corridor. As a supplementary BioRank assessment, the peak of each ATD response was compared as a single point to the mean plus/minus one standard deviation of the corridor.

Face Rigid Disk Impact. The face rigid disk impact biomechanical response requirement was developed by Melvin and Shee (1989) based on the responses of five PMHS subjected to impact from a 13 kilogram impactor with a 152 millimeter diameter flat disk impact surface at 6.7 meters per second. A response corridor was developed for the impactor force time-history, defining a peak force of 6,300 ± 1,900 Newtons with a rise time of 3.6 ± 0.9 milliseconds. This loading condition generally represents the impact of the face of an occupant to a flat surface such as the instrument panel in the motor vehicle crash occupant environment.

To evaluate ATD biofidelity, face rigid disk impact tests were conducted using both the THOR-50M and H3-50M (Table 2). In each case, the ATD was impacted by a 13 kilogram impactor with a 152 millimeter diameter flat disk impact surface at a velocity of 6.7 meters per second. The impactor acceleration was recorded and multiplied by the impactor mass to determine impact force. The THOR used in test b11345, THOR-50M S/N 9799, meets the specifications of the THOR-50M August 2016 drawing package (NHTSA, 2016a). However, the response of this THOR did not meet the specifications of the Face Qualification test procedure defined in the THOR-50M Qualification Procedures Manual (NHTSA, 2016b), which is identical to the face rigid disk impact test condition.

To quantify the biofidelity of the THOR-50M and H3-50M responses, BioRank was calculated over the time domain of the response corridor. As in the face rigid bar impact condition, ATD responses were phase shifted such that the peak force occurred in the temporal center of the defined peak duration (3.6 milliseconds). Additionally, the peak of each ATD response was compared as a single point to the mean plus/minus one standard deviation of the corridor.

Neck

Three test conditions were used to assess neck biofidelity: frontal flexion, lateral flexion, and torsion.

Table 3. Test Information: Neck

	THOR-50M	H3-50M
Neck Frontal Flexion		
ATD Description	S/N 015 (Mod Kit)	N/A
Data Source	b10999	b09711
Neck Lateral Flexion		
ATD Description	S/N 015 (Mod Kit)	N/A
Data Source	b11005	b09714
Neck Torsion		
ATD Description	S/N 9207 (Metric)	Digitized from Myers et al. (1989)
Data Source	b11559	

Neck Frontal Flexion. The neck flexion biomechanical response requirement was based on what is known as the NBDL condition, as it was developed from volunteer testing conducted by the Naval Biodynamics Laboratory. In this test series, volunteers restrained by shoulder straps, a lap belt, and additional pelvic straps were subjected to an acceleration pulse with nominal 15g plateau (Thunnissen et al., 1995). The kinematic response of the head, neck, and thoracic spine at the level of T1 were monitored using photo markers and accelerometers. A total of nine experiments were conducted using five human volunteers, with all but one of the subjects tested twice. The results were post-processed by Thunnissen et al. (1995) to correct for the motion of T1 instrumentation mount relative to the T1 vertebral body, and kinematic measurements were presented relative to T1 using a two-pivot model.

The THOR-50M and H3-50M were subjected to a test condition representative of the volunteer experiments (Table 3). These tests were conducted by attaching the base of the neck of each ATD to a sled and applying the measured sled acceleration pulse presented by Thunnissen et al. (1995). The sled pulse was applied instead of the measured T1 acceleration pulse because the multiple peaks and complexity of the T1 pulse could not be recreated on a deceleration sled system. Additionally, the anatomical T1 location on the THOR is not coincident with the base of the lower neck load cell, so even if the T1 acceleration pulse could be applied directly, it would be applied at a location inferior to the ATD representation of T1.

The basis for biofidelity assessment of the THOR-50M and H3-50M implemented herein were the volunteer corridors presented by Thunnissen et al. (1995), which were digitized for this study. To compare the ATD responses to the Thunnissen corridors, several steps were necessary to prepare the data on an equivalent basis.

1. Motion tracking was conducted using high-speed video to track the head CG, OC, marker placed at the approximate location of T1, the base of the lower neck load cell, and two markers on the sled. The motion tracking data based on the timestamp on the video file (ignoring the trigger light) was confirmed to be synchronized with the data recorded in the data acquisition system by tracking the sled velocity from the video and comparing to the integrated sled accelerometer recorded in the data acquisition system (DAS). Measurements were converted from pixel domain to the spatial domain using measurements documented in the associated test photographs.

2. To align the data in the time domain with the Thunnissen corridors, both the data recorded in DAS and the motion tracking data were shifted forward in time by 25 milliseconds.

3. For the ATD tests, the neck link was defined as the line connecting the marker at the approximate location of T1 to the OC. In the THOR-50M test, the T1 marker was located just above the 2nd lowest neck plate. In the H3-50M test, the T1 marker was located above the lower neck load cell but on the same rigid body.

Additionally, the frontal flexion moment vs. rotation characteristic of the ATDs during this test was compared to the PMHS corridor presented by Mertz and Patrick (1971). The moment vs. rotation characteristic for the ATD tests was calculated using the neck moment at the OC with respect to the head angle relative to its initial position. For THOR-50M, the neck moment represents total neck section moment at the OC (TSTNO b10999, CURNO 28).

The THOR used in test b10999, THOR Mod Kit S/N 015, is assumed to be functionally equivalent to the THOR-50M as specified in the August 2016 drawing package (NHTSA, 2016a) since there were no significant design changes to the head and neck between the Mod Kit and Metric versions of the THOR. It is assumed that the response of the THOR-50M would be identical, provided that the qualification specifications of the August 2016 THOR-50M Qualification Procedures Manual (NHTSA, 2016b) are met.

Neck Lateral Flexion. The neck lateral flexion biomechanical response requirement was also based on volunteer sled testing conducted by NBDL (Wismans and Spenny, 1983). The data published in this series included 16 tests on 6 volunteers, of which the most severe tests were used to define performance requirements for a mechanical neck evaluation. This test condition amounted to a nominal 6.25 m/s input with a sled pulse with a nominal 7g plateau. The kinematic response of the head, neck, and thoracic spine at the level of T1 were monitored using photo markers and accelerometers.

To evaluate ATD biofidelity, the neck lateral flexion test was conducted using the THOR-50M and H3-50M (Table 3). As in the NBDL frontal flexion condition, the sled pulse was applied to the base of the neck. As noted by Wismans and Spenny (1983), the variation in the T1 accelerations did not significantly influence the head-neck motion in volunteer tests. Therefore, it is assumed that the application of the sled acceleration to the base of the neck in the ATD tests is equivalent to the volunteer loading condition for the purposes of a comparison to kinematic response. To evaluate the strength of this assumption, the applied acceleration pulse in the ATD tests is compared to both the sled acceleration and the T1 acceleration pulses.

The basis for biofidelity assessment of the THOR-50M and H3-50M implemented herein were the corridors presented in the THOR-NT Biomechanical Response Requirements (GESAC, 2005a), which were obtained in electronic format. A comparison to the Patrick and Chou (1976) moment vs. rotation corridor was performed for each ATD using the moment measured at the upper neck load cell and the head angle relative to its initial position.

To compare the THOR-50M and H3-50M responses to the specified response corridors, high-speed video was processed as described in the previous section. However, a discrepancy in timing was identified, as the sled pulse begins at 0 milliseconds (Figure 17) while the T1 pulse does not begin until almost 100 milliseconds (Figure 18). In contrast, the neck frontal flexion sled (Figure 8) and T1 (Figure 9) acceleration pulses start at nearly the same time. Due to this uncertainty, each ATD response was phase-shifted in time such that BioRank was minimized.

The THOR used in test b11005, THOR Mod Kit S/N 015, is assumed to be functionally equivalent to the THOR-50M as specified in the August 2016 drawing package (NHTSA, 2016a). While THOR S/N 015 is of the Mod Kit vintage, there were no significant design changes to the head and neck between the Mod Kit and Metric versions of the THOR. It is assumed that the response of the THOR-50M would be identical, provided that the qualification specifications of the August 2016 THOR-50M Qualification Procedures Manual (NHTSA, 2016b) are met.

Neck Torsion. The neck torsion biomechanical response requirement is different from most of the corridors defined herein, as instead of an average response corridor, the upper and lower limits of neck torsional stiffness are based on dynamic and quasi-static neck torsion stiffness. Neck torsion stiffness is defined as the Z-axis neck moment with respect to the axial rotation of the neck column. The lower stiffness boundary was based on the corridor presented by Myers et al. (1989), based on the response of five PMHS cervical spines loaded to failure in axial rotation at a constant angular velocity of 500 degrees per second. While Myers et al. (1989) present a mean plus/minus one standard deviation response corridor for neck torsion of PMHS, this corridor does not represent active musculature which could be expected in a live human response. As suggested by Myers et al. (1989), the influence of neck musculature can be assessed using the data from the Wismans and Spenny (1983) analysis of the NBDL lateral loading tests, which induced axial rotation of the neck of volunteers. For the purposes of this evaluation, the active musculature condition was interpreted as the upper stiffness boundary, while PMHS condition was interpreted as the lower stiffness boundary. This corridor does not meet the requirements of BioRank since it is not calculated using a mean plus/minus one standard deviation corridor, thus it is not included in the BRBR. That said, it is evaluated informationally since the neck torsion response drives the head Z-axis angular velocity, which plays a significant role in frontal oblique impact occupant kinematics (Saunders et al., 2015).

To evaluate ATD biofidelity, neck torsion tests were carried out using the neck of the THOR-50M in a representative environment to the tests conducted by Myers et al. (1989). A portion of the head/neck assembly of THOR-50M, from the head/neck mounting platform superiorly to the lower neck load cell inferiorly, was mounted in a torsion fixture and loaded at a rate of 500 degrees per second up to a maximum angle of 85 degrees. The applied angle was measured, along with the moment at the upper and lower neck load cells and the base of the torsion fixture.

The THOR used in test RT04CMLFAIL4, THOR-50M S/N 9207, meets the specifications of the August drawing package (NHTSA, 2016a). As recent data from the H3-50M in this loading condition was not available, the H3-50M response was digitized from the data presented by Myers et al. (1989).

While not included in the BRBR, BioRank was calculated by assuming that the generalized upper and lower stiffness boundaries represent a mean plus/minus one standard deviation corridor. The calculation range of BioRank was constrained to the maximum angle of each ATD response. Since the maximum of the H3-50M response occurs before the beginning of the upper stiffness corridor, BioRank could not be calculated for this ATD.

Thorax

Two test conditions were used to assess thoracic biofidelity: sternal impact and lower ribcage oblique impact.

Table 4. Test Information: Thorax

	THOR-50M	H3-50M
Sternal Impact		
ATD Description	S/N DL9207 (Metric)	S/N 202
Data Source	b11362	b10992
Lower Ribcage Oblique Impact		
ATD Description	S/N 006 (Mod Kit)	S/N 43
Data Source	b11584	b11583

Sternal Impact. The sternal impact test condition described in the THOR-NT Biomechanical Response Requirements (GESAC, 2005a) involves a blunt thoracic impact with a 23.4 kilogram pendulum with a 152.4 millimeter diameter flat face impacting the center of the sternum. Response corridors were presented for two impact velocities, 4.3 and 6.7 meters per second, each defined by piecewise linear representations as presented by Neathery (1974). As shoulder belt loading typically results in loading rates in the range of 1 to 4 meters per second (Schneider et al., 1989), the 6.7 meter-per-second sternal impact was lowered in priority in favor of a more exposure-appropriate 4.3 meter-per-second sternal impact during the Mod Kit design update (Ridella and Parent, 2011).

Parent et al. (2013) evaluated the biofidelity of the H3-50M and several iterations of the THOR, including the NT, the Mod Kit, and the Metric versions, the latter both with the standard shoulder and with the SD-3 shoulder assembly installed. The configuration described as “THOR Metric w/SD-3” is functionally equivalent to the THOR-50M as defined by the August 2016 THOR-50M drawing package (NHTSA, 2016a). In this study, the responses of the ATDs to thoracic impact at 4.3 meters per second with a blunt 23.4 kilogram impactor were qualitatively compared to two existing low-speed thoracic impact response corridors: the Kroell corridor (as presented in GESAC, 2005a), based on skeletal deflection, and the Lebarbé corridor (Lebarbé and Petit, 2012), based on external deflection.

While the Lebarbé corridor was available in the time domain for calculation of BioRank based on force and deflection time-histories, it was necessary to develop force and deflection time-histories representing the Kroell corridor, which existed only as an idealized, linearized response envelop of forces in the deflection domain. Development of these time-histories was achieved through the formulation and optimization of a spring-mass-damper system, specifically the simplified Lobdell model (Lobdell et al., 1973), to meet the mid-points of the Kroell corridor. The individual force and deflection time-histories meeting the corridor mid-points were considered to be the mean and scaled upward and downward by 15% (as in Neathery, 1974) to form the upper and lower boundaries of the force and deflection time-histories.

Lower Ribcage Oblique Impact. The lower ribcage oblique impact condition is based on PMHS tests carried out by Yoganandan et al. (1997). This condition involves a blunt thoracic impact with a 23.4 kilogram pendulum with a padded 152.4 millimeter diameter disc impacting the approximate level of the eighth rib with the subject rotated right to left by 15 degrees. In contrast to the blunt thoracic impact test, which uses a nearly identical impactor, the lower ribcage oblique impact adds a 19 millimeter thick foam rubber pad at the impact interface. This condition was used to define the biomechanical response requirements for the THOR-NT (GESAC, 2005a), which included both a force-deflection characteristic as a primary requirement and deflection and force time-history corridors as a secondary requirement. These corridors appear to have been developed based on the data presented by Yoganandan et al. (1997), though the development process is not described. Further, the force-deflection response purports to present upper and lower response corridors at plus/minus one standard deviation, though the three loading curves are coincident. Such a corridor is not appropriate for the calculation of BioRank. To proceed in quantification of biofidelity in the lower ribcage oblique impact condition, it was necessary to obtain the underlying data and recalculate the response corridors.

To recalculate the lower oblique ribcage impact response corridors, the individual force and deflection time-histories were acquired for the first 6 of the 7 subjects described by Yoganandan et al. (1997) (Table 5) and scaled using the mass-scaling approach developed by Eppinger et al. (1984). The force time-histories were aligned in time using cross-correlation, and for each subject the same time shift was applied identically to both the force and deflection time-histories. Corridors created for the deflection and force time-histories were in turn used to develop a composite force-deflection corridor, which was constructed with an upper boundary formed by the mean plus one standard deviation of force and mean minus one standard deviation of deflection and a lower boundary formed by the mean minus one standard deviation of force and mean plus one standard deviation of deflection. The force-deflection corridor was carried out up to the maximum deflection of the subject with the lowest overall deflection, otherwise discontinuities resulted.

Table 5. Key anthropometry and response metrics from lower ribcage oblique impacts (from Yoganandan et al., 1997).

Test ID (PC*)	101	102	103	104	105	106
TSTNO	3085	N/A	N/A	N/A	N/A	N/A
Sex	M	M	M	M	M	M
Age (years)	72	81	84	86	62	70
Stature (cm)	170	175	168	170	174	178
Mass (kg)	82	63	68	56	61	91
Velocity (m/s)	4.3	4.3	4.3	4.3	4.3	4.3
Peak Force (N)	1864	2742	2082	2136	2631	1934
Peak Defl. (mm)	86	34	62	104	57	90
Slope (N/mm)	21.7	80.5	33.8	20.6	46.6	21.5

BioRank was calculated for THOR-50M and H3-50M for all four of the presented corridors. Since the response corridor was created by aligning the force time-histories by cross-correlation, the ATD force time-histories were also phase-shifted to minimize the BioRank value. The resulting phase shift in the force time-history for each ATD was also applied to the deflection time-history.

Abdomen

Three test conditions were used to assess abdomen biofidelity: upper abdomen steering wheel impact, lower abdomen rigid bar impact, and abdomen belt loading.

Table 6. Test Information: Abdomen

	THOR-50M	H3-50M
Upper Abdomen Steering Wheel Impact		
ATD Description	S/N 9207 (Metric)	S/N 43
Data Source	b11388	b11582
Lower Abdomen Rigid Bar Impact		
ATD Description	S/N 9799 (Metric)	S/N 43
Data Source	b11580	b11581
Abdomen Belt Loading		
ATD Description	S/N 006 (Mod Kit)	S/N 43
Data Source	b11576	b11571

Upper abdomen steering wheel impact. The response requirement for upper abdomen impact was derived from PMHS data collected by Nusholtz and Kaiker (1994) from a series of steering wheel impact tests with engagement at the vertical level of the 2nd lumbar vertebrae (L2). Six tests were performed with an 18-kg pendulum mass at impact speeds of 3.9 m/s to 10.8 m/s with an average speed of 8.0 m/s. The results were presented by Nusholtz and Kaiker (1994) as force-deflection characteristics, though time-histories of each response for the individual subjects can be found in a more detailed report on these tests Nusholtz et al. (1988). The response requirement in the THOR-NT Biomechanical Response Requirements (GESAC, 2005a) was specified as a generalized force-deflection corridor generally outlining the individual responses presented by Nusholtz and Kaiker (1994).

As this generalized corridor is not appropriate for calculation of BioRank, new response corridors for deflection time-history and force time-history using Approach B described above, which were in turn used to develop two possible force-deflection corridors. The force and deflection time-histories from each subject (Table 7) were acquired and scaled using the mass-scaling approach developed by Eppinger et al. (1984). This approach was selected based on the insensitivity of the force-deflection characteristic to impact velocity, and the individual responses were not corrected for impact velocity. Test number 86m062 was excluded as this subject was impacted in the "Below Sternum" location as opposed to the "Abdomen" location of the remaining five subjects (Nusholtz et al., 1988). Time-history corridors were formed by calculating the mean and standard deviation of the deflection or force values from the five included subjects at each point in time. The composite force-deflection corridor was developed with an upper boundary formed by the mean plus one standard deviation of force and mean minus one standard deviation of deflection and a lower boundary formed by the mean minus one standard deviation of force and mean plus one standard deviation of deflection.

Table 7. Key response metrics from upper abdominal steering rim impacts (from Nusholtz and Kaiker, 1994).

Test Number	86m006	86m016	86m026	86m042	86m052	86m062
Sex	Male	Female	Female	Male	Female	Male
Age (years)	63	52	44	46	55	61
Mass (kg)	70.1	40.2	57.5	50.0	70.3	61.9
Stature (cm)	180.0	168.4	164.5	176.2	161.8	178.4
Velocity (m/s)	10	6.5	7.5	10.8	9.3	3.9
Peak Force (N)	8900	5300	6700	8400	6700	3000
Peak Deflection (mm)	170	90	100	140	150	70
Slope (N/mm)	52	59	67	60	45	43

To evaluate ATD biofidelity, upper abdomen impact tests were conducted using both the THOR-50M and H3-50M (Table 6). In each case, the ATD was impacted with an 18-kg pendulum mass with a steering wheel shaped impact interface at a velocity of 8.0 m/s. The impactor acceleration was recorded and multiplied by the impactor mass to determine impact force. Deflection was determined through differential double integration of accelerometers on the pendulum and an accelerometer installed on the lower spine of the ATD. The THOR used in test b11388, THOR Metric S/N 9207, is believed to be functionally equivalent to the THOR-50M as specified in the August 2016 drawing package (NHTSA, 2016a). BioRank was calculated for THOR-50M and H3-50M for two time-history corridors and two force-deflection corridors.

Lower abdomen rigid bar impact. The response requirement for lower abdomen impact was derived from data developed by Cavanaugh et al. (1986) based on rigid bar impacts at the vertical level of the third lumbar vertebrae (L3) as to involve little or no rib contact. The subjects in the Cavanaugh study were grouped by impact velocity, and used to develop low-velocity and high-velocity response corridors. Only the low-velocity corridor, developed from the responses of five subjects impacted by a 31.24 or 31.52 kilogram impactor at velocities ranging from 4.87 to 7.24 meters per second, was used in the THOR-NT biomechanical response requirement (GESAC, 2005a). As defined therein, the test uses the average impact velocity of the low-velocity cohort (6.1 m/s) and a response corridor similar to the corridor presented in Figure 9 of Cavanaugh et al. (1986). This corridor was created based on data filtered and normalized using the Eppinger mass-scaling method (Eppinger et al., 1984).

As with the upper abdomen impact test, Approach B was used to develop BioRank-appropriate corridors. Deflection and force time-histories from each subject (Table 8) were digitized and scaled using the mass-scaling approach developed by Eppinger et al. (1984). Time-history corridors were formed by calculating the mean and standard deviation of the deflection or force values from the five included subjects at each point in time. The composite force-deflection corridor was developed with an upper boundary formed by the mean plus one standard deviation of force and mean minus one standard deviation of deflection and a lower boundary formed by the mean minus one standard deviation of force and mean plus one standard deviation of deflection.

Table 8. Key response metrics from lower abdomen rigid bar impacts (from Cavanaugh et al., 1986).

Test Number	14	19	24	28	33
Sex	M	F	M	F	F
Age (years)	56	43	57	57	51
Stature (m)	1.82	1.59	1.87	1.63	1.63
Mass (kg)	68	53	45	75	68
Velocity (m/s)	6.84	5.00	4.87	6.66	7.24
Peak Force (N)	3070	2030	2370	2380	4230
Peak Penetration (mm)	140.0	120.0	125.5	184.6	172.7
Peak Compression (%)	49.5	51.9	48.8	67.0	66.2
Slope (N/mm)	34.2	25.5	25.2	20.2	26.9

To evaluate ATD biofidelity, upper abdomen impact tests were conducted using both the THOR-50M and H3-50M (Table 6). In each case, the ATD was impacted with a 32-kg pendulum mass with a rigid bar impact interface at a velocity of 6.1 m/s. The impactor acceleration was recorded and multiplied by the impactor mass to determine impact force. Deflection was determined through differential double integration of accelerometers on the pendulum and an accelerometer installed on the lower spine of the ATD. The THOR used in this test condition, THOR Metric S/N 9799, is believed to be functionally equivalent to the THOR-50M as specified in the August 2016 drawing package (NHTSA, 2016a).

Abdomen belt loading. The original biomechanical response requirements for the THOR-NT (GESAC, 2005a) did not include an abdomen belt loading test condition, but the belt loading test condition conducted by Hardy et al. (2001) was proposed as an additional biomechanical requirement. However, it was not possible to recreate this test condition directly since the input used to drive the belt displacement was varied for each subject (Hardy et al., 2001). Instead, a more recent set of tests were used as the basis for abdomen belt loading biofidelity evaluation. Ramachandra et al. (2016) subjected seven PMHS to seat belt loading at the mid-abdomen level in a free-back condition. The belt was initially in contact with the anterior surface of the abdomen and was pulled posteriorly using a ram driven by a pneumatic piston of known accumulator pressure. Primary metrics were the abdominal penetration distance, measured as the difference between the seat belt motion and the spine motion, and the applied force, measured as the sum of two seat belt load cells and confirmed by an inertially-compensated load cell attached to the ram.

Ramachandra et al. (2016) developed a force-penetration response corridor using responses of the seven PMHS tested under identical loading conditions, referred to as Test Condition A. The individual responses were scaled using the Eppinger mass-scaling methodology (Eppinger et al., 1984), and a force-penetration response corridor was developed using the ellipse method (Shaw et al., 2006). As the resulting corridor boundaries were not directly available in the penetration domain, the corridor was approximated by extracting several points on the upper and lower boundaries of the graphical corridor representation.

To evaluate ATD biofidelity, the THOR-50M and H3-50M were subjected to a reproduction of Test Condition A presented by Ramachandra et al. (2016). For the THOR-50M test, the belt was centered on the vertical position of the anterior attachment point of the IR-TRACCs, and for the H3-50M test, the belt was vertically centered on the top edge of the pelvis flesh near the center of the abdomen. BioRank was calculated for the THOR-50M and H3-50M in the penetration domain, constrained to the deflection up to the peak penetration of each ATD response.

Knee/Thigh/Hip (KTH)

Two test conditions were used to assess biofidelity of the knee/thigh/hip complex: femur compression and knee shear.

Table 9. Test Information: KTH

	THOR-50M	H3-50M
Femur Compression		
ATD Description	N/A	N/A
Data Source	b11578	b6958
Knee Shear		
ATD Description	S/N 9799 (Metric)	Digitized from Balasubramanian et al. (2004)
Data Source	b11349	

Femur compression. Biomechanical response corridors have been developed by Rupp et al. (2003) to describe the response of the femur when subjected to an axial impact at the intact knee while rigidly supported at the femoral head. This testing involved subjecting whole knee/femur complexes to axial compression along the long axis of the femur by rigidly supporting the femoral head and loading the knee through a molded cup. The loading was applied by pneumatically accelerating a 250 kilogram mass into a transfer ram initially in contact with the knee. The resulting loading rate was nominally 1.2 meters per second. The responses of twenty femurs from eleven unembalmed PMHS were evaluated and used to calculate a response corridor representing the force applied at the knee with respect to the compression of the knee/femur complex. Unscaled responses were used to construct the corridor, as an attempted mass-scaling approach (Eppinger et al., 1984) did not reduce the variability in the response data (Rupp et al., 2003).

Since the data referenced by Rupp et al. (2003) are available in the NHTSA Biomechanics Database, the corridors presented in the literature were recalculated to allow quantification of biofidelity using BioRank. Response data from twenty tests (Table 10) were processed as follows:

1. Ram force, ram acceleration, and ram deflection data for each test were debiased by subtracting the average value of each response between 20 and 10 milliseconds before recorded time zero.
2. Time zero was standardized across all tests by determining the phase shifting necessary such that that time zero occurs when the ram force first exceeds 100 Newtons; an identical phase shift was applied to the force, acceleration, and deflection within each test.
3. Applied force was calculated by mass-compensating the ram force using the ram acceleration and the mass between the load cell center-of-gravity and the knee surface as provided in the associated test reports (Table 10).
4. The end of each test was determined to be the time of peak applied force.
5. Each response was resampled to achieve a consistent timestep of 1 millisecond.

Table 10. Data source for femur compression corridor development.

TestID Rupp 2003	TSTNO in NHTSA BioDB	Load Cell Mass Compensation (kg)
19LF	6104	1.47
19RF	6106	1.47
22LF	6178	1.39
22RF	6180	1.39
24LF	6188	1.39
24RF	6190	1.39
25LF	6214	1.39
25RF	6216	1.39
26LF	6218	1.95
27LF	6243	1.35
27RF	6245	1.35
28LF	6247	2.20
28RF	6249	2.20
30LF	6494	1.39
30RF	6496	1.39
31LF	6498	1.44
31RF	6500	1.44
32LF	6502	1.44
32RF	6503	1.44
33RF	6526	2.00

The resulting response data was used to develop mean plus/minus one standard deviation corridors for both the deflection and force time-histories, which were in turn used to develop a composite force-deflection corridor as well as a corridor based on the force-deflection responses in the deflection domain. The composite force-deflection corridor was developed with an upper boundary formed by the mean plus one standard deviation of force and mean minus one standard deviation of deflection and a lower boundary formed by the mean minus one standard deviation of force and mean plus one standard deviation of deflection. The force-deflection corridors were developed for the loading portion of the characteristic (e.g. to the point of peak force).

The H3-50M and THOR-NT ATDs were also subjected to this test condition, and found to be excessively stiff compared to the PMHS corridor (Rupp et al., 2003). This was addressed in the Mod Kit update to the THOR with a 57% increase in the length of the compliant element in the femur that allows axial compression (Ridella and Parent, 2011). The effectiveness of this design update was evaluated during the Mod Kit project, though the exact test apparatus could not be used. Instead, the femur was supported in a dynamic compression device and driven using a target displacement time-history similar to the PMHS deflection time-history corridor. BioRank was calculated for THOR-50M and H3-50M for the force and deflection time-history corridors as well as the two force-deflection corridors.

Knee shear. The THOR-50M includes a sliding joint at the interface between the distal femur and the proximal tibia at the knee, which allows linear translation perpendicular to the tibia, which represents both bending of the proximal tibia and extension of the posterior cruciate ligament (PCL). The THOR-NT design included neither biomechanical response requirements nor certification requirements to define the response of this interface. In lieu of this, it had been previously assumed that the response requirements match those of the H3-50M knee slider mechanism, which is of similar form and function.

The H3-50M knee slider performance requirement is defined in the Hybrid III User's Manual (SAE, 2009), though it is not referenced by NHTSA for either regulation or consumer information testing. This requirement defines an isolated impact test to the knee slider by rigidly supporting the knee assembly and impacting a load distribution bracket attached in place of the knee clevis. A 12.0 kilogram pendulum impacts the load distribution bracket at 2.75 meters per second, and the reaction force at the femur load cell and translation of the knee slider are measured. Response requirements are specified as an upper and a lower reaction force at two different knee displacements: between 1,260 and 1,720 Newtons at 10.2 millimeters of displacement and between 2,270 and 3,100 Newtons at 17.8 millimeters of displacement (SAE, 2009).

More recent biomechanical response data in a similar loading condition presented by Balasubramanian et al. (2004) indicated that the response of the H3-50M at levels of knee displacement below the 10.2 millimeter response requirement was stiffer than the PMHS response. To address this in the THOR-50M, an additional biomechanical response requirement was added during the Mod Kit project (Ridella and Parent, 2011). This requirement added an additional measurement point at 5 millimeters of knee displacement with a force between 100 and 500 Newtons. The THOR-50M requirements also relegated the measurement point at 10.2 millimeters of deflection to a secondary requirement, as it was shown to be at the high end of the underlying PMHS corridors.

To develop response corridors suitable for calculation of BioRank, the individual force-displacement responses presented by Balasubramanian et al. (2004) were digitized and a corridor was calculated as described in the reference. This corridor was created using the entire data set (N=14), as including all subjects in a single response corridor facilitates comparison and does not presuppose an injury mechanism. The resulting corridor (All) is similar to both the existing PCL mid-substance rupture group (PCL) and fracture of the tibial metaphysis group corridors presented by Balasubramanian et al. (2004) (Figure 2), and is consistent with the design requirements for both the H3-50M and THOR-50M (Figure 3).

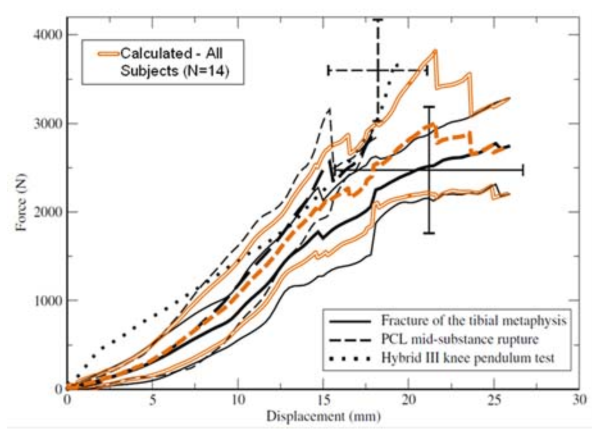

Figure 2. Knee shear response corridor calculated using all subjects presented by Balasubramanian et al. (2004), with corridor calculated from all subject responses overlaid.

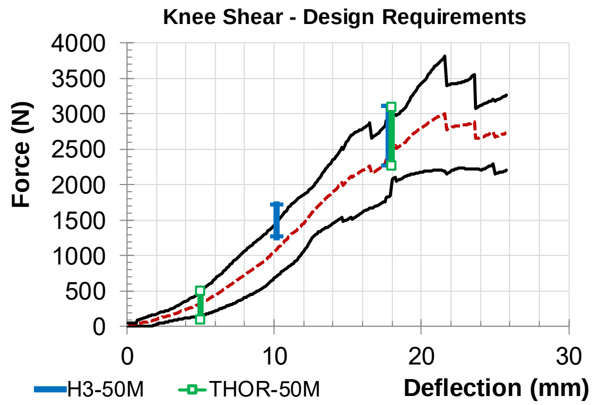

Figure 3. ATD design requirements in knee shear compared with force-deflection corridor calculated from the "All" subjects group of Balasubramanian et al. (2004).

To evaluate ATD biofidelity, the knee slider mechanisms of the THOR-50M and H3-50M were subjected to loading from the impact of a 12.0 kilogram pendulum at 2.75 meters per second through a common load distribution bracket. The deflection measured at the knee slider and the reaction force measured at the femur load cell were used to create a force-deflection characteristic to compare to the three PMHS corridors. BioRank was calculated with the calculation range constrained to the deflection up to the peak force for each ATD in order to focus on the loading portion of the response, and calculated at a resolution of 0.1 millimeters.

Lower Extremity

Three test conditions were used to assess biofidelity of the lower leg: heel impact, tibia axial compression, and dorsiflexion. The lower extremity biofidelity assessment is complicated because the foot and shoe of the THOR-50M are integrated, whereas most of the biofidelity response corridors for the human foot were developed without shoes. Therefore, in conditions where the absence or presence of a shoe would influence the response, namely the heel impact and dorsiflexion conditions, additional steps to demonstrate biofidelity are described in the respective sections.

Table 11. Test Information: Lower Extremity

Heel Impact				
ATD Description	THOR-50M Foot only	THOR-50M Foot plus MIL-spec shoe	THOR-50M Molded shoe	H3-50M Foot only
Data Source	b11588	b11589	b11590	b09763
Dorsiflexion				
ATD Description	THOR-50M Foot only	THOR-50M Foot plus MIL-spec shoe	THOR-50M Molded shoe	
Data Source	b11585	b11586	b11587	
Tibia Axial Compression				
ATD Description	THOR-50M Prototype molded shoe	THOR-50M Foot plus MIL-spec shoe		
Data Source	b11525 (3.1 m/s) b11532 (5.3 m/s)	b11529 (5.3 m/s)		

Heel impact. The heel impact biofidelity condition is based on PMHS specimen tests presented by Yoganandan et al. (1996). In these tests, PMHS lower limb specimens were potted at the proximal tibia, mounted to a mini-sled ballasted to 16 kilograms which allowed translation parallel to the tibia, and impacted with a 24 kilogram pendulum at between 2.2 and 7.6 meters per second. As data from these subjects are available in the NHTSA Biomechanics Database, response corridors were developed for time-histories of both impact force, using the measured pendulum acceleration, and proximal tibia reaction force, using the load cell between the tibia and the mini-sled. The force time-histories were aligned in time using cross-correlation and corridor boundaries were defined by the mean plus/minus one standard deviation of the included forces at each point in time. Two sets of corridors were created – one using data from all of the specimens available in the database (Table 12), and one using only a subset of these tests conducted between 3.3 and 4.5 meters per second (highlighted rows in Table 12). The former set represents a wider range of input energies, thus is expected to be a liberal interpretation of the response corridor, while the latter was a more conservative interpretation based only on tests with a similar impact velocity (4.0 ±1.0 m/s) to that of the ATD tests.

Table 12. Data sources for PMHS response corridor development in heel impact condition.

TSTNO	TSTREF	Age	Stature	Mass	Velocity	Fracture?
3604	PCLE106	74	185	104	2.2	No
3605	PCLE109	58	183	73	7.5	No
3606	PCLE111	27	175	66	7.6	No
3607	PCLE113	27	175	66	7.6	No
3608	PCLE1181	27	180	77	2.2	No
3609	PCLE1182	27	180	77	6.7	Yes
3610	PCLE119	55	175	82	6.7	Yes
3611	PCLE120	60	178	75	5.6	Yes
3612	PCLE121	60	178	75	4.5	Yes
3613	PCLE126	67	163	57	6.7	Yes
3614	PCLE127	67	163	57	4.5	Yes
3615	PCLE128	67	178	82	5.6	Yes
3616	PCLE129	67	178	82	3.4	Yes
3617	PCLE130	64	166	70	6.7	Yes
3618	PCLE131	64	166	70	2.2	No
3619	PCLE132	50	185	93	3.3	No
3620	PCLE133	50	185	93	5.6	No

Tests in an identical test condition were conducted using the H3-50M and presented by Kuppa et al. (1998), though the associated data are not available in the NHTSA Biomechanics Database. Likewise, no THOR-50M data are available in the identical test condition. As an alternative, impact data are available in the qualification test condition, which consists of a 5.0 kilogram pendulum impact to the heel of the foot in a direction parallel to the long axis of the tibia at 4.0 meters per second, with the upper tibia load cell rigidly supported. This test condition is described in more detail in the THOR-50M Qualification Procedures Manual (NHTSA, 2016b).

Since the THOR-50M molded shoe component integrates the foot and shoe into a single response element, correction is necessary before comparing the response to the PMHS corridor. Heel impact tests were conducted according to the THOR-50M Qualification Procedure Manual (NHTSA, 2016b) of the same lower leg with three different foot configurations: molded shoe, foot plus MIL-spec shoe, and foot only. The objective of these tests was to develop transfer functions to relate the impact force (external biofidelity) and tibia force (internal biofidelity) between the molded shoe and foot alone configurations, such that later molded shoe components can be evaluated for biofidelity without the intermediate steps.

BioRank was calculated to compare the transferred THOR-50M response and the measured H3-50M response to the four available corridors. As the data associated with the specimens used to calculate the PMHS response corridor were not well-controlled for impact time, the absolute value of the time component of the corridors is not particularly meaningful. Due to this uncertainty, phase-shifting was implemented to align the ATD responses with the PMHS corridor such that the BioRank value was minimized.

Dorsiflexion. The dorsiflexion test condition is based on a Rudd et al. (2004) study of dynamic dorsiflexion response of 20 specimens, 11 of which sustained ankle fractures. This test condition was intended to represent a motor vehicle crash environment with the foot of the driver placed on an intruding brake pedal. This test condition was experimentally reproduced using a test fixture which supported the lower leg horizontally at the knee and applied an impulse to a representation of a brake pedal initially in contact with the ball of the foot (Rudd et al. 2004). This impulse was applied through impact of a pneumatic impactor with a padded interface on a transfer piston attached to the brake pedal, which resulted in pure horizontal translation of the brake pedal at velocities between 3.1 m/s and 6.9 m/s. Response corridors for the time-history of reaction moment at the ankle joint as well as the relationship between ankle reaction moment and ankle rotation were developed by Lebarbé et al. (2015b) based on 18 of the 20 specimens.

Tests in an identical test condition were not available for the THOR-50M or H3-50M. As an alternative, impact data are available for the THOR-50M in the dynamic dorsiflexion qualification test condition, which consists of a 5.0 kilogram pendulum impact to the ball of the foot in a direction parallel to the long axis of the tibia at 5.0 meters per second with the lower tibia load cell rigidly supported (NHTSA, 2016b). The ankle moment evaluated in this study is the *ankle resistive moment* defined in the qualification procedure, which is calculated by summing moments about the ankle Y-axis rotation joint. Data in a similar condition for the H3-50M could not be located.

As with the heel impact, tests were run in this condition with the THOR-50M molded shoe, foot plus MIL-spec shoe, and foot only configurations in order to determine whether transfer functions were necessary to relate the response between the molded shoe and foot alone configurations. BioRank was calculated to quantify the transferred THOR-50M response to the ankle moment time-history and ankle moment-rotation characteristic corridors.

Tibia axial compression. Biofidelity of the tibia in axial compression was assessed using the methodology presented by Funk et al. (2000), which represents lower leg loading in an automotive crash environment where the knee is entrapped and the lower leg is compressed due to toepan intrusion. This condition was experimentally reproduced using a test fixture which supported the lower leg horizontally at the knee and applied an impulse to a plate initially in contact with the foot. This impulse was applied through impact from a pendulum of 33 kilogram effective mass traveling at 7 meters per second to a transfer piston rigidly attached to a load cell and a foot plate with a total mass of 6.54 kilograms. A total of 20 PMHS specimens were evaluated in this test condition.

Based on the Funk et al. (2000) data, Lebarbé et al. (2015b) developed response corridors representing tibia axial force as a function of time as well as tibia axial force as a function of footplate displacement. Corridors were developed using 15 of the 20 subjects, excluding 5 which sustained only a tibia fracture. Means and standard deviations were calculated at each point in time for the tibia force and footplate displacement time-histories, and average standard deviations in force and displacement were calculated. These corridors were recreated for this effort using the data provided in the Supplemental Material associated with the Lebarbé et al. (2015b) publication. The tibia axial force time-history corridor boundaries were formed using the mean plus or minus the average standard deviation of tibia axial force for the 15 subjects. The corridor for tibia axial force as a function of footplate displacement was formed by superimposing the average standard deviations on the force versus mean displacement characteristic to form a plus/minus one standard deviation ellipse at each point in time. The upper and lower corridor boundaries were then formed by interpolating to determine the minimum and maximum tibia forces at each tenth of a millimeter of footplate displacement.

Tests in a similar configuration were conducted using two different configurations of the THOR-50M, one with a MIL-spec shoe and one with a prototype molded shoe (Table 11). There were three differences between the tests on the THOR-50M (Kim et al. 2017) and the PMHS tests (Funk et al. 2000): first, the ballistic mass used in the THOR-50M tests was 28.4 kilograms; second, the THOR-50M tests were conducted at impact velocities of 3.1 and 5.3 meters per second; and third, the THOR-50M tests were conducted with shoes. A transfer function to relate the THOR-50M with-shoe response to predict a foot only response was not considered in this case, as the measured tibia axial force in matched pair tests of with-shoe and without-shoe PMHS specimens showed minimal differences (Kim et al., 2017). No phase correction was made for the time-history comparison, as impact time was well controlled in the study and the PMHS and ATD tests were conducted using a similar test fixture.

Whole Body

To evaluate the ATD in its intended application of crash testing in frontal and frontal oblique test modes, biofidelity evaluation in as close to this condition as possible is desired. However, there are many tradeoffs that prevent an exact replication of a motor vehicle crash event in a laboratory environment suitable for PMHS response evaluation, including but not limited to the repeatability and reproducibility of the test apparatus, the feasibility of instrumentation to collect meaningful biomechanical response measurements, the ability to visually capture high-speed video and motion tracking information without interference from the vehicle or test apparatus, and the selection of a crash pulse that is severe enough to provide a meaningful kinematic and kinetic response assessment while not inducing severe injuries to the PMHS which may compromise the integrity of the results.

This section presents four sled test conditions of increasing representativeness of the motor vehicle crash environment: Gold Standard 1, the most simplified of the sled conditions, which uses a rigid seat and standard lap and shoulder belts without pretensioners or load limiters and represents a 40 km/h frontal crash; Gold Standard 2, which adds a load limiter but is conducted at a lower speed (30 km/h) to allow measurement of skeletal thoracic deflection; Gold Standard 3, which is identical to Gold Standard 2 except that the sled is rotated 30 degrees to represent an oblique loading condition; and Far Side Oblique (FSO), which represents the occupant environment in an Oblique Moving Deformable Barrier (OMDB) (NHTSA, 2015b) crash test and includes a standard vehicle seat, a three-point seat belt with a pretensioner and load limiter, and a front passenger air bag. As the similarity of the test condition to the frontal and frontal oblique crash test modes increases, the ability to measure the internal and external biomechanical response of the PMHS used in the biofidelity tests decreases. For example, in the Far Side Oblique test, the air bag deployment prevents measurement of skeletal thoracic deflection using a motion capture system due to obstruction of the visual targets at the time of peak belt loading.

Except for three of the eight PMHS tests conducted in the Gold Standard 1 condition, all of the data, reports, photos, and videos from the biofidelity and ATD tests referenced in this section are available in the NHTSA Biomechanics Database. As such, the information presented in this section will be intentionally brief; the curious reader is invited to review the referenced papers and associated information.

Gold Standard 1. The Gold Standard 1 (GS1) sled test condition reported by Shaw et al. (2009) is a simplified representation of a mid-size passenger car crash into a rigid barrier at 40 kilometers per hour. Subjects were positioned on a flat, rigid seat pan and restrained by a shoulder belt and a lap belt with anchor geometry selected to match the right front passenger seat of a typical U.S. mid-size passenger sedan. The restraint system did not include a load limiter or retractor. The lower legs of the subject were restrained by a rigid knee bolster and foot pan apparatus initially in contact with the subject and intended to minimize motion inferior to the pelvis. The key measurements recorded for each test were the restraint forces and kinematics of the head, spine, and torso skeletal deformation at five locations on the anterior rib cage, including the sternum and four locations representative of the THOR IR-TRACC attachment points.

To allow quantification of biofidelity, corridors were recreated using the five subjects available in the NHTSA Biomechanics Database (Table 13). Time-history corridors were developed for shoulder belt forces, chest deflections, head and T1 displacements, head acceleration, and head angular rates by calculating the mean and the mean plus/minus one standard deviation of the five responses at each tenth of a millisecond over the span of 0 to 0.2 seconds. Chest deflections were calculated and presented as X-axis deflections with respect to the T8 coordinate system. Head and T1 displacements were calculated and presented as the X, Y, and Z axis displacement with respect to the sled coordinate system.

The THOR-50M and H3-50M were evaluated in the Gold Standard 1 test condition using the same test apparatus (Table 13). Since 3D motion tracking data was not collected during the evaluation of THOR-50M S/N 9207, the data set is supplemented with an earlier data set using a Mod Kit THOR (S/N 016) with the SD-3 shoulder assembly installed. The H3-50M was equipped with string potentiometers installed at four locations on the chest, which differ from the THOR measurement locations; the “straight” measurements from each quadrant, which measure X-axis deflection relative to the spinebox, were used in this evaluation.

Table 13. Data sources for Whole Body tests

Gold Standard 1					
TSTREF	UVA 1294	UVA 1295	UVA 1378	UVA 1379	UVA 1380
TSTNO	b09546	b09547	b11014	b11015	b11016
Sex	Male	Male	Male	Male	Male
Age (years)	76	47	72	40	37
Stature (cm)	178	177	184	179	180
Mass (kg)	70	68	81	88	78
Chest Depth (mm)	239	230	218	270	225
ATD	THOR-50M (kinematics)		THOR-50M (kinetics)		H3-50M
ATD Description	S/N 016 (Mod Kit*)		S/N 9027 (Metric)		S/N 048
TSTREF	UVA0096		S0158		UVAS0110
TSTNO	b11472		b11119		b11485
Gold Standard 2					
TSTREF	UVA S028	UVA S029	UVA S0302	UVA S0303	UVA S0304
TSTNO	b11468	b11469	b11509	b11510	b11511
Sex	Male	Male	Male	Male	Male
Age (years)	59	66	67	67	74
Stature (cm)	178	179	177	173	183
Mass (kg)	68	70	68	68	70
Chest Depth (cm)	24	35	24	22	23
ATD	THOR-50M (kinematics)		THOR-50M (kinetics)		H3-50M
ATD Description	S/N 016 (Mod Kit*)		S/N 9027 (Metric)		S/N 048
TSTREF	UVA0099		S0161		UVAS0107
TSTNO	b11475		b11122		b11484
Gold Standard 3					
TSTREF	UVAS0313		UVAS0314		UVAS0315
TSTNO	b11518		b11519		b11520
Sex	Male		Male		Male
Age (years)	69		66		67
Stature (cm)	173		172		177
Mass (kg)	69		76		64
Chest Depth (mm)	248		227		243
ATD	THOR-50M			H3-50M	
ATD Desc.	S/N 9027 (Metric)			S/N 0169	
TSTREF	UVAS0312			UVAS0307	
TSTNO	b11517			b11513	
Far Side Oblique					
TSTREF	UVAS0243		UVAS0244		UVAS0245
TSTNO	b11500		b11501		b11502
Sex	Male		Male		Male
Age (years)	73		83		63
Stature (cm)	178		178		183
Mass (kg)	73		81.6		68
Chest Depth (mm)	251		264		219
ATD	THOR-50M	THOR-50M	THOR-50M	H3-50M	H3-50M
ATD Description	S/N 016 (Mod Kit*)			S/N 048	S/N 048 (belt loads)
	Position A	Position B	Position C		
TSTREF	UVA S0249	UVA S0250	UVA S0251	UVA S0246	UVA S0246
TSTNO	b11504	b11505	b11506	b11499	b11498

** The Mod Kit THOR used in the whole body sled tests included the SD-3 shoulder*

Gold Standard 2. The Gold Standard 2 (GS2) sled test condition reported by Shaw et al. (2014) is nearly identical to the GS1 condition except for the sled pulse, which represents a frontal crash at 30 kph, and the restraint system, which represents a 3 kN load-limited shoulder belt. The GS2 test condition was carried out using five nominally 50th percentile male PMHS (Table 13). From this data, response corridors were calculated for the same set of kinematic and kinetic measurements as in the GS1 condition.

The THOR-50M and H3-50M were evaluated in the Gold Standard 2 test condition using the same test apparatus (Table 13). Since 3D motion tracking data was not collected during the evaluation of THOR-50M S/N 9207, the data set is supplemented with an earlier data set using a Mod Kit THOR (S/N 016) with the SD-3 shoulder assembly installed. As in the GS1 condition, the H3-50M used for comparison was equipped with string potentiometers installed at four locations on the chest.

Gold Standard 3. The Gold Standard 3 (GS3) sled test condition reported by Montesinos Acosta et al. (2016) is similar to the GS2 condition with two exceptions: first, the sled was angled 30 degrees counterclockwise to represent the right front passenger in a near-side frontal oblique impact; second, bilateral wedges were added to the rigid seat to reduce the risk of the pelvis sliding laterally off of the seat. The GS3 test condition was carried out using three nominally 50th percentile male PMHS (Table 13). From this data, response corridors were calculated for the same set of kinematic and kinetic measurements as in the GS1 and GS2 conditions.

The THOR-50M and H3-50M were evaluated in the Gold Standard 3 test condition using the same test apparatus (Table 13). As in the previous Gold Standard conditions, the H3-50M used for comparison was equipped with string potentiometers installed at four locations on the chest, which differ from the THOR measurement locations.

Far Side Oblique. In most OMDB research crash tests conducted by NHTSA, the far-side occupant was observed to move laterally inboard to the extent that the shoulder belt was no longer in contact with the shoulder at the point of peak forward excursion (Saunders et al., 2015). To gain understanding of the interaction of a far-side occupant with the shoulder belt in an oblique crash, a sled test series was developed to represent the environment of a mid-sized passenger vehicle in an OMDB crash test. A sled buck was constructed using a mid-sized passenger car body-in-white representing a similar vehicle as used in two OMDB crash tests: one with two THOR-50M (TSTNO v09123) and one two H3-50M (TSTNO v09224), both available in the NHTSA Vehicle Database. The sled buck was angled 20 degrees clockwise to best approximate both the average rotation of the vehicle as well as the translation of the vehicle CG location up to the point of peak head excursion. The crash pulse applied was the resultant acceleration calculated from the local X-axis and Y-axis accelerometers mounted to the right rear sill during test v09224, as there were data anomalies in test v09123. Original equipment manufacturer (OEM) components were used for the right front passenger seat, seat belts, front passenger air bag, instrument panel, and knee bolster. The belt pretensioner and frontal air bag were triggered at the same time as they were in the full-scale vehicle OMDB test. The seat back was replaced with a minimal support system to allow subject positioning without impeding the field of view of VICON cameras used to track occupant kinematics. PMHS subjects were instrumented with chest bands to measure chest deformation as well as marker plates to track head and spine motion with respect to the buck, as recorded and processed using the VICON system.

This test condition, referred to as the Far Side Oblique (FSO) condition, was carried out using three nominally 50th percentile male PMHS (Table 13). From this data, response corridors were calculated for whole-body kinematics and shoulder belt forces. While chest bands were used to measure external chest deflection in the PMHS tests, they were not used in the ATD tests, thus chest band response corridors are not presented herein.

The THOR-50M and H3-50M were evaluated in the FSO test condition using the same test apparatus (Table 13). Three different postures and D-ring positions were evaluated for the THOR-50M: Position A, matching the posture and D-ring position in the full-scale vehicle OMDB crash test; Position B, with a posture closest to the subject in UVAS0244 but a D-ring location inboard of the OEM D-ring plane; and Position C, using a posture closest to the subject in UVAS0244 and a D-ring location consistent with the OEM D-ring plane. The H3-50M used for comparison was run in only the baseline posture and D-ring position, and only one such test was conducted with the VICON system (b11499). However, this test is missing shoulder belt load data, so the shoulder belt loads from b11498, an otherwise identical H3-50M test that did not collect VICON data, were used instead. The TCBR was calculated for all of the belt position and posture combinations assessed for the THOR-50M, though the results from Position C are used in the overall BioRank calculation as it is believed that the posture and belt position used in this test is most representative of that used in the associated PMHS tests.

RESULTS

Head

Table 14. BioRank Results: Head

	THOR	H3
Head Drop Test		
INT: Head resultant acceleration	0.155	0.013
Whole-body Head Impact		
EXT: Peak impact force	0.261	0.004
Face Rigid Bar Impact		
EXT: Impact force time-history	0.967	2.385
EXT: Peak impact force	3.742	23.952
TCBR: External	*2.355*	*13.169*
Face Disk Bar Impact		
EXT: Impact force time-history	0.737	1.874
EXT: Peak impact force	0.892	11.618
TCBR: External	*0.815*	*6.746*
Head BRBR: Internal	**0.155**	**0.013**
Head BRBR External	**1.143**	**6.640**

Isolated Head Drop. The peak resultant head acceleration for the THOR-50M and H3-50M are compared to the mean plus/minus one standard deviation of the PMHS response (Figure 4). The BioRank results show that both the THOR-50M and H3-50M achieve excellent biofidelity compared to the standard deviation corridor (Table 14).

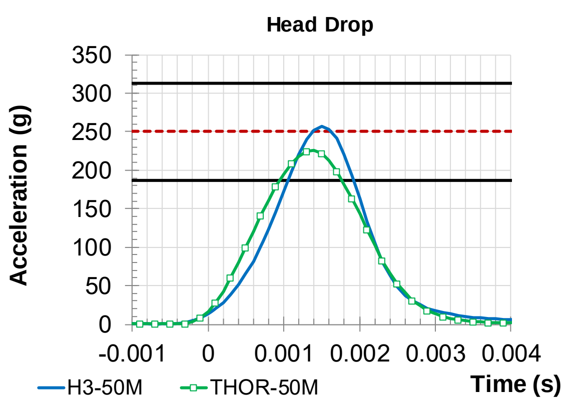

Figure 4. Head drop test response.

Whole-body Head Impact. The responses of the THOR-50M and H3-50M are compared to the mean plus/minus one standard deviation of the PMHS response (Figure 5). The BioRank results show that both the THOR-50M and the H3-50M demonstrate excellent biofidelity in the head impact biofidelity test condition (Table 14).

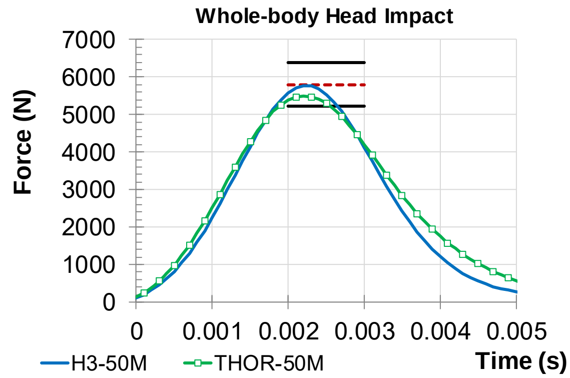

Figure 5. Whole-body head impact test response.

Face Rigid Bar Impact. Qualitatively, the ATD responses were similar in shape to the biofidelity corridor, but higher in magnitude (Figure 6). The BioRank results (Table 14) show that the THOR-50M demonstrates excellent external biofidelity relative to the impact force time-history, but poor external biofidelity considering just the peak impact force alone, as the peak is outside of the response corridor. On average, the external biofidelity score for THOR-50M is marginal in this test condition. The H3-50M demonstrates poor external biofidelity for this test condition, with a marginal classification for the impact force time-history corridor comparison alone and a poor classification for the peak impact force, which is higher than the biofidelity corridor mean by a factor of more than two.

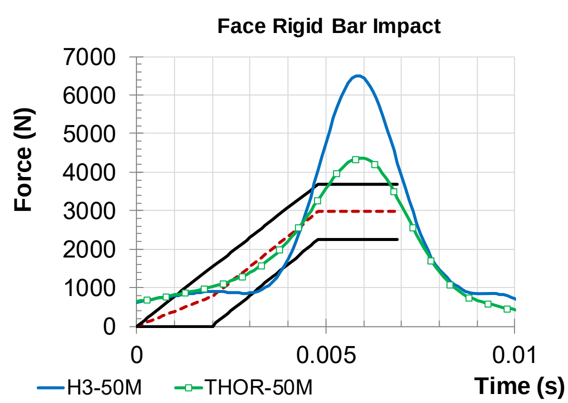

Figure 6. Face rigid bar impact test response.

Face Rigid Disk Impact. Qualitatively, the ATD responses were similar in shape to the biofidelity corridor, with the THOR-50M force peak within the peak corridor force but later in time, and the H3-50M force peak above the upper boundary of the corridor but earlier in time. The BioRank results (Table 14) demonstrate excellent external biofidelity for the THOR-50M based on both the impact force time-history corridor as well as the peak impact force alone. The H3-50M shows good biofidelity in the impact force time-history corridor comparison, but poor biofidelity with respect to the peak impact force alone. The peak impact force comparison isolates the BioRank score at a single point in time, thus it does not account for the fact that the H3-50M response does follow the corridor for a portion of the ramp up to the peak force (Figure 7); however, the H3-50M peak force is over a factor of two higher than the corridor mean.

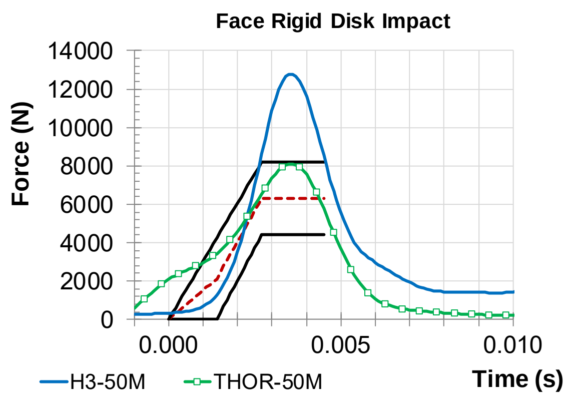

Figure 7. Face rigid disk impact test response.

Neck

Neck Frontal Flexion. Comparisons of the resulting THOR-50M and H3-50M responses to the Thunnissen corridors are shown in Figure 8 through Figure 16. The resulting BioRank calculations are summarized in Table 15. The BioRank results show the THOR-50M and H3-50M demonstrate similar internal biofidelity (marginal), while the THOR-50M demonstrates marginal external biofidelity compared to the poor external biofidelity of the H3-50M. The key differences appear to be in the head CG X-axis motion (Figure 11), where THOR-50M shows more forward motion than the H3-50M, which subsequently influences the head and neck angle time-histories and the associated head lag corridor (Figure 15).

Table 15. BioRank Results: Neck

	THOR	H3
Neck Frontal Flexion		
Input: Sled pulse	2.087	2.036
Input: T1 resultant acceleration	1.649	1.641
INT: Head resultant acceleration	2.155	2.185
EXT: Head CG X-axis displ.	1.440	5.747
EXT: Head CG Z-axis displ.	2.557	3.013
EXT: Head angle	3.078	4.052
EXT: Neck angle	1.896	3.866
EXT: Head lag corridor	1.857	16.974
EXT: Moment-vs-rotation corridor	2.320	2.028
TCBR: Internal	*2.155*	*2.185*
TCBR: External	*2.191*	*5.947*
Neck Lateral Flexion		
Input: Sled pulse	3.710	3.855
Input: T1 resultant acceleration	1.177	1.177
EXT: Head CG X-axis displ.	1.647	3.548
EXT: Head CG Z-axis displ.	0.249	3.881
EXT: Head angle	1.779	2.311
EXT: Moment-vs-rotation corridor	0.975	1.016
TCBR: External	*1.163*	*2.689*
Neck Torsion		
EXT: Moment-vs-rotation corridor	3.027	N/A
TCBR: External	*3.027**	*N/A*
Neck BRBR: Internal	**2.155**	**2.185**
Neck BRBR External	**1.677**	**4.318**

** Not included in BRBR since corridor does not represent mean plus/minus one standard deviation*

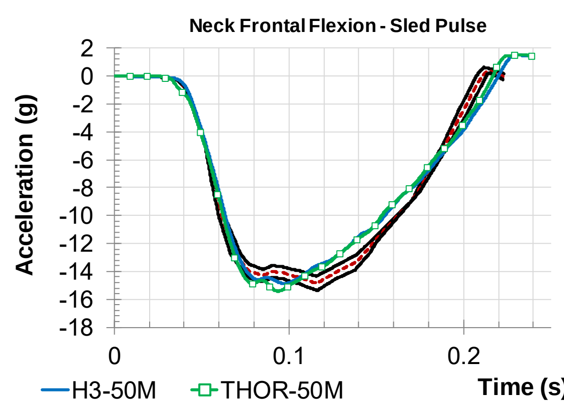

Figure 8. Neck frontal flexion, sled acceleration pulse.

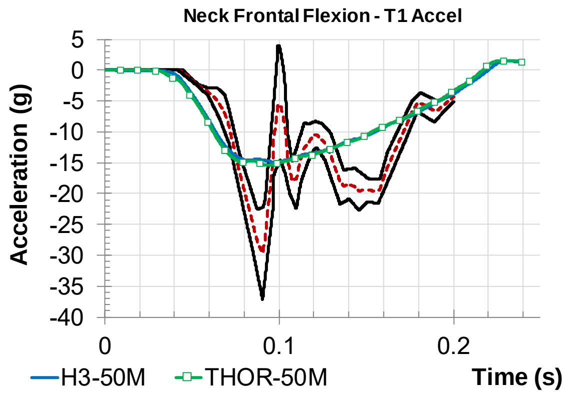

Figure 9. Neck frontal flexion, T1 acceleration pulse compared to acceleration pulse applied to the base of the neck in the ATD tests.

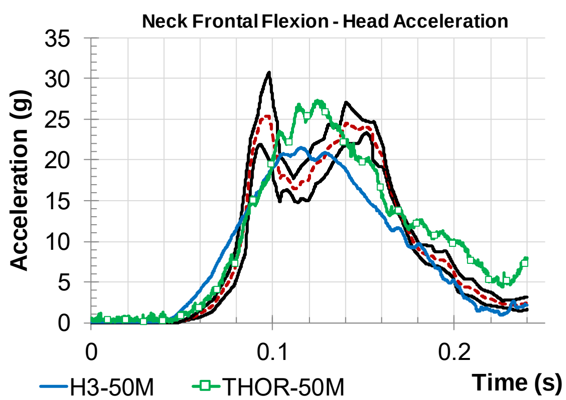

Figure 10. Neck frontal flexion, head resultant acceleration

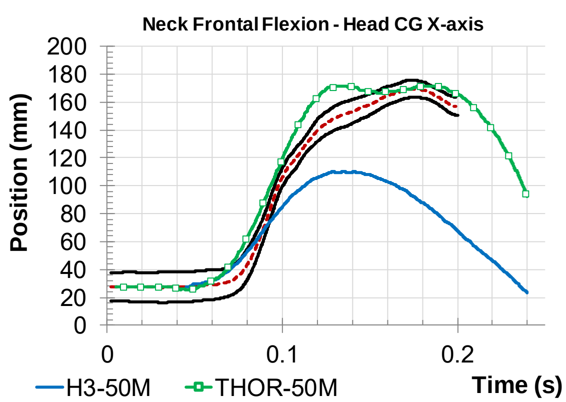

Figure 11. Neck frontal flexion, head CG x-axis motion

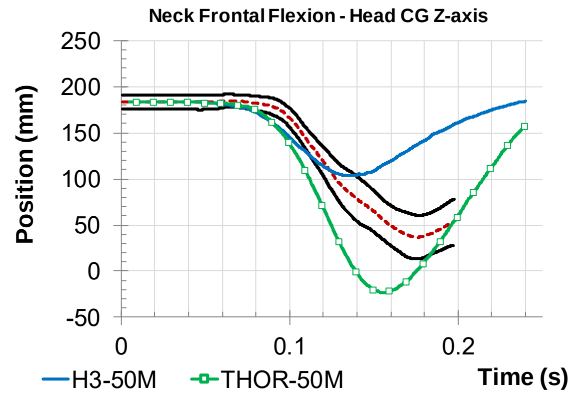

Figure 12. Neck frontal flexion, head CG z-axis motion

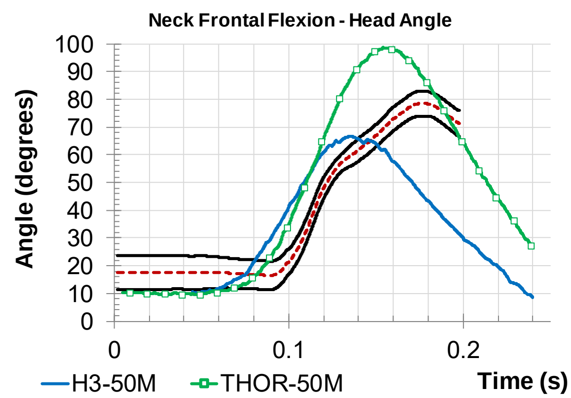

Figure 13. Neck frontal flexion, head angle

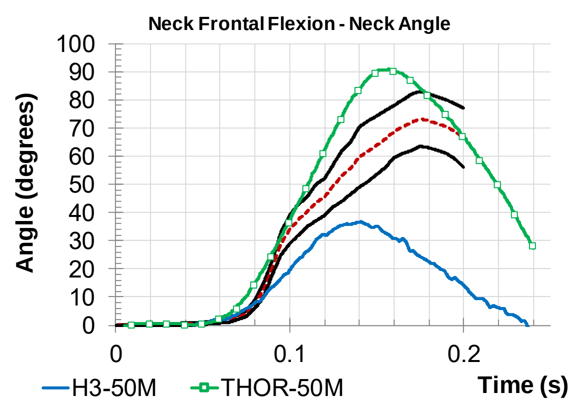

Figure 14. Neck frontal flexion, neck angle

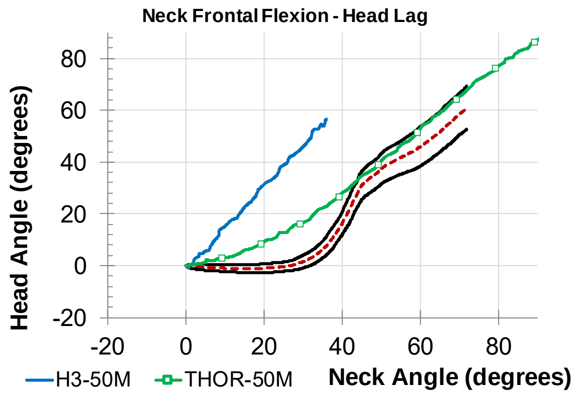

Figure 15. Neck frontal flexion, head lag

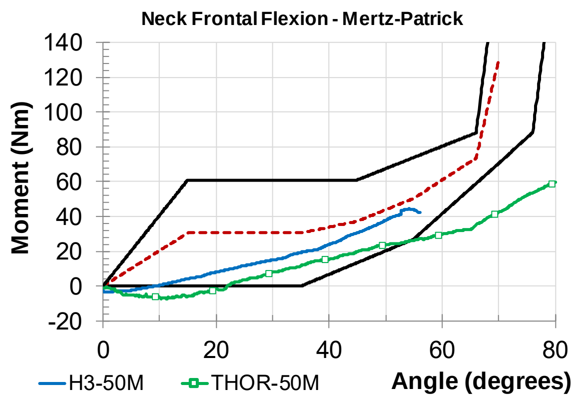

Figure 16. Neck frontal flexion, Mertz and Patrick (1971) moment-angle response corridor

Neck Lateral Flexion. Comparisons of the resulting THOR-50M and H3-50M responses to the prescribed response corridors are shown in Figure 17 through Figure 22. The BioRank results show that the THOR-50M demonstrates superior biofidelity to the H3-50M for all measurements in this test mode. As there are no internal biofidelity measurements in this test mode, the TCBR consists of only external biofidelity measurements. Based on the External TCBR, the THOR-50M demonstrates excellent biofidelity, while the H3-50M demonstrates good biofidelity.

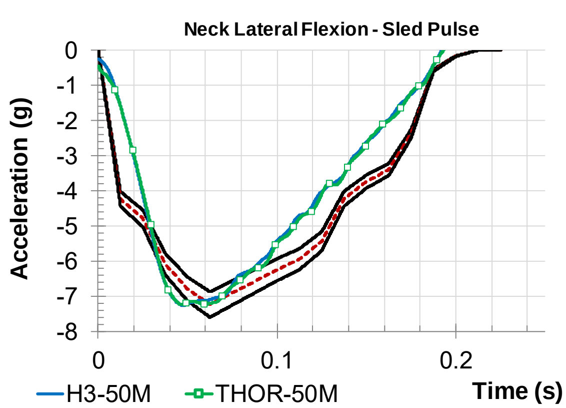

Figure 17. Neck lateral flexion, sled acceleration pulse

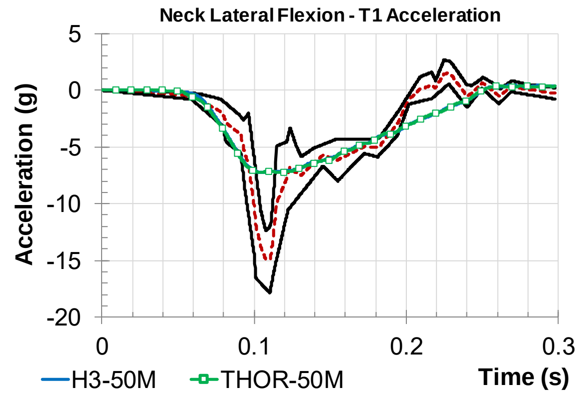

Figure 18. Neck lateral flexion, T1 acceleration vs. applied acceleration pulse

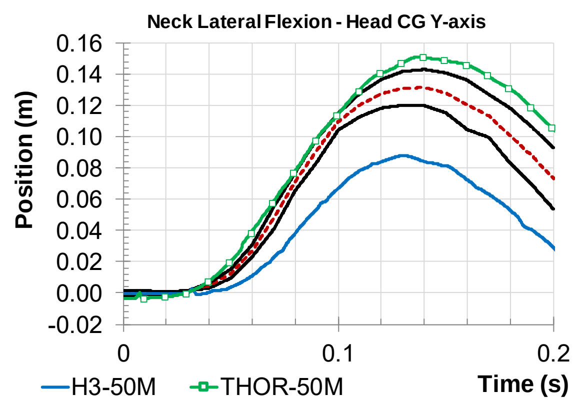

Figure 19. Neck lateral flexion, head CG y-axis position

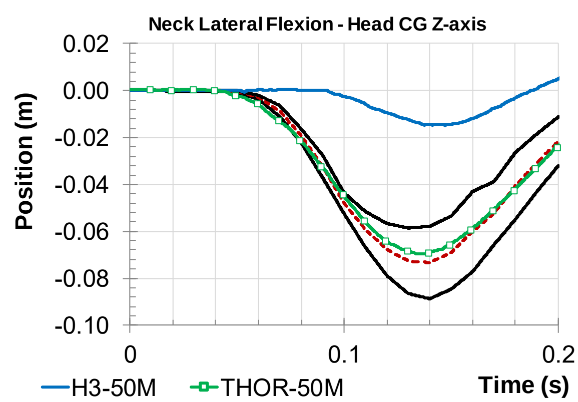

Figure 20. Neck lateral flexion, head CG z-axis position

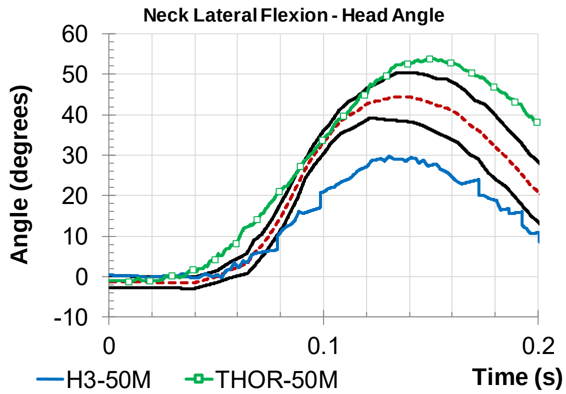

Figure 21. Neck lateral flexion, head angle

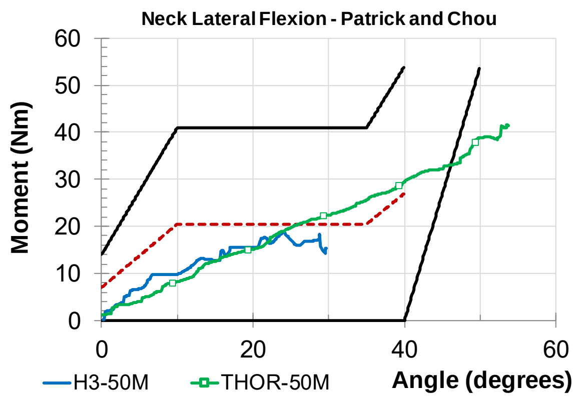

Figure 22. Neck lateral flexion, Patrick and Chou (1976) moment-angle response corridor

Neck Torsion. Qualitatively, the THOR-50M response shows a similar loading slope to the response corridor (nominally 0.5 Newton-meters per degree), but where the human response exhibits a low-moment toe region, or the relatively low resistance over the first 50 to 75 degrees of rotation, the THOR-50M resistance increases soon after the onset of rotation (Figure 23). The H3-50M demonstrates a much stiffer moment-rotation response than both the THOR-50M and the biofidelity corridor.

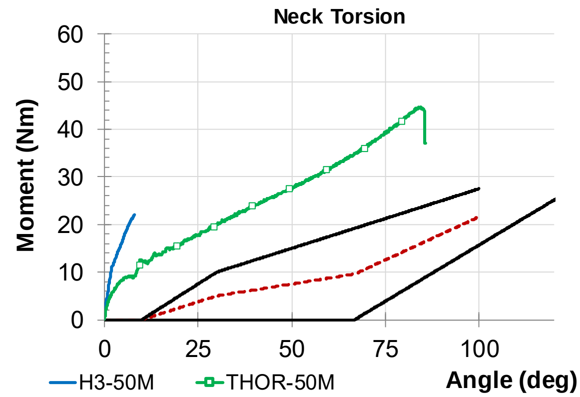

Figure 23. Neck torsion moment-vs-rotation response

The BioRank results show that the THOR-50M demonstrates poor biofidelity compared to the generalized moment-rotation corridor, though since this corridor does not represent a mean plus/minus one standard deviation response as defined in the BioRank methodology, the resulting score and classification may not be meaningful and as such is not included in the BRBR score for the neck.

Thorax

Table 16. BioRank Results: Thorax

	THOR	H3
Sternal Impact		
Parent et al., 2013 (skeletal deflection)		
INT: Deflection	0.581	2.648
EXT: Force	0.905	1.844
EXT: Force-deflection	0.607	1.999
Lebarbé et al., 2012 (external deflection)		
INT: Deflection	1.049	2.364
EXT: Force	0.769	2.923
EXT: Force-deflection	0.647	2.621
TCBR: Internal	*0.815*	*2.506*
TCBR: External	*0.732*	*2.347*
Lower Ribcage Oblique Impact		
INT: Deflection	1.019	0.700
EXT: Force	1.733	2.627
EXT: Force-deflection corridor calculated at each point in time	0.647	1.538
EXT: Force-deflection corridor calculated at each point in deflection	1.110	1.212
TCBR: Internal	*1.019*	*0.700*
TCBR: External	*1.163*	*1.792*
Thorax BRBR: Internal	**0.917**	**1.603**
Thorax BRBR External	**0.948**	**2.070**

Sternal Impact. Comparisons of the THOR-50M and H3-50M responses to the Kroell and Lebarbé force-deflection corridors are shown in Figure 24 and Figure 25, respectively. The TCBR (Table 16) was calculated by averaging the individual measurements for both the skeletal deflection and external deflection corridors.

The Internal TCBR consists of the deflection time-history corridor comparison, while the External TCBR consists of the force time-history and force-deflection corridor comparisons. The THOR-50M demonstrates excellent biofidelity based on both the Internal and External TCBR values, while the H3-50M demonstrates marginal biofidelity. The H3-50M shows a stiffer response than both the THOR-50M and the biofidelity corridor, thus for an identical impact the H3-50M would be expected to measure less ribcage deflection.

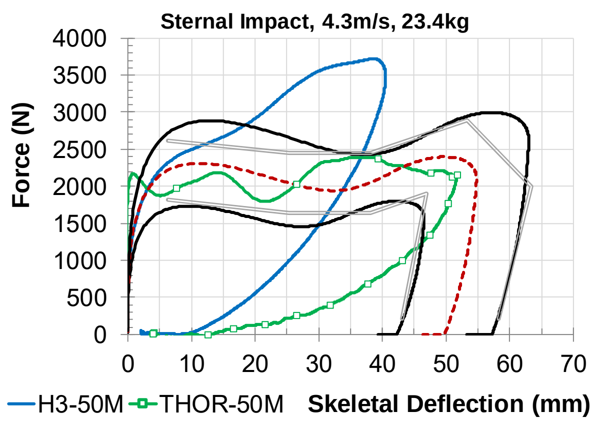

Figure 24. Sternal impact response corridor, expressed as force vs. skeletal deflection characteristic; Kroell corridor (from GESAC, 2005a) shown in grey double lines as reference.

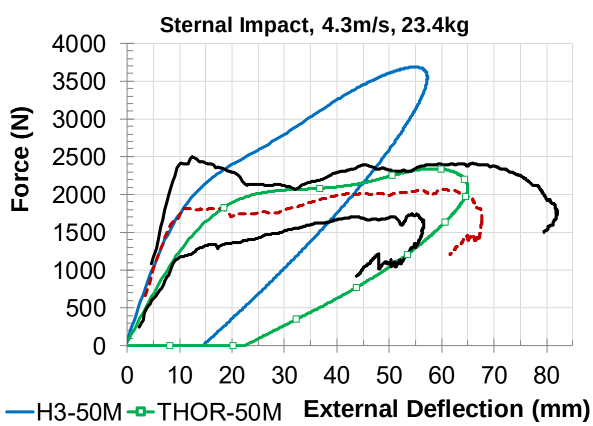

Figure 25. Sternal impact response corridor, expressed as force vs. external deflection characteristic

Lower Ribcage Oblique Impact. THOR-50M and H3-50M responses were compared to the deflection time-history (Figure 26), force time-history (Figure 27), and the two force-deflection corridors developed from the time-history data (Figure 28 and Figure 29). BioRank was calculated for all four comparisons (Table 16). The BioRank results show that the THOR-50M demonstrates good biofidelity according to both the Internal and External TCBR scores, while the H3-50M showed good internal biofidelity and marginal external biofidelity.

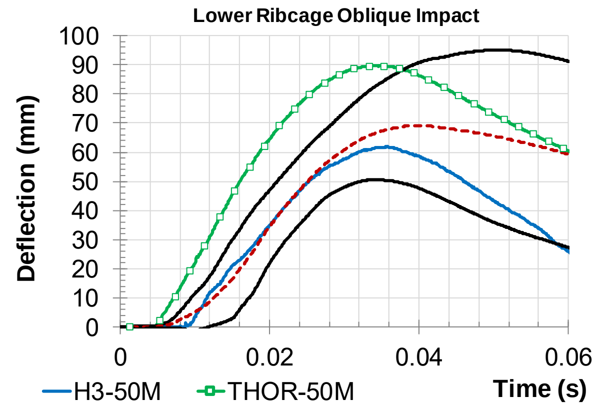

Figure 26. Lower ribcage oblique impact deflection time-history corridor

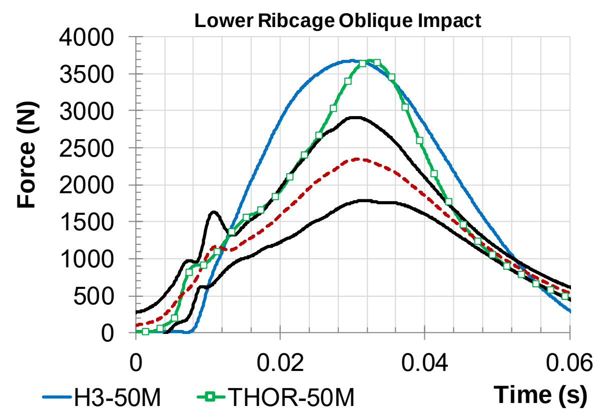

Figure 27. Lower ribcage oblique impact force time-history corridor

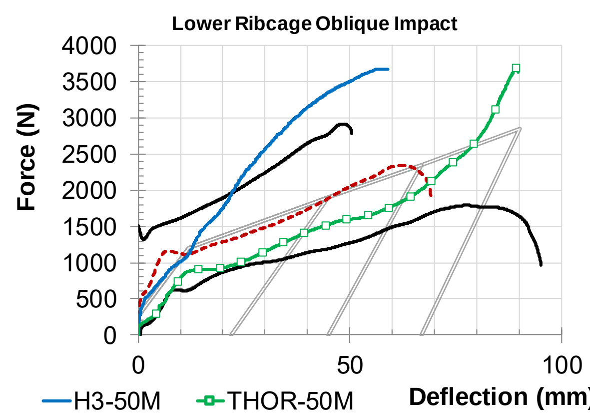

Figure 28. Lower ribcage oblique impact composite force-deflection response corridor; reference corridor shown for comparison (GESAC, 2005a).

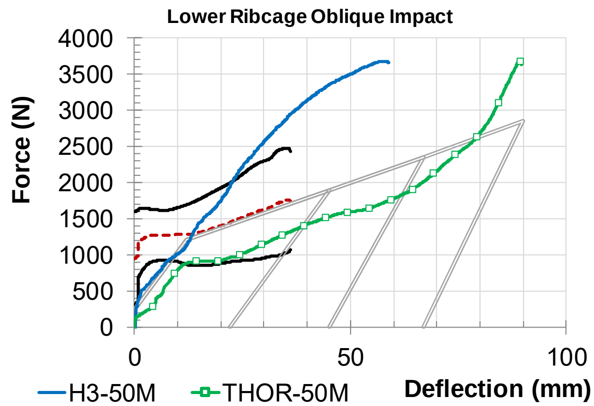

Figure 29. Lower ribcage oblique impact force-deflection corridor calculated in deflection domain; reference corridor shown for comparison (GESAC, 2005a).

Abdomen

Table 17. BioRank Results: Abdomen

	THOR	H3
Upper Abdomen Steering Wheel Impact		
INT: Deflection	0.968	0.552
EXT: Force	2.185	0.881
EXT: Force-deflection corridor calculated at each point in time	0.563	0.433
EXT: Force-deflection corridor calculated at each point in deflection	0.748	0.515
TCBR: Internal	*0.968*	*0.552*
TCBR: External	*1.165*	*0.610*
Lower Abdomen Rigid Bar Impact		
INT: Deflection	1.972	2.705
EXT: Force	4.652	6.865
EXT: Force-deflection corridor calculated at each point in time	4.973	6.549
EXT: Force-deflection corridor calculated at each point in deflection	9.288	11.401
TCBR: Internal	*1.972*	*2.705*
TCBR: External	*6.304*	*8.272*
Abdomen Belt Loading		
EXT: Force-deflection corridor calculated at each point in deflection	0.938	1.541
Abdomen BRBR: Internal	**1.470**	**1.629**
Abdomen BRBR External	**2.803**	**3.474**

Upper abdomen steering wheel impact. Both the THOR-50M and H3-50M reach peak deflection earlier in time than the PMHS corridor (Figure 30). The THOR-50M reaches a peak force slightly earlier than the PMHS peak, and this peak exceeds the upper boundary of the PMHS corridor, while the H3-50M peak force occurs slightly later than the PMHS peak, but remains within the corridor (Figure 31). Both ATD responses follow the general trend in stiffness of the PMHS corridor (Figure 32 and Figure 33), with the THOR-50M response exceeding the upper boundary of the PMHS corridor calculated in the deflection domain after roughly 110 millimeters of deflection while the H3-50M response remains within the corridor up to its peak deflection. The BioRank results for the upper abdomen steering wheel impact condition demonstrate excellent internal and good external biofidelity for THOR-50M, and excellent internal and external biofidelity for H3-50M.

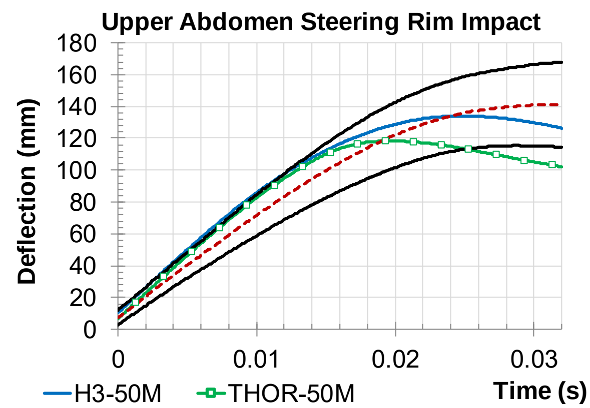

Figure 30. Upper abdomen impact, deflection time-history corridor.

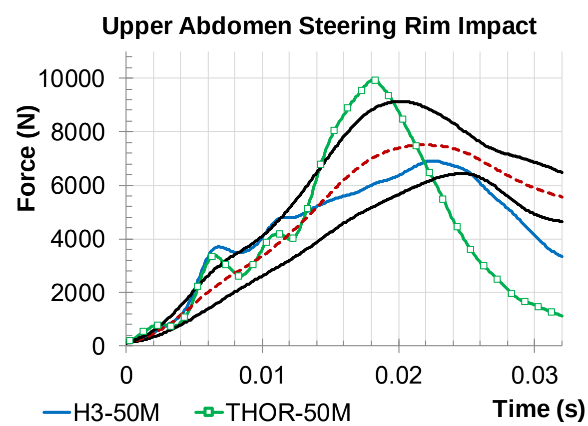

Figure 31. Upper abdomen impact, force time-history corridor.

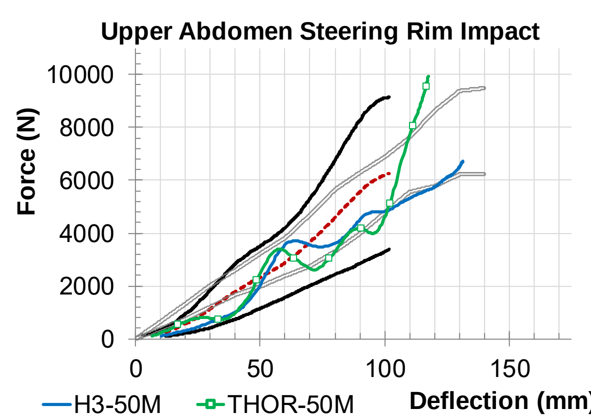

Figure 32. Upper abdomen impact, composite force-deflection corridor; reference corridor shown for comparison (GESAC, 2005a).

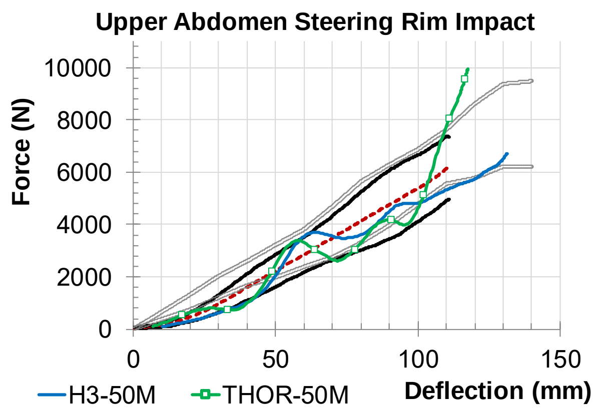

Figure 33. Upper abdomen impact, force-deflection corridor calculated in deflection domain; reference corridor shown for comparison (GESAC, 2005a).

Lower abdomen rigid bar impact. Both ATDs exhibit responses that are more stiff than the PMHS corridors, showing higher peak deflections and forces. The THOR-50M response follows the lower boundary of the deflection time-history until it reaches its peak at roughly 120 millimeters of deflection, compared to the peak of 100 millimeters for the H3-50M (Figure 34). The THOR-50M and H3-50M both reach higher and earlier peak forces than the PMHS corridor (Figure 35). Both ATDs exceed the upper boundary of the force-deflection characteristics, though for both corridors the THOR-50M remains within the PMHS upper boundary up to a higher level of deflection (Figure 36 through Figure 39). The TCBR results in good internal biofidelity for the THOR-50M and marginal biofidelity for the H3-50M, while the external biofidelity is poor for both ATDs.

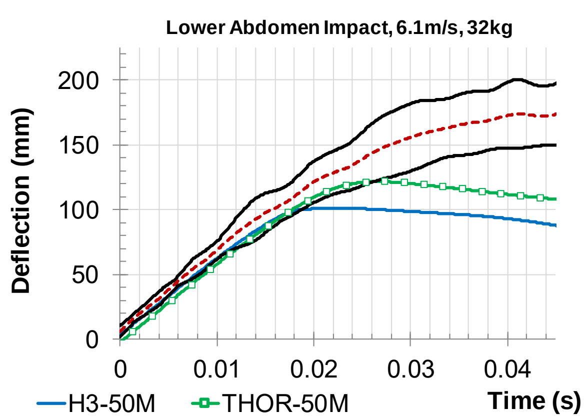

Figure 34. Lower abdomen rigid bar impact, deflection time-history corridor.

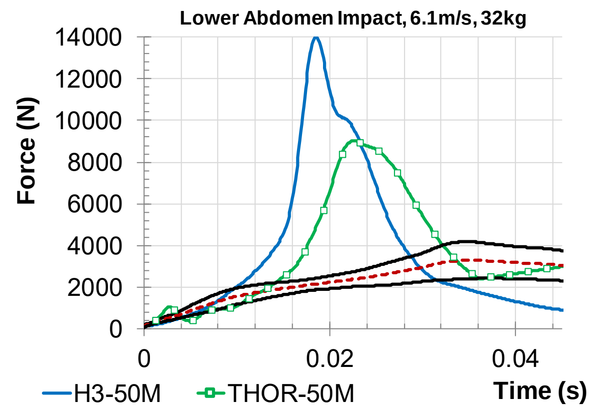

Figure 35. Lower abdomen rigid bar impact, force time-history corridor.

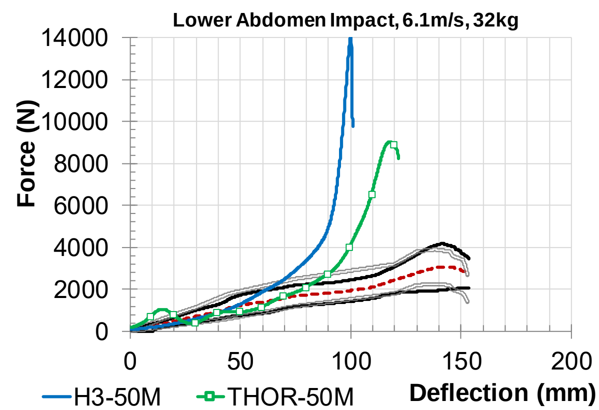

Figure 36. Lower abdomen rigid bar impact, composite force-deflection corridor; reference corridor shown for comparison (GESAC, 2005a).

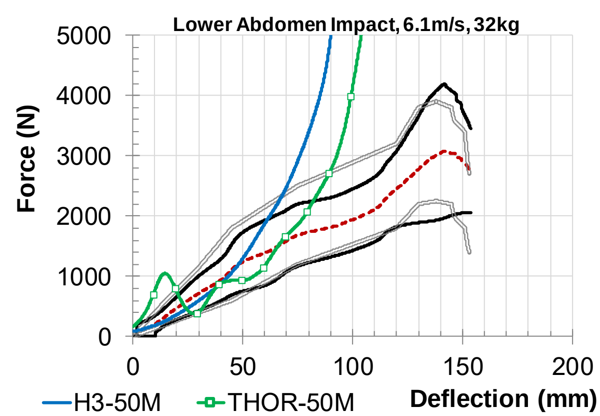

Figure 37. Lower abdomen rigid bar impact, composite force-deflection corridor; reference corridor shown for comparison (GESAC, 2005a); cropped at 5 kN for visibility.

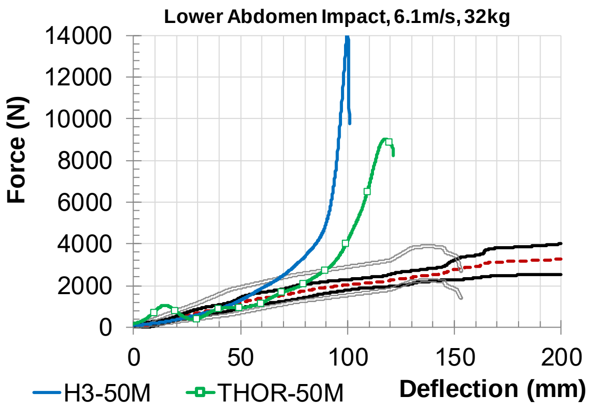

Figure 38. Lower abdomen rigid bar impact, force-deflection corridor calculated in deflection domain; reference corridor shown for comparison (GESAC, 2005a).

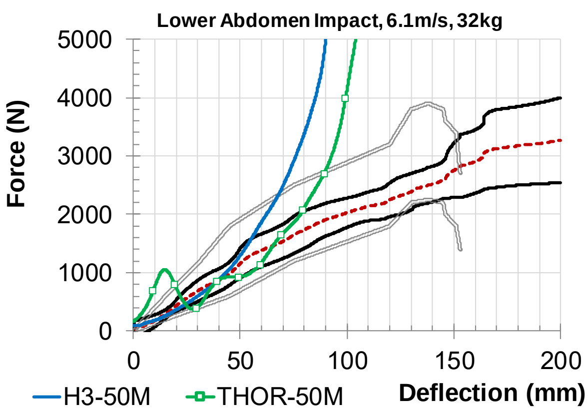

Figure 39. Lower abdomen rigid bar impact, force-deflection corridor calculated in deflection domain; reference corridor shown for comparison (GESAC, 2005a); cropped at 5 kN for visibility.

Abdomen belt loading. The response of the THOR-50M abdomen lies within the response corridor for the first 75 millimeters of penetration before the force exceeds the upper boundary of the corridor (Figure 40). In contrast, the H3-50M response exceeds the upper boundary of the corridor after only 37 millimeters of penetration. The BioRank results demonstrate excellent biofidelity for the THOR-50M and good biofidelity for the H3-50M.

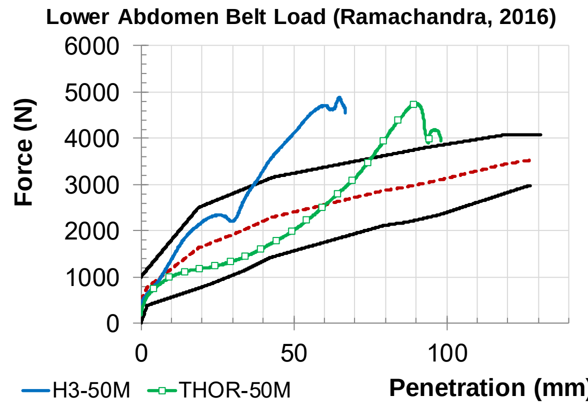

Figure 40. Response of belt loading to the abdomen compared to mean plus/minus one standard deviation corridor from Ramachandra et al. (2016).

Knee/Thigh/Hip

Table 18. BioRank Results: KTH

	THOR	H3
Femur Compression		
INT: Deflection	1.400	3.875
EXT: Force	1.897	2.917
EXT: Force-deflection corridor calculated at each point in time	0.583	11.913
EXT: Force-deflection corridor calculated at each point in deflection	1.059	21.963
TCBR: Internal	*1.400*	*3.875*
TCBR: External	*1.180*	*12.264*
Knee Shear		
EXT: Force-deflection corridor	2.282	1.070
TCBR: External	*2.282*	*1.070*
KTH BRBR: Internal	**1.400**	**3.875**
KTH BRBR External	**1.731**	**6.667**

Femur compression. The deflection of the H3-50M in the femur compression condition is much smaller than that of the THOR-50M (Figure 41), though the peak forces are comparable in magnitude (Figure 42). As a result, the H3-50M femur is much stiffer than the THOR-50M (Figure 43 and Figure 44). Based on the TCBR calculated as the average of the available measurements, the THOR-50M demonstrates good internal and external biofidelity. The H3-50M, on the other hand, demonstrates poor internal and external biofidelity. This finding is to be expected given that Rupp et al. (2003) showed that that the H3-50M was between 2.4 and 16 times stiffer than the upper boundary of the PMHS corridor.

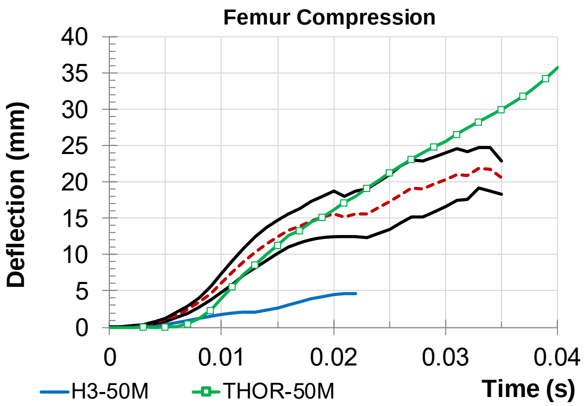

Figure 41. Femur compression input deflection time-history for THOR-50M and H3-50M tests, compared to input measured from PMHS tests.

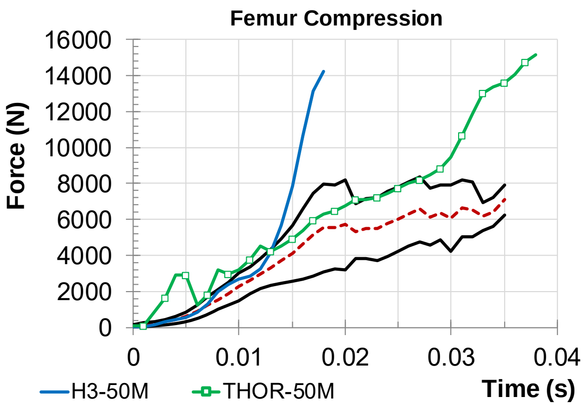

Figure 42. Femur compression force time-history for THOR-50M and H3-50M tests, compared to response measured from PMHS tests.

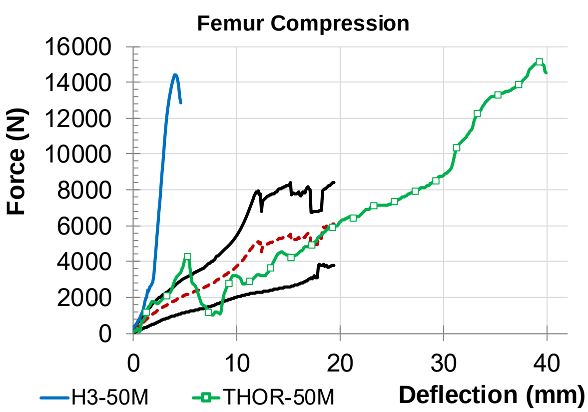

Figure 43. Femur compression composite force-deflection corridor.

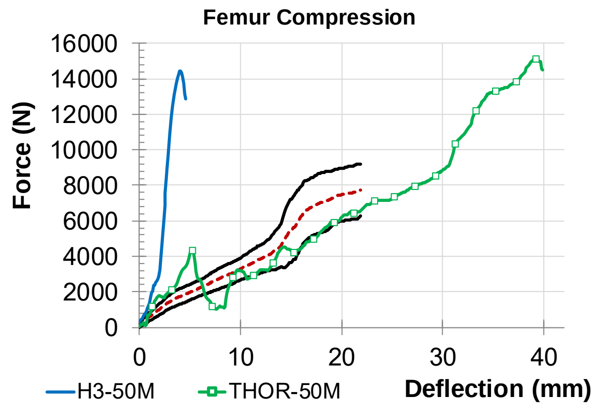

Figure 44. Femur compression force-deflection corridor calculated in the deflection domain.

Knee shear. Comparisons of the THOR-50M and H3-50M responses to the force-deflection response corridor shows that the response of the THOR-50M is initially less stiff than the corridor, but after about 15 millimeters of compression, the stiffness increases drastically above that of the PMHS corridor (Figure 45). The H3-50M is initially stiffer than the PMHS response and ends at a higher force than each corridor, but is on average closer to the corridor mean than the THOR-50M. The resulting BioRank values confirm this qualitative comparison. As there are no internal biofidelity measurements in this test condition, the TCBR consists of only external biofidelity. The THOR-50M demonstrates marginal external biofidelity, while the H3-50M demonstrates good external biofidelity.

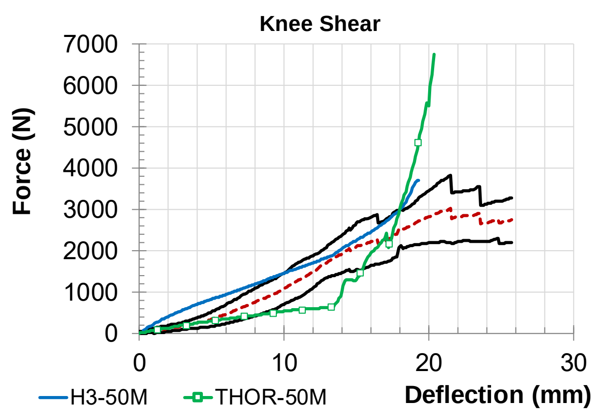

Figure 45. Knee shear response corridor calculated using all subjects from Balasubramanian et al. (2004).

Lower Extremity

Table 19. BioRank Results: Lower Extremity

	THOR	H3
Heel Impact		
EXT: Impact force (All)	0.720	0.923
INT: Tibia force (All)	0.655	0.681
EXT: Impact force (4.0±1.0m/s)	1.022	1.293
INT: Tibia force (4.0±1.0m/s)	1.622	0.983
TCBR: Internal	*1.139*	*0.832*
TCBR: External	*0.871*	*1.108*
Dorsiflexion		
INT: Ankle moment	0.675	N/A
INT: Ankle moment-rotation	0.747	N/A
TCBR: Internal	*0.711*	*N/A*
Tibia Axial Compression		
INT: Tibia force time-history (3.1m/s)	1.764	N/A
INT: Tibia force-displacement (3.1m/s)	0.864	N/A
INT: Tibia force time-history (5.3m/s)	1.768	N/A
INT: Tibia force-displacement (5.3m/s)	4.399	N/A
TCBR: Internal	*2.199*	*N/A*
LX BRBR: Internal	**1.349**	**0.832**
LX BRBR External	**0.871**	**1.108**

Heel impact. Qualitatively, the impact force in the foot only configuration demonstrates an earlier and higher force peak than both shoe configurations (Figure 46). The foot plus MIL-spec shoe and molded shoe configurations are similar in shape and phase, though foot plus MIL-spec shoe configuration shows a higher initial peak with a deeper subsequent valley, and a similar secondary peak. The added mass and effectively softer impact stiffness of the molded shoe results in a response that appears to be a filtered version of the foot only and foot plus MIL-spec shoe configurations.

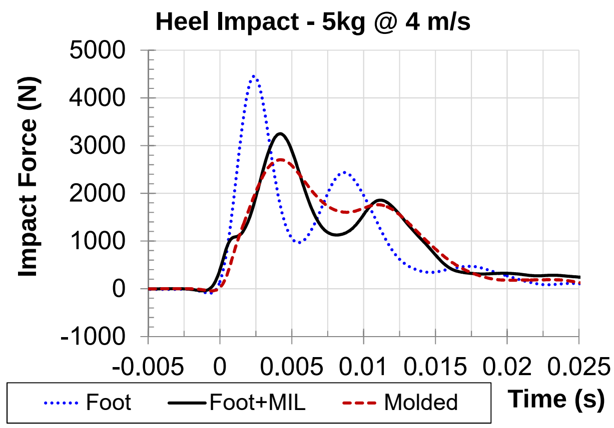

Figure 46. Impact force in the heel impact test condition, comparing foot alone, foot plus MIL-spec shoe, and molded shoe configurations.

While filtering of the response in the foot only configuration is surprisingly effective in predicting the molded shoe response, this approach is unfortunately not uniquely reversible. Instead, a simple scaling approach was implemented to predict the foot only response based on the molded shoe response (Equation 1); while not as mechanically meaningful, was found to provide a similar relationship between the predicted foot-only and the measured foot-only responses (Figure 47). The scaling coefficient for force was determined by comparing the average peak force from 6 foot-only tests (4686 N) with the average peak force from 12 molded shoe tests (2660 N), while the scaling coefficient for time was determined from visual inspection.

$$\boldsymbol{F_{foot,predicted}(t) = 1.76 \times F_{molded}(t)} \quad (1)$$

$$t_{foot,predicted} = 0.7 \times t_{molded} \quad (2)$$

where

$F_{foot,predicted}(t)$ = Predicted impact force time-history for a foot only configuration

$F_{molded}(t)$ = Measured impact force time-history for a molded shoe configuration

$t_{foot,predicted}$ = Predicted time for a foot only configuration

t_{molded} = Measured time for a molded shoe configuration

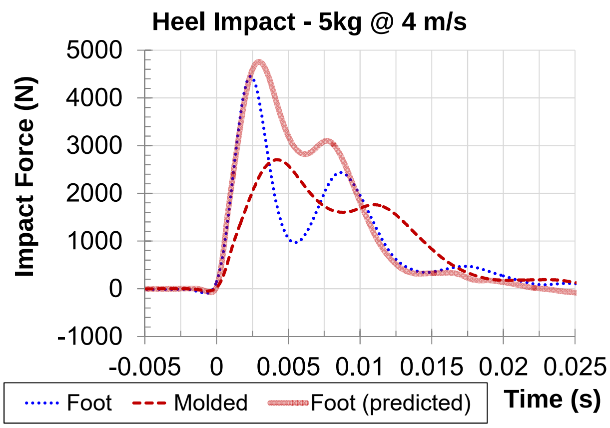

Figure 47. Impact force in the heel impact test condition, showing the prediction of foot response based on measured molded shoe response.

The lower tibia force in the foot only configuration demonstrates an earlier initial peak than the foot plus MIL-spec shoe and molded shoe configurations, though this peak is not the overall peak force (Figure 48). The overall peak tibia force occurs at roughly the same time for all three foot/shoe configurations, and the range of peak forces (417 N) is smaller than the draft qualification specifications (632 N) (NHTSA, 2016b), therefore the response difference is within the expected range of test-to-test variation. Thus, while a transfer function may be necessary to relate the impact force between foot/shoe configurations, any differences in impact force appear to be attenuated in the shoe and/or foot and not transferred to the tibia.

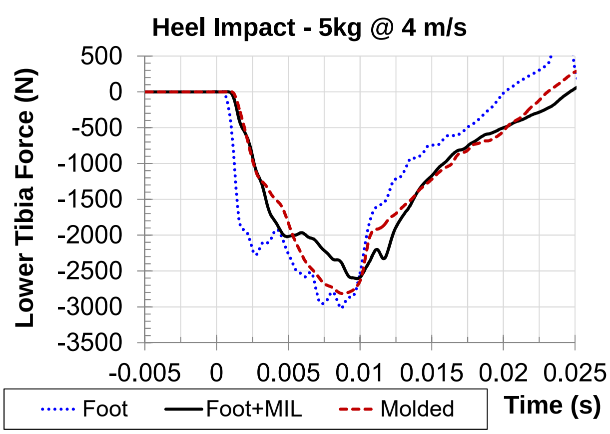

Figure 48. Tibia force in the heel impact test condition, comparing foot alone, foot plus MIL-spec shoe, and molded shoe configurations.

For the THOR-50M impact response comparisons (Figure 49, Figure 51), the measured force time-history in the molded shoe condition was corrected based on the transfer functions in Equations 1 and 2, while correction was not necessary for the H3-50M as a shoe was not installed for these tests. The tibia forces (Figure 50, Figure 52) were not corrected for either ATD.

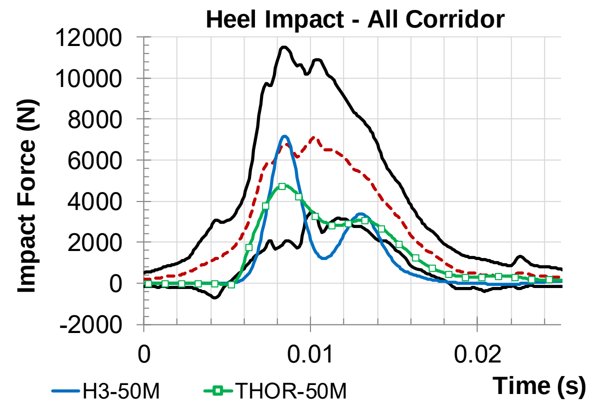

Figure 49. Impact force response for heel impact test condition compared to corridor created from all observations.

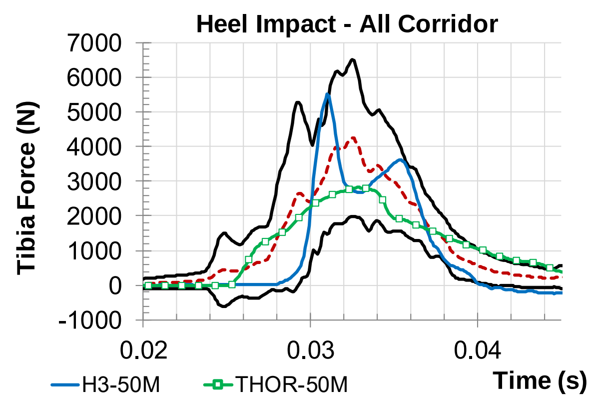

Figure 50. Tibia force response for heel impact test condition compared to corridor created from all observations.

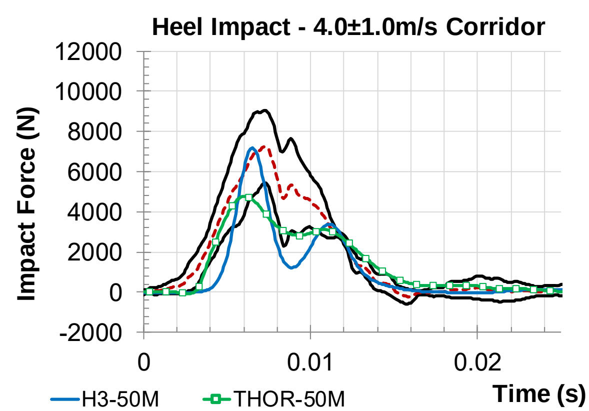

Figure 51. Impact force response for heel impact test condition compared to corridor created from PMHS tests at 4.0±1.0 m/s.

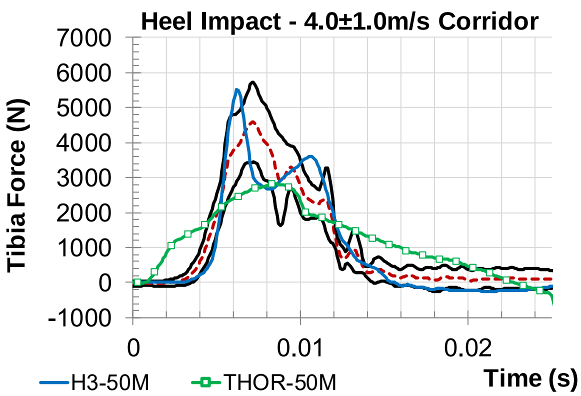

Figure 52. Tibia force response for heel impact test condition compared to corridor created from PMHS tests at 4.0±1.0 m/s

The resulting BioRank calculations are summarized in Table 19. The TCBR is calculated by averaging the results from both corridor comparisons. Based on the TCBR, the THOR-50M demonstrates good internal biofidelity and excellent external biofidelity, while the H3-50M demonstrates excellent internal biofidelity and good external biofidelity.

Dorsiflexion. Qualitatively, the impact force in the foot only configuration demonstrates an earlier and higher force peak than both shoe configurations (Figure 53), though not as pronounced a difference as in the heel impact condition. When presented with respect to the ankle dorsiflexion angle, the ankle moments of all three configurations follow a similar slope, though the foot only configuration results in a larger moment and angle (Figure 54). As the foot plus MIL-spec shoe and the molded shoe configurations show a similar phase, shape, and magnitude, they appear to dissipate impact energy in a similar fashion. Based on this relationship, a scaling methodology is proposed to relate the measured molded shoe response to a predicted foot-only response (Equations 3, 4, and 5). When applied to both the ankle moment time-history (Figure 55) and ankle moment-rotation characteristic (Figure 56), the predicted foot-only response shows good agreement with the measured foot-only response.

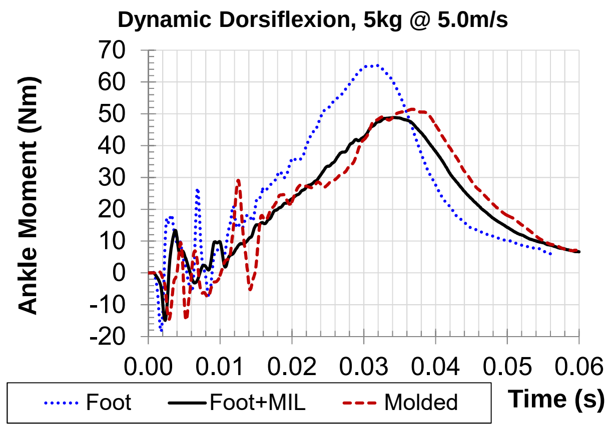

Figure 53. Ankle moment in the dynamic dorsiflexion test condition, comparing foot alone, foot plus MIL-spec shoe, and molded shoe configurations.

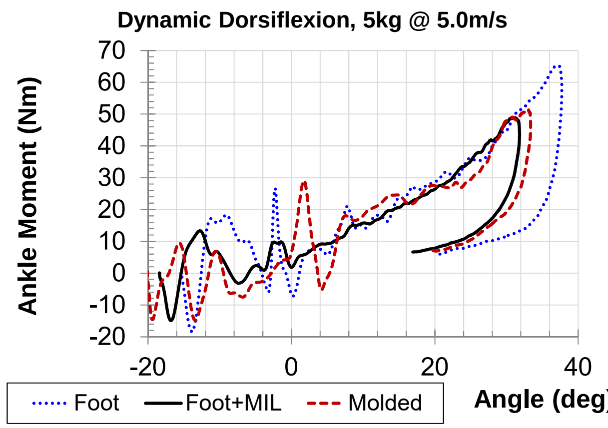

Figure 54. Ankle moment vs. ankle rotation angle in the dynamic dorsiflexion test condition, comparing foot alone, foot plus MIL-spec shoe, and molded shoe configurations.

$$\boldsymbol{M_{foot,predicted}(t) = 1.25 \times M_{molded}(t)} \tag{3}$$

$$\boldsymbol{\theta_{foot,predicted}(t) = 1.15 \times \theta_{molded}(t)} \tag{4}$$

$$t_{foot,predicted} = 0.85 \times t_{molded} \tag{5}$$

where

$M_{foot,predicted}(t)$	=	Predicted ankle moment time-history for a foot only configuration
$M_{molded}(t)$	=	Measured ankle moment time-history for a molded shoe configuration
$\theta_{foot,predicted}(t)$	=	Predicted ankle dorsiflexion angle time-history for a foot only configuration
$\theta_{molded}(t)$	=	Measured ankle dorsiflexion angle time-history for a molded shoe configuration
$t_{foot,predicted}$	=	Predicted time for a foot only configuration
t_{molded}	=	Measured time for a molded shoe configuration

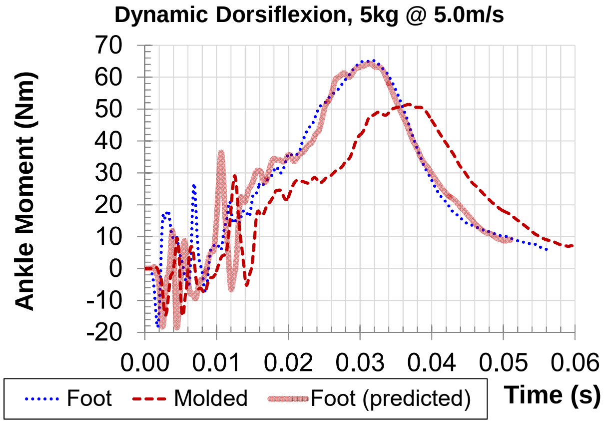

Figure 55. Ankle moment time-history in the dynamic dorsiflexion test condition, showing the prediction of foot response based on measured molded shoe response.

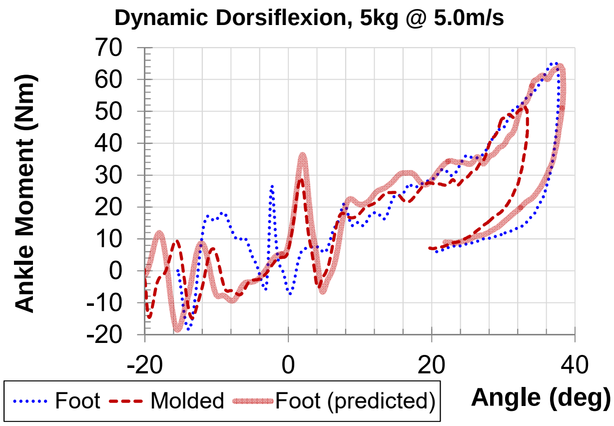

Figure 56. Ankle moment vs. ankle rotation angle in the dynamic dorsiflexion test condition, showing the prediction of foot response based on measured molded shoe response.

Using the predicted foot-only response based on the measured response in the molded shoe configuration and the relationship presented in Equations 3, 4, and 5, the THOR-50M shows good agreement with the response corridors for ankle moment time-history (Figure 57) and ankle moment-rotation characteristic (Figure 58). The resulting BioRank calculations are summarized in Table 19. There are no external biofidelity metrics in the dorsiflexion condition, thus the TCBR consists of only the internal biofidelity assessment and is calculated as the average of the two available corridor comparisons. Based on the TCBR, the THOR-50M demonstrates excellent internal biofidelity based on the foot response predicted from the molded shoe response. For reference, the foot-only response would similarly demonstrate an excellent internal biofidelity rating.

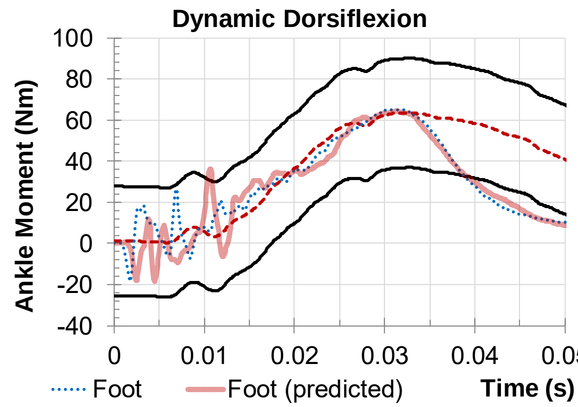

Figure 57. Ankle moment time-history in the dynamic dorsiflexion test condition, showing both predicted foot response based on measured molded shoe response and measured foot-only response.

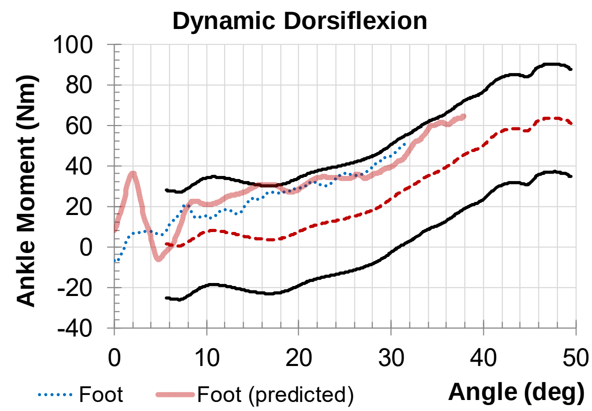

Figure 58. Ankle moment vs. ankle rotation angle in the dynamic dorsiflexion test condition, showing both predicted foot response based on measured molded shoe response and measured foot-only response.

Tibia axial compression. Comparing the 3.1 m/s and 5.3 m/s loading rates, the difference in velocity is evident in the tibia force time-history response (Figure 59) but the tibia force vs. footplate displacement characteristic (Figure 60) is largely insensitive to impact velocity over the loading portion of the force-displacement corridor. At larger deflections, the deformable bushing in the THOR-50M tibia bottoms out and the forces do increase beyond the corridor. The resulting BioRank calculations are summarized in Table 19. As there are no external biofidelity measurements in this test condition, the TCBR consists of only internal biofidelity, and is calculated from an average of the molded shoe tests at 3.1 m/s and 5.3 m/s. Based on the TCBR, the THOR-50M demonstrates good internal biofidelity in this test condition. For reference, the biofidelity in this condition in the MIL-spec shoe configuration would be nearly identical.

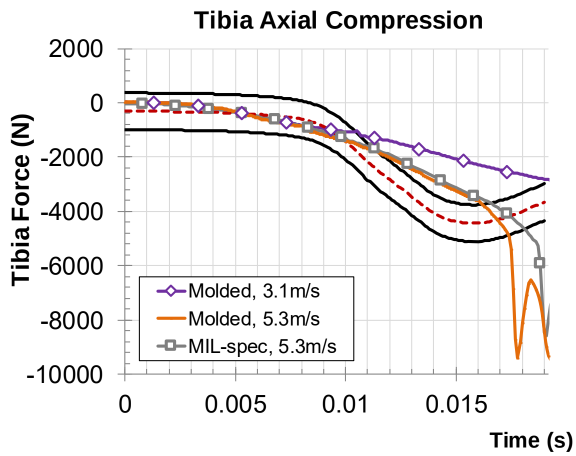

Figure 59. Tibia force time-history corridor for tibia axial compression test condition.

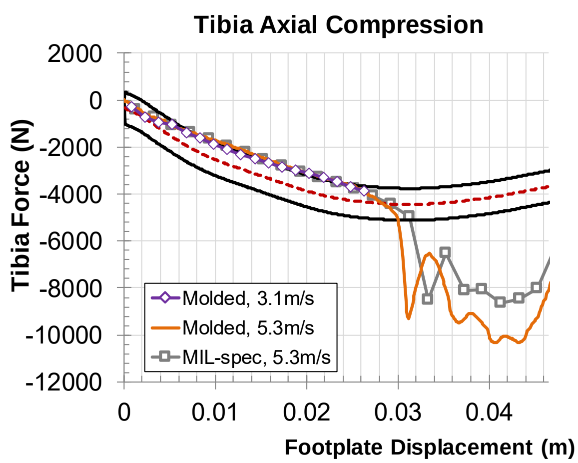

Figure 60. Tibia force vs. footplate displacement corridor for tibia axial compression test condition.

Whole Body

A summary of the individual measurements, TCBR scores, and BRBR scores for the whole body sled test conditions is shown in Table 20.

Gold Standard 1. Based on the TCBR calculation (Table 20), the H3-50M internal and external biofidelity scores are slightly better than those of the THOR-50M, though both the THOR-50M and H3-50M demonstrate good biofidelity. The THOR-50M demonstrates excellent biofidelity in several key areas relevant to injury prediction: head X-axis displacement (Figure 61), which is an indicator of head contact to vehicle interior structures; head resultant acceleration (Figure 62), used to calculate the head injury criterion (HIC); head Y-axis angular velocity (Figure 63), the key component of the brain injury criterion (BrIC) in a frontal crash; and upper left chest deflection (Figure 64), the quadrant of peak chest deflection in the PMHS tests. For the same measurements, the H3-50M, shows good, good, good, and excellent biofidelity respectively.

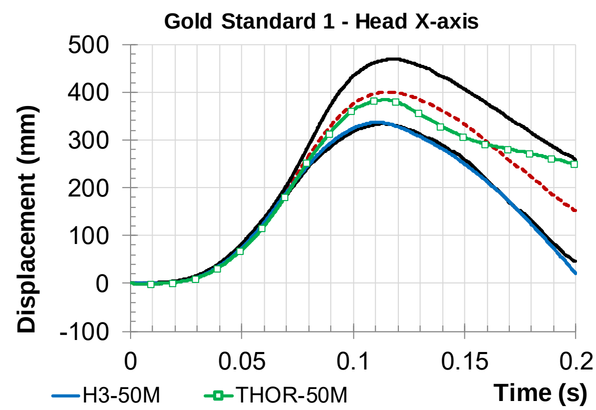

Figure 61. Head X-axis displacement time-history in the GS1 whole-body test condition.

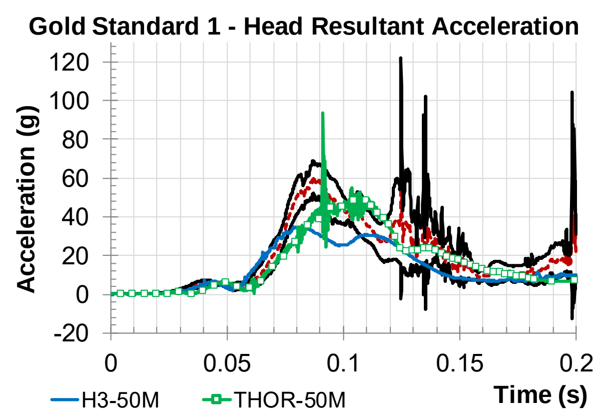

Figure 62. Head resultant acceleration time-history in the GS1 whole-body test condition.

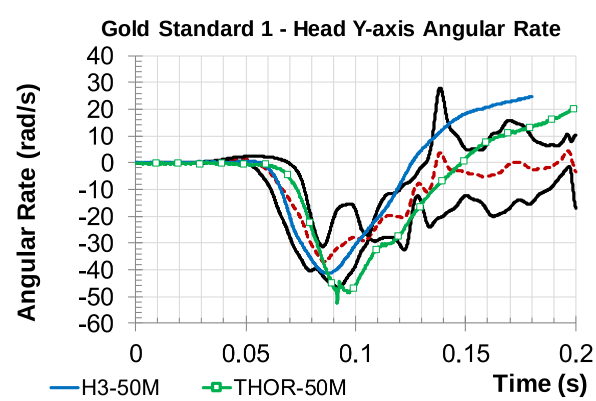

Figure 63. Head Y-axis angular velocity time-history in the GS1 whole-body test condition.

Table 20. BioRank results for the Whole Body test conditions.

	BioRank ($\sqrt{R}$)	Gold Standard 1		Gold Standard 2		Gold Standard 3		Far Side Oblique	
	ATD	THOR	H3	THOR	H3	THOR	H3	THOR	H3
INT/EXT	TSTNO	b11472	b11485	b11475	b11484	b11517	b11513	b11506	b11499
Ext	Head X-axis displacement	0.502	1.055	1.813	3.191	3.861	1.936	2.937	0.763
Ext	Head Y-axis displacement	3.446	2.467	1.415	0.399	3.858	2.571	0.679	1.167
Ext	Head Z-axis displacement	1.241	1.596	3.746	1.272	1.018	2.435	1.529	1.531
Ext	T1 X-axis displacement	0.947	2.319	0.500	1.599	0.845	2.154	0.800	1.420
Ext	T1 Y-axis displacement	2.439	0.978	0.708	1.121	2.613	1.169	1.834	3.294
Ext	T1 Z-axis displacement	2.105	1.224	3.118	1.495	1.050	2.163	0.388	1.038
	TSTNO (if different)	b11119		b11122					*b11498
Int	Head resultant acceleration	0.883	1.082	0.575	0.780	2.325	2.401	1.083	
Int	Head X-axis angular velocity	2.500	1.406	1.939	0.898	0.922	1.146	1.884	2.104
Int	Head Y-axis angular velocity	0.966	1.238	0.904	1.446	1.748	2.785	1.226	1.432
Int	Head Z-axis angular velocity	1.315	1.771	0.708	0.883	3.636	3.817	0.983	1.024
Ext	Upper shoulder belt	1.344	0.985	2.102	1.659	3.272	1.943	0.966	1.160*
Ext	Lower shoulder belt	2.764	1.261	3.556	2.556	5.066	5.965	1.183	1.071*
Int	Upper left chest deflection	0.524	0.969	1.084	1.449	0.649	1.385		
Int	Upper right chest deflection	0.784	0.563	1.295	1.386	1.451	1.058		
Int	Lower left chest deflection	1.126	0.752	2.015	1.688	1.021	0.678		
Int	Lower right chest deflection	2.575	2.793	3.284	3.390	2.522	2.522		
	TCBR: Internal	*1.334*	*1.322*	*1.476*	*1.490*	*1.784*	*1.974*	*1.294*	*1.520*
	TCBR: External	*1.849*	*1.486*	*2.120*	*1.662*	*2.698*	*2.542*	*1.290*	*1.431*

	THOR	**H3**
Whole Body BRBR: Internal	**1.472**	**1.576**
Whole Body BRBR External	**1.989**	**1.780**

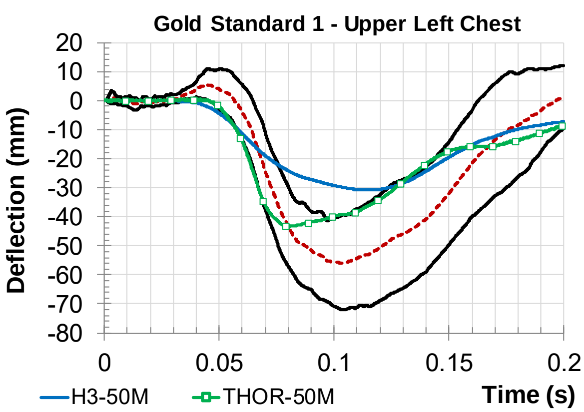

Figure 64. Upper left chest deflection time-history in the GS1 whole-body test condition.

Gold Standard 2. Based on the TCBR calculation (Table 20), the THOR-50M internal biofidelity score is slightly better than that of the H3-50M, but the H3-50M external biofidelity score and classification (good) is better than that of the THOR-50M (marginal). Areas where the H3-50M demonstrates categorically-improved external biofidelity than THOR-50M are the head Y- and Z-axis displacement, T1 Z-axis displacement, head X-axis angular velocity (Figure 65), upper and lower shoulder belt forces (Figure 66 and Figure 67), and lower left chest deflection (Figure 68). On the other hand, the THOR-50M shows categorically better biofidelity than the H3-50M include head X-axis displacement, T1 X- and Y-axis displacement, and head Y-axis angular velocity (Figure 69).

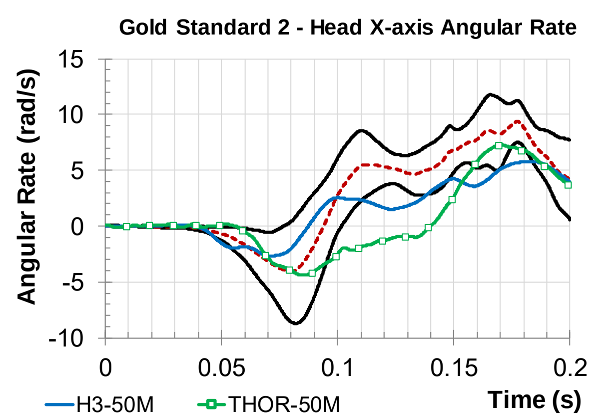

Figure 65. Head X-axis angular velocity time-history in the GS2 whole-body test condition.

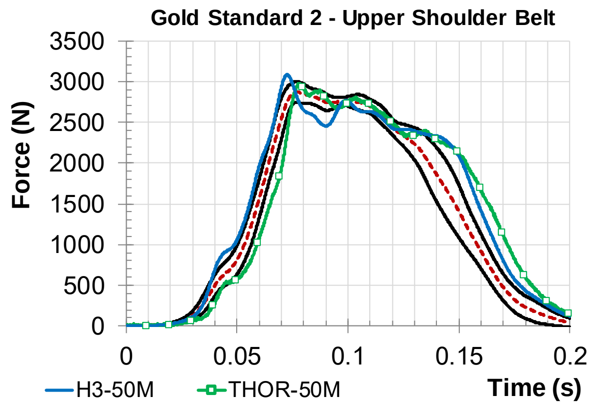

Figure 66. Upper shoulder belt force time-history in the GS2 whole-body test condition.

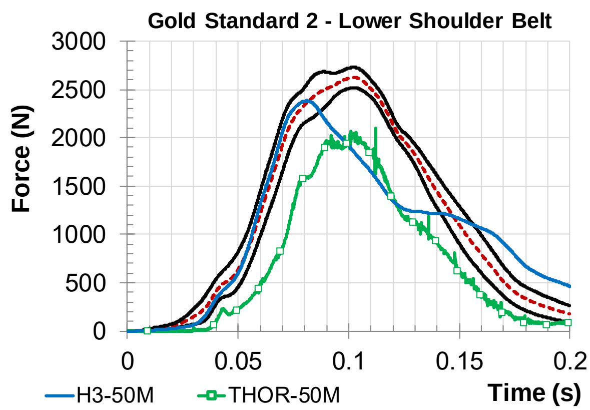

Figure 67. Lower shoulder belt force time-history in the GS2 whole-body test condition.

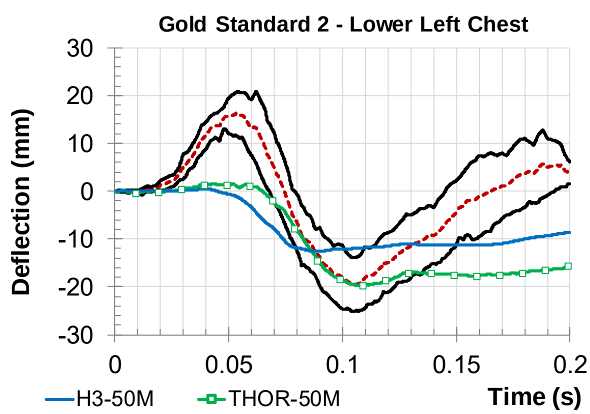

Figure 68. Lower left chest deflection in the GS2 whole-body test condition.

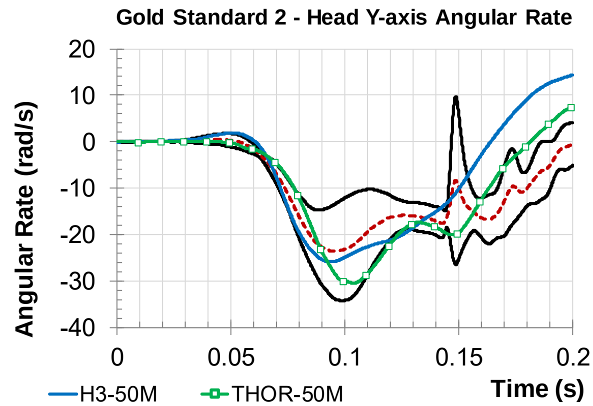

Figure 69. Head Y-axis angular velocity in the GS2 whole-body test condition.

Gold Standard 3. Both ATDs demonstrated good internal biofidelity and marginal external biofidelity (Table 20), with the THOR-50M registering slightly better internal and slightly worse external biofidelity. The highest BioRank score for both ATDs was the comparison to the lower shoulder belt force time-history (Figure 71). This corridor is noticeably narrow compared to the other biofidelity corridors in this test mode, which may result from the load-limited nature of the upper shoulder belt. The narrow corridor results in a smaller denominator in the BioRank calculation, which in turn amplifies any differences between the ATD and PMHS responses. Despite the high BioRank score, the peak lower shoulder belt load measured for the THOR-50M falls within the peak PMHS corridor.

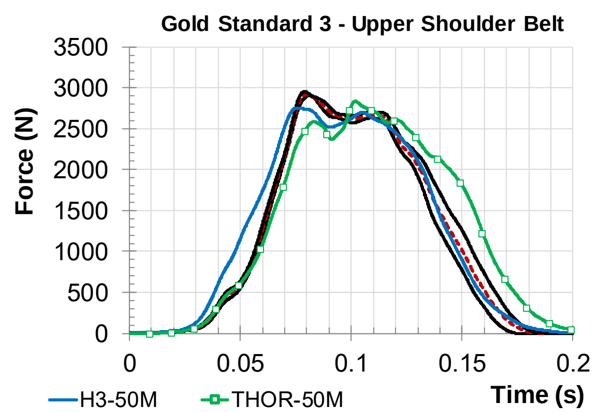

Figure 70. Upper shoulder belt force time-history in the GS3 whole-body test condition.

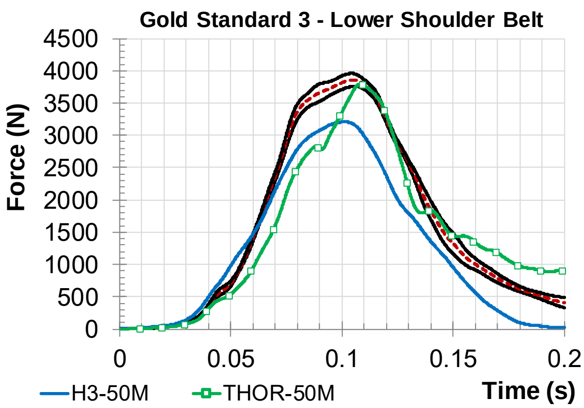

Figure 71. Lower shoulder belt force time-history in the GS3 whole-body test condition.

There are a few noteworthy findings in the GS3 condition as it relates to injury prediction. First, both ATDs show poor biofidelity with respect to head Z-axis angular velocity. In the PMHS tests, the head naturally rotates about the local Z-axis as it pitches forward about the global Y-axis, perhaps due to the lack of resistance to Z-axis rotation at low magnitudes of torsion (see neck torsion condition). The ATDs do not exhibit this motion, resulting in a large difference in angular rate between the ATDs and the PMHS corridor (Figure 74). The X- and Y-axis angular rates of the THOR-50M, however, are more similar to the PMHS corridors (Figure 72 and Figure 73) both qualitatively and quantitatively, with BioRank scores demonstrating excellent and good biofidelity, respectively, compared to the good and marginal ratings of the H3-50M. A caveat to this finding is that the head response in this condition represents completely free motion, which is unlikely to occur in a frontal and oblique crash in a vehicle with good air bag coverage.

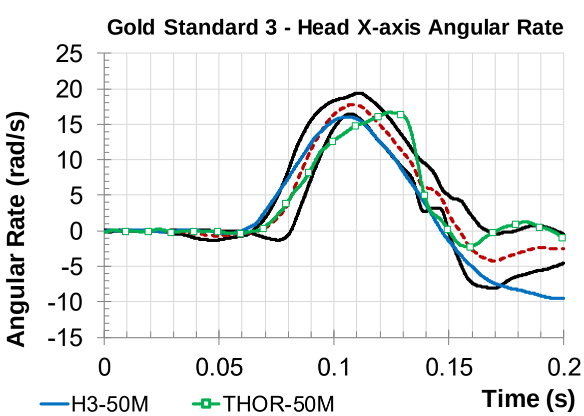

Figure 72. Head X-axis angular velocity in the GS3 whole-body test condition.

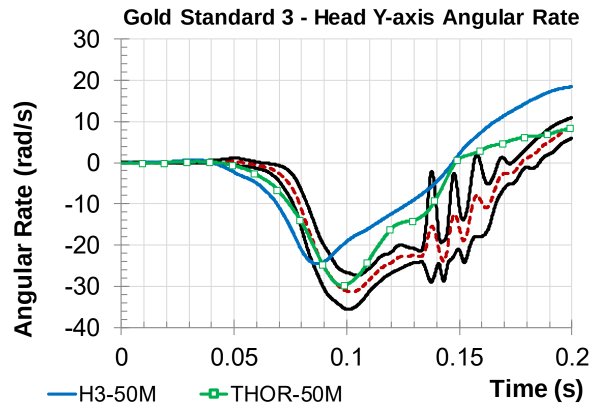

Figure 73. Head Y-axis angular velocity in the GS3 whole-body test condition.

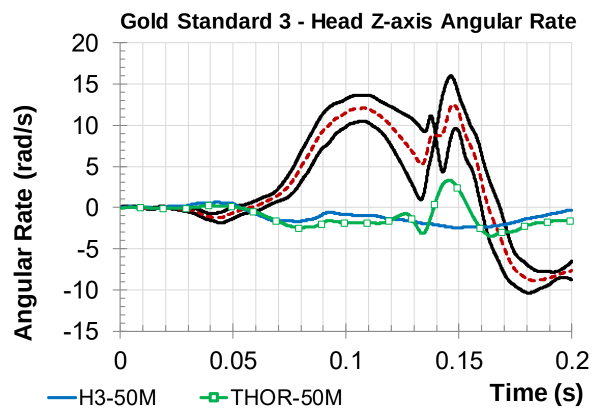

Figure 74. Head Z-axis angular velocity in the GS3 whole-body test condition.

Far Side Oblique. The internal and external TCBR subtotals for the tests of various posture and belt positions in the FSO condition for the THOR-50M all resulted in good biofidelity. As expected based on the similarity of the posture and belt position to the PMHS tests, Position C demonstrates the best internal and external biofidelity. Position C also results in the most PMHS-like interaction with the front passenger air bag, as evidenced by the good (X-axis, Figure 75; Y-axis, Figure 76) and excellent (Z-axis, Figure 77) head angular velocity BioRank scores. The THOR-50M demonstrates good internal and external biofidelity based on BioRank scores of 1.294 and 1.290, respectively, while the H3-50M demonstrates good internal and external biofidelity but with a slightly higher TCBR scores of 1.520 and 1.431, respectively.

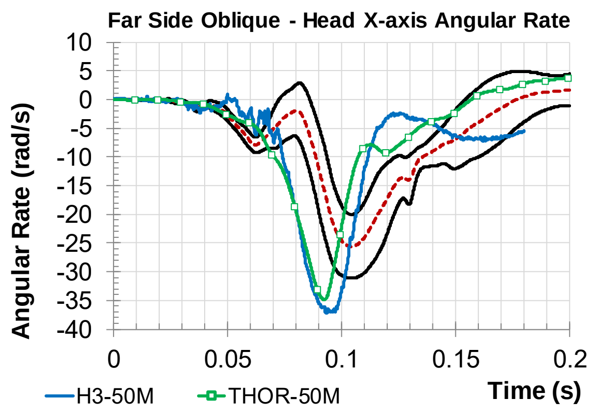

Figure 75. Head X-axis angular velocity in the FSO whole-body test condition.

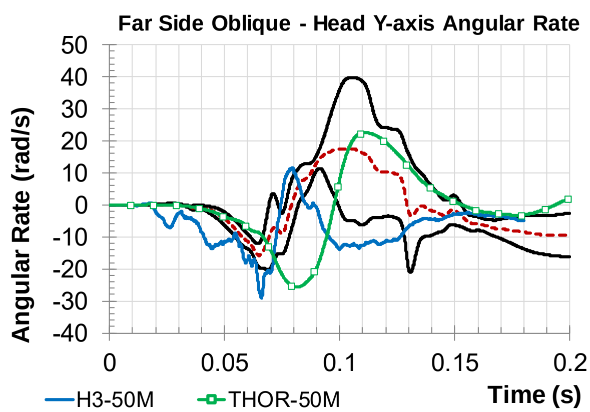

Figure 76. Head Y-axis angular velocity in the FSO whole-body test condition.

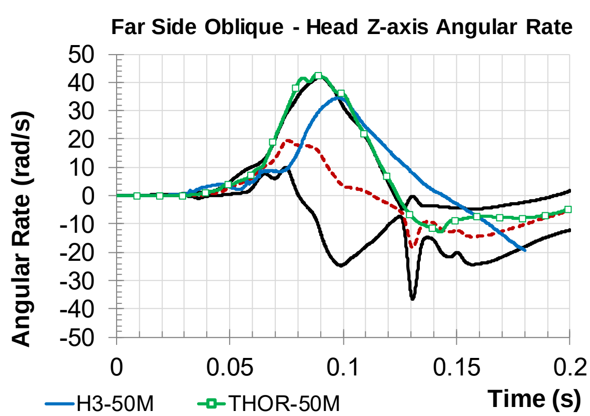

Figure 77. Head Z-axis angular velocity in the FSO whole-body test condition.

Summary

The internal and external TCBR scores from each test condition and for each ATD are summarized in Table 21. Blank cells indicate conditions where either there were no metrics associated with internal or external biofidelity, or the ATD was not instrumented to record the given metric.

In 7 of the 12 test conditions where internal biofidelity TCBR scores were available for both ATDs, the THOR-50M score was lower than that of the H3-50M. Of the 14 available internal biofidelity scores for the THOR-50M, 4 were classified as excellent and 8 were classified as good. The tibia axial compression response was classified as marginal, as the THOR-50M tibia compressive element bottoms out after roughly 30 millimeters of footplate displacement. During the first 30 millimeters of footplate displacement, however, the THOR-50M response would achieve an excellent classification. The neck frontal flexion condition, was classified as marginal. In this test condition, there was only one internal biofidelity metric: head resultant acceleration. In the volunteer tests used to develop the biofidelity corridors, the sled pulse was applied to the entire body of the restrained subjects. The ATD tests were a simplification of this test that applied the same sled pulse to the isolated head/neck assembly, since the more detailed acceleration measured at T1 of the volunteers could not be replicated on the sled. While the sled pulse is effectively a filtered version of the T1 pulse (see Figure 9) thus provides a similar global input to the head/neck, the local acceleration pulse measured at the head CG of the ATDs would not be expected to follow the same detailed acceleration measured in the volunteer tests.

Of the 12 available internal biofidelity measurements available for the H3-50M, 4 were classified as excellent, 4 were good, 3 were marginal, and 1 was poor. There were 5 test conditions which showed better internal biofidelity for the H3-50M than the THOR-50M: isolated head drop, lower thorax oblique, upper abdomen steering rim, heel impact, and Gold Standard 1. In all but the heel impact test, the THOR-50M biofidelity classification was the same as the H3-50M.

Table 21. Test Condition BioRank (TCBR) Summary

Body Region	Test Condition	Corridor Approach (See Methods)	THOR-50M INT	THOR-50M EXT	H3-50M INT	H3-50M EXT
Head	Isolated Head Drop	D	0.155		0.013	
	Whole-body Head Impact	D		0.261		0.004
	Face Rigid Bar	A		2.355		13.169
	Face Rigid Disk	A		0.815		6.746
Neck	Neck Frontal Flexion	A	2.155	2.191	2.185	5.947
	Neck Lateral Flexion	A		1.163		2.689
	Neck Torsion	A		3.027*		
Thorax	Sternal Impact	C	0.815	0.732	2.506	2.347
	Lower Ribcage Oblique	B	1.019	1.163	0.700	1.792
Abdomen	Upper Abdomen Steering Rim	B	0.968	1.165	0.552	0.610
	Lower Abdomen Rigid Bar	B	1.972	6.304	2.705	8.272
	Abdomen Belt Loading	A		0.938		1.541
KTH	Femur Compression	B	1.400	1.180	3.875	12.264
	Knee Shear	B		2.282		1.070
Lower Extremity	Dynamic Heel Impact	B	1.139	0.871	0.832	1.108
	Tibia Axial Compression	A	2.199			
	Dynamic Dorsiflexion	A	0.711			
Whole-body	Gold Standard 1	B	1.334	1.849	1.322	1.486
	Gold Standard 2	B	1.476	2.120	1.490	1.662
	Gold Standard 3	B	1.784	2.698	1.974	2.542
	Far Side Oblique	B	1.294	1.290	1.520	1.431

** Not included in BRBR since corridor does not represent mean plus/minus one standard deviation*

In 11 of the 17 test conditions where external biofidelity TCBR scores were available, the THOR-50M score was lower than that of the H3-50M. Of the 17 available external biofidelity scores for the THOR-50M, 5 were classified as excellent, 6 good, 5 marginal, and 1 poor. In the lower abdomen rigid bar impact, the THOR-50M followed the biofidelity force-deflection corridor up to roughly 80 millimeters of deflection before a steep increase in stiffness. The H3-50M showed a similar increase in stiffness but at a lower magnitude of deflection, resulting in a higher TCBR in this test condition. The results of the lower abdomen rigid bar test for the THOR-50M may have been influenced by the selection of loading location, where the point of loading was intended to engage the anterior attachment point of the IR-TRACC sensors as a priority over the loading location specified in the biofidelity test.

For each body region, the internal and external TCBR scores were averaged to determine the BRBR (Table 22), which were then averaged to develop overall internal and external BioRank scores for each ATD. Overall, the THOR-50M demonstrates good internal and external biofidelity. The THOR-50M exhibits excellent head and thorax internal biofidelity, good abdomen, KTH, and lower extremity internal biofidelity, and marginal neck internal biofidelity. The marginal internal biofidelity of the neck is based on a single measurement of head resultant acceleration discussed above. The external biofidelity of the THOR-50M is classified as excellent for the thorax and lower extremity, good for the head, neck, and KTH, and marginal for the abdomen. In response to whole-body sled test conditions, the THOR-50M demonstrates good biofidelity for both internal and external assessments. Compared to the H3-50M, the THOR-50M shows lower internal biofidelity scores in 5 of the 7 body regions and lower external biofidelity scores in 6 of the 7 body regions, and the overall internal and external biofidelity scores for the THOR-50M are lower than those of the H3-50M.

Table 22. Body Region BioRank (BRBR) Summary.

Body Region	THOR-50M INT	THOR-50M EXT	H3-50M INT	H3-50M EXT
Head	0.155	1.143	0.013	6.640
Neck	2.155	1.677	2.185	4.318
Thorax	0.917	0.948	1.603	2.070
Abdomen	1.470	2.803	1.629	3.474
KTH	1.400	1.731	3.875	6.667
Lower Extremity	1.349	0.871	0.832	1.108
Whole-body	1.472	1.989	1.576	1.780
OVERALL	1.274	1.594	1.673	3.722

DISCUSSION

Overall, the THOR-50M and H3-50M both demonstrated categorically good internal biofidelity, though the THOR-50M BioRank score was 24% lower (better) than the H3-50M. The intent of the internal biofidelity evaluation is to assess the ability of the ATD itself, not the test apparatus, to collect measurements that are useful in prediction of response and injury criteria in a test condition that is not as well instrumented, such as the interior of a vehicle. One caveat to this analysis is that the internal biofidelity quantification was sometimes calculated using differential acceleration or an externally-installed chestband device to enable comparison to the associated biofidelity corridor. If the internal biofidelity evaluation were limited to the instrumentation installed on the ATD, the H3-50M would be at a disadvantage in the thorax and abdomen test conditions, since the only deflection instrumentation available to the H3-50M is the sternum potentiometer measurement of anterior-posterior deflection. The THOR-50M, on the other hand, is capable of recording ribcage deformation in the anterior-posterior, lateral, and vertical directions at four locations on the rib cage and two location on the lower abdomen.

Considering external biofidelity, the THOR-50M demonstrated good biofidelity, compared to the poor biofidelity of the H3-50M. Since a majority of the test conditions included involved pure frontal loading, and several involved oblique and lateral loading such as the neck lateral flexion, neck torsion, lower thorax oblique, Gold Standard 3, and Far Side Oblique test conditions, these findings are expected to extend to frontal and frontal oblique crash test conditions. The findings may not, however, extend to other loading conditions, such as pure lateral or rear impacts, without further research.

ATD Version Equivalence

Since many of the biomechanical response requirements involve specialized instrumentation or test equipment, these tests are not intended to be carried out as certification or qualification tests conducted between crash tests or sets of crash tests to confirm that specified ATD response requirements are met. Due to their relative complexity and instrumentation requirements, biomechanical response requirements are enacted at a design level and typically evaluated on a limited number of samples to confirm that the design requirements are met by the physical ATDs. Except where the biofidelity tests are identical to the qualification tests in some instances, the biofidelity tests are not always conducted on each ATD produced or used in vehicle crash testing. Instead, simplified and standardized versions of these requirements, configured to use internal instrumentation where possible, have been developed as qualification procedures (NHTSA, 2016a). Because the qualification specifications are based on the expected variation in response of the ATD, not the underlying human response, the qualification requirements specify a much smaller allowable range in response than the biomechanical response requirements. Therefore, it is expected that all THOR units that meet the specifications of the qualification procedures would demonstrate similar biofidelity.

Where possible, an attempt was made to conduct biofidelity assessment testing of the ATDs in identical test configurations to those used to develop the PMHS response corridors. As this was not always possible due to contractual, financial, and ATD availability limitations, some compromises had to be made. In several test conditions, testing was completed on an earlier version of the THOR and was not able to be repeated on the THOR-50M hardware. Generally, it is assumed that the earlier version of the THOR is equivalent to the current version, as defined by the August 2016 drawing package (NHTSA, 2016a) and August 2016 qualification specifications (NHTSA, 2016b) since there were no specific changes expected to influence the response of the given body region.

In some cases, equivalence can be demonstrated by comparing the response of the same ATD in a similar qualification procedure. One example of this is the head drop test, which was conducted with a Mod Kit version of the THOR. As there were no changes to the head between the Mod Kit design and the THOR-50M August 2016 design, the response of the Mod Kit THOR is used to represent the THOR-50M here. This representation is substantiated by the fact that the specific THOR hardware tested in the head drop condition was also used for the whole-body head impact condition, which resulted in a peak force of 5,504 N. This response is within the peak force specification of 5,498 N to 5,660 N defined in the THOR-50M Qualification Procedures Manual (NHTSA, 2016b). Since the qualification specifications are a narrower corridor within the biofidelity corridor, the response of a THOR that meets the THOR-50M qualification specifications would result in an equivalent biofidelity assessment. Therefore, the biofidelity assessment of both the head drop test and the whole-body head impact are expected to be equivalent for the Mod Kit and THOR-50M designs, as both test conditions focus on the compression of the head skin in the forehead region.

In other cases, qualification procedures do not exist or are sufficiently different that the performance in the biofidelity test is not directly transferrable. For example, there is no longer an upper abdomen steering wheel impact condition in the THOR-50M qualification procedures (NHTSA, 2016b), thus version equivalence cannot be demonstrated using qualification data. Also, the lower abdomen qualification procedure is conducted at a lower speed and with a different impactor. This limitation was minimized where possible by conducting tests on the same THOR-50M used to develop the qualification specifications. Thus, it is assumed that if the THOR in question meets the qualification specification for a given body region, it would also provide an equivalent biofidelity assessment.

Version equivalence is even more difficult to quantify in the whole-body sled test conditions, where the overall response is a function of the performance of multiple body regions and deformable elements. While some deformable elements of the ATD that may contribute to the response do have performance requirements specified by the qualification procedures (e.g. neck flexion), others are specified by drawing specifications alone (e.g. lumbar spine flex joint). Therefore, while it is assumed that the response of the Mod Kit design and the THOR-50M August 2016 design are equivalent, it is not possible to directly compare these responses. Specifically, since motion tracking data was not used in the Gold Standard 1 and 2 whole-body sled test conditions, it is a known limitation that the version used to assess motion tracking data may not provide the same result as the THOR-50M August 2016 design. To minimize the influence of this limitation, the Mod Kit THOR was only used for the kinematic measurements in these two test conditions, while a THOR believed to meet the August 2016 design and qualification requirements was used for the kinetics.

Similarly, a THOR Mod Kit ATD was used in the FSO whole-body test condition as a surrogate for the THOR-50M. While there were no significant changes between the THOR Mod Kit and THOR-50M thorax designs or performance requirements aside from the inclusion of the SD-3 shoulder assembly, Parent et al. (2013) demonstrated a difference in biofidelity in the blunt thoracic impact condition between the THOR Mod Kit, referred therein as the "THOR Mod Kit w/SD-3" and the THOR-50M, referred to therein as the "THOR Metric w/SD-3." The THOR Mod Kit showed a higher force and a different shape of the force-deflection characteristic compared to the THOR-50M, with BioRank scores demonstrating excellent biofidelity for the THOR-50M and good biofidelity for the THOR Mod Kit. As an approximation of the THOR-50M thoracic response in the FSO test condition, the THOR Mod Kit ATD may provide a conservative estimate of biofidelity as it has been shown to underestimate the biofidelity of the thorax. However, this is expected to be secondary effect, as thoracic biofidelity is not directly assessed in the FSO condition.

Calculation Methodology

For the purposes of this analysis, historical PMHS response corridors were not recreated unless doing so was required to create a corridor appropriate for calculation of BioRank which is electronically reproducible and known to represent the mean response plus/minus one standard deviation. Where corridors were recreated based on individual subject responses, the intent was to reproduce the previously-published PMHS response corridors to minimize the need for additional out-of-scope analysis and documentation. This approach also remains true to most of the original biomechanical response design requirements of the THOR design (GESAC, 2005a). A limitation of this approach is that alternate methods of corridor development through scaling and/or subject normalization, such those of Irwin and Mertz (2002) or Moorhouse (2013), could indeed result in PMHS response corridors of different magnitudes and widths, which in turn could in different BioRank values.

To investigate the implications of this limitation, an investigation was carried out using one test condition, upper abdomen steering wheel impact. The THOR biomechanical response requirement was developed to envelope the individual force-deflection responses published by Nusholtz and Kaiker (1994). In recreating this corridor in a format appropriate for BioRank, the individual responses were mass-scaled and averaged at each point in the resulting deflection. The resulting force-deflection corridor calculated in the deflection domain (*Mass-scaled* in Figure 78) shows a similar magnitude and width as the reference corridor. Two additional corridors were created: *Velocity-scaled*, using the velocity ratio methodology presented Irwin and Mertz (2002), and *Eff Mass & Eff Stiff*, using the effective mass and effective stiffness normalization strategy proposed by Moorhouse (2013). All three corridors follow a similar slope as the reference corridor (Figure 78), though the *Velocity-scaled* and *Eff Mass & Eff Stiff* corridors are noticeably narrower.

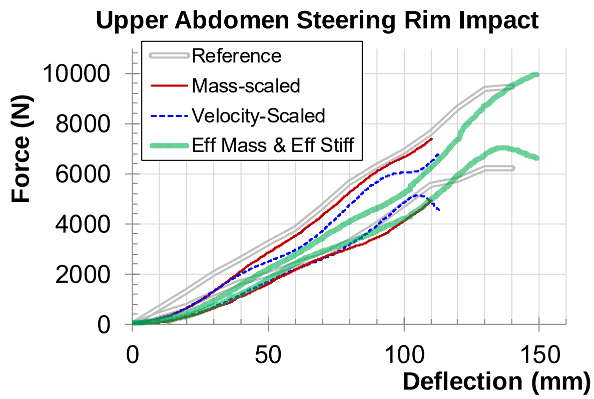

Figure 78. Comparison of upper abdomen steering rim impact response corridors calculated using different scaling methodologies.

The BioRank calculations were carried out for each corridor creation strategy and compared to the results presented earlier for the *Mass-scaled* method (Table 23). Using the *Mass-scaled* approach, the internal biofidelity of the THOR-50M and H3-50M were both categorized as excellent, compared to good and marginal for the *Velocity-scaled* approach and good and excellent for the *Eff Mass & Eff Stiff* approach. The *Mass-scaled* and *Eff Mass & Eff Stiff* approaches were the most similar, differing by only 0.128 and 0.182 for the THOR-50M and H3-50M respectively. Per Rhule et al. (2009), differences in √R less than or equal to 0.2 are not significant, and the biofidelity is essentially the same. All three methods resulted in the same external biofidelity categorization for the THOR-50M and H3-50M: good and excellent, respectively. This example demonstrates that different approaches can be taken to develop PMHS response corridors without any appreciable change in the end result. Therefore, the additional time and effort necessary to develop new PMHS corridors based on more involved strategies does not appear to be warranted for the sake of this analysis.

More generally, previous publications (e.g. Lebarbé et al., 2015a and 2015b) have presented PMHS response corridors calculated using plus/minus the average standard deviation across the entirety of the independent parameter, either time or deflection/rotation. While such an approach may be useful for response target generation for the design of future ATDs, averaging the standard deviation across an entire time-history masks the fact that subject-to-subject variation is often smaller during initial or well-controlled portions of a response, such as chest deflection during the ride-down portion of a sled test before peak belt load, and larger during certain intervals of the time-history, such as chest deflection at the time of peak belt load.

Table 23. Comparison of BioRank results for different corridor creation strategies in the upper abdomen steering rim impact condition

	Mass-scaled		Velocity-scaled		Eff Mass & Eff Stiff	
	THOR	H3	THOR	H3	THOR	H3
INT: Deflection	0.968	0.552	1.842	2.377	1.096	0.734
EXT: Force	2.185	0.881	3.476	1.432	2.108	0.963
EXT: Force-deflection corridor calculated at each point in time	0.563	0.433	1.374	0.858	1.337	0.812
EXT: Force-deflection corridor calculated at each point in deflection	0.748	0.515	0.885	0.444	0.542	0.361
TCBR: Internal	*0.968*	*0.552*	*1.842*	*2.377*	*1.096*	*0.734*
TCBR: External	*1.165*	*0.610*	*1.912*	*0.911*	*1.329*	*0.712*

One perceived side-effect of not averaging standard deviations is that force-deflection or moment-rotation corridors can have discontinuities where an individual subject has reached peak deflection or rotation, thus the next increment of deflection includes one less observation over which to calculate the standard deviation. An example of this can be seen in Figure 45, where there are discontinuities in both the mean and plus/minus one standard deviation responses at deflections of roughly 16, 22, and 24 millimeters. While these discontinuities may be visually unappealing, the BioRank calculation can continue unhindered up to the last point in time (or other independent parameter) for which there exists a mean and corridor boundary.

Test Condition Limitations

Throughout this study, THOR-50M and H3-50M were presented in test conditions intended to be the same as the test conditions used in the original PMHS tests used to develop the associated response corridors. There were several limitations preventing the identical test conditions from being recreated, some general and some specific to certain test modes. One such general limitation is that the ATDs do not have representations of some of the anthropometric landmarks used to position test apparatus in the PMHS tests, thus the test apparatus or loading surfaces cannot be confirmed to be placed in identical locations. Another general limitation is that while ATDs are intended to represent live humans in a motor vehicle crash environment, many of the response corridors were developed from testing of PMHS which lack active musculature. In some test conditions, such as sternal impact, the influence of active musculature has been shown to have a minimal influence on the response to dynamic loading (Kent et al., 2006). In conditions where active musculature has been shown to influence the response, this limitation is minimized by using volunteer data instead of PMHS data to develop corridors for the evaluation of ATD response.

Neck Flexion. In the neck frontal and lateral flexion conditions, a simplification was made in the execution of the ATD tests. Instead of recreating the volunteer sled tests using the complete ATDs, the head/neck system was isolated and the sled pulse was input at the base of the neck. While this may result in the application of an acceleration pulse different than the measured T1 pulse corridor from the volunteer tests, this simplification is expected to have a negligible influence on head kinematics.

To examine this further, simulations were conducted using a finite element model representation of the THOR using either the sled pulse or the T1 pulse input to the base of the neck. While the peak head resultant acceleration was 11% different between the two inputs, the remaining outputs were at most 5.8% different, all slightly greater in magnitude for the T1 pulse input (head angle: 1.8%; x-axis displacement: 2.3%; z-axis displacement: 5.8%; total neck section moment: 3.4%). These differences were assumed to be negligible relative to the difference in response between the THOR-50M and the H3-50M. Moreover, Wismans and Spenny (1983) stated that, at least in the lateral flexion test condition, the large variability in T1 accelerations did not significantly affect the head-neck kinematics. In both the frontal and lateral neck flexion tests, the input sled acceleration is actually closer to the volunteer acceleration corridor than the input sled pulse corridor using BioRank. Therefore, it is assumed that application of the sled pulse to the base of the ATD neck is appropriate for the purposes of evaluating head-neck kinematics. An additional limitation to this simplification is that the initial spine, neck, and head angles of the ATDs cannot be compared directly to the human volunteers in an identical seat configuration. Future work could be done to validate this assumption by running complete ATDs in the same seat and restraint conditions as the NBDL volunteers.

Neck Torsion. While not included in the calculation of BioRank because the corridor was not developed using the mean plus/minus one standard deviation method, the neck torsion condition would have resulted in a poor external biofidelity classification for both ATDs. Though the THOR-50M demonstrated a similar moment-rotation slope to the biofidelity corridor, it lacked the low-resistance toe region of the human response. The H3-50M demonstrated an even stiffer response than the THOR-50M, but since the peak moment occurred at a rotation angle lower than the beginning of the biofidelity corridor, it could not be quantified. Qualitatively, however, the neck of the THOR-50M demonstrates a much more biofidelic response than that of the H3-50M in torsion, as seen in Figure 23.

Of the test conditions included in this study, the neck flexion and torsion conditions are the most likely to be influenced by active musculature. In the neck frontal flexion condition, volunteers pre-tensed their muscles (Thunnissen et al., 1995). The response of the THOR-50M shows similar x-axis motion (Figure 11) but more z-axis motion (Figure 12) and head rotation (Figure 13) than the volunteer response corridor. Therefore, the THOR-50M neck response can be considered more relaxed than a pre-tensed human volunteer in frontal flexion. In the neck lateral flexion condition, the THOR-50M neck response shows similar head z-axis motion (Figure 20), but slightly more y-axis motion (Figure 19) and head rotation (Figure 21), suggesting a slightly more relaxed neck response than the pre-tensed human volunteers in lateral flexion. In the neck torsion condition, the THOR-50M shows resistance to motion earlier than the pre-tensed volunteers, suggesting a more tensed muscle state. Such a tradeoff may be necessary for a repeatable and reproducible test device, as a head with minimal initial resistance to rotation would be difficult to consistently position in a motor vehicle crash test. In contrast to the THOR-50M, the H3-50M exhibits a much higher neck stiffness than the pre-tensed volunteer corridors in all three neck test conditions, which leads to its poor external biofidelity classification.

Abdomen Belt Loading. In the abdomen belt loading tests conducted by Ramachandra et al. (2016), three of the seven subjects were tested twice. For two of these subjects, a previous test was conducted before the Condition A test. This previous test, intended to investigate the influence of pressurization on the force-penetration response, used the same accumulator pressure but did not perfuse the abdominal vessels. The authors suggest that pressurization of the vasculature in the second test resulted in increased abdominal penetration, though it is possible that the increase in penetration simply resulted from repeated loading. While it would be possible to develop a force-deflection response corridor by excluding these two subjects due to this uncertainty, doing so would be unlikely to change the corridor enough to result in a different assessment of H3-50M or THOR-50M biofidelity and thus was not investigated in this effort.

An additional limitation in the abdomen belt loading condition relates to belt positioning in the ATD tests.

In the PMHS tests, the belt was positioned at the level of the umbilicus. Since neither ATD portrays the anatomical location of the umbilicus, an identical test condition could not be confirmed. Instead, the belt was positioned in a location most likely to result in a successful test execution. For the H3-50M, the belt was positioned near the center of the abdomen insert, along the top edge of the pelvis flesh. It is not clear how this position compares to the anatomical location of the umbilicus. For the THOR-50M, this location was at the vertical level of the anterior attachment point of the abdomen IR-TRACCs. Cross-referencing the THOR-50M drawing package with the anthropometry of motor vehicle occupants (AMVO) landmarks presented by Robbins (1983), the IR-TRACC attachment points are approximately 29 millimeters inferior to the anatomical location of the umbilicus, which in turn puts the bottom edge of the belt less than 10 millimeters above the superior surface of the anterior-superior iliac spine (ASIS) load cell. The ASIS, in turn, is roughly 100 millimeters posterior of the anterior surface of the abdomen. If the ASIS did influence the force-penetration response of the THOR, it would have been close to point of peak penetration. Unfortunately, different belt locations were not evaluated, and the ASIS load cell data was not recorded during the THOR tests. Thus, conclusions cannot be drawn regarding the influence of belt location on the abdomen force-deflection response for either ATD.

Lower Extremity. In two of the lower extremity test modes, heel impact and dorsiflexion, the ATD tests were carried out using a different test configuration than the PMHS tests. Ideally, the exact test procedure would be replicated, but doing so was not possible in this case. Instead, the ATD qualification test data was compared to the PMHS response corridor. In the qualification test, a 5 kilogram pendulum impacts the heel at 4.0 meters per second with the tibia fixed. In contrast, the PMHS test condition used a 24 kilogram mass to impact the heel at between 2.2 and 7.6 meters per second with the tibia attached to a translating mini-sled ballasted to 16 kilograms. While the impactor mass in the ATD tests is lower than that of the biofidelity condition, the attachment of the proximal tibia to the mini-sled in the biofidelity condition results in a lower effective mass. As a compromise, an effort was made to evaluate the ATD test condition against a subset of the PMHS tests conducted at similar impact velocities. This difference between the ATD test condition and the biofidelity condition is nonetheless a known limitation to this comparison.

In the dorsiflexion condition, the tibia was fixed in both the PMHS tests and the ATD tests. However, the precise input to the PMHS tests is not clear aside from the fact that it was driven by a pneumatic impactor, and that the peak pedal velocity is known for each subject. While an attempt was made to compare THOR-50M tests within the range of peak pedal velocities in the PMHS tests, it is uncertain how the input energy of a pendulum impact with an initial velocity of 5.0 meters per second compares to an average pedal velocity of 5.6 meters per second in the Rudd et al. (2004) test fixture. This uncertainty would influence the moment time-history comparison more than the moment-rotation comparison, as a larger or smaller input energy could change the magnitude of moment or rotation, but would not be expected to result in appreciable changes in the shape of the moment-rotation response.

In the tibia axial compression condition, the ATD tests were conducted with less input energy than the PMHS, as the ATD tests used a lighter ballistic mass and a lower impact velocity than the PMHS tests. While Kim et al. (2017) note that the impact velocity was chosen based on Funk et al. (2002), they also confirm that the test condition was not identical. The influence of impact velocity can be seen in the magnitude of force and/or deflection, as seen in the deflection time-history comparison between the THOR-50M tests at 3.1 m/s and 5.3 m/s in Figure 59, though the difference in the shape of the force-displacement response is negligible. A later set of tests presented by Funk et al. (2002) simulated muscle tension through application of a pretension force to the Achilles tendon. These tests are not presented herein since Achilles tendon pretension, while possible in the THOR-50M lower leg, was not applied in the associated ATD tests.

In both the dorsiflexion and tibia axial compression conditions, data for the H3-50M were not available. The excellent biofidelity of the THOR-50M in the dorsiflexion test condition may in part result from the cable-spring mechanism represents the Achilles tendon load path. Since the H3-50M does not include such a mechanism, it is unlikely to exhibit better biofidelity than the THOR-50M. In the tibia axial compression test condition, the tibia compressive element of the THOR-50M acts to dissipate energy in response to axial impact. While this element was effective in the 3.1 m/s condition, it appears to have bottomed out in the 5.3 m/s condition (Kim et al., 2017). Since the H3-50M does not include a compressive element in the tibia, the response in the tibia axial compression condition is unlikely to exhibit better biofidelity than the THOR-50M at either impact velocity.

Whole Body. While the ATD tests were conducted using the same test apparatus as the PMHS tests, there are some limitations to the comparison of ATD response to PMHS corridors. First, the Gold Standard PMHS tests were intended primarily to assess thoracic response to shoulder belt loading; while kinematics of the spine and head were measured, the response did not necessarily represent the expected kinematics of an occupant in a frontal crash due to the lower body restraint necessary to isolate and measure the torso response.

Second, the Gold Standard tests did not include frontal airbags, thus the free-motion head kinematics were measured as opposed to forced-motion kinematics induced by an airbag. As such, the utility of the comparison of ATD head kinematics to PMHS corridors is limited to free-motion kinematics, with the caveat that specimen preparation did not consider the condition of the brain, which may have deteriorated by the time the tests were conducted and subsequently influenced the moment of inertia of the head. In the Gold Standard 3 condition, both ATDs show poor biofidelity with respect to head Z-axis angular velocity. In the PMHS tests, the head naturally rotates about the local Z-axis as it pitches forward about the global Y-axis, perhaps due to the lack of resistance to Z-axis rotation at low magnitudes of torsion (see Results: Neck Torsion). ATDs do not exhibit this motion, resulting in a large difference in angular rate between the ATDs and the PMHS corridor. The X- and Y-axis angular rates of the THOR-50M, however, are more similar to the PMHS corridors both qualitatively and quantitatively, with BioRank scores demonstrating excellent and good biofidelity, respectively, compared to the good and marginal ratings of the H3-50M. A caveat to this finding is that the head response in this condition represents completely free motion, which is unlikely to occur in a frontal and oblique crash in a vehicle with adequate airbag coverage. The occupant environment in the Far Side Oblique condition, on the other hand, provides for a more meaningful comparison of head kinematics in vehicles with frontal airbags. In this condition, the kinematics of the head are forced through interaction with the frontal airbag, resulting in primarily Z-axis rotation. In the FSO condition, the THOR-50M demonstrates good, good, and excellent internal biofidelity with respect to X-, Y-, and Z-axis angular rates, while the H3-50M shows marginal, good, and good internal biofidelity respectively. This finding suggests that the THOR-50M would be a more biofidelic evaluation tool to assess the risk of brain injury, for which head angular velocity has been shown as a correlate (Takhounts et al., 2013), in an oblique crash test mode.

Third, the chest deflection measurements differed between the PMHS and ATDs. In the PMHS tests, chest deflection was recorded using an optoelectronic stereophotogrammetric system (OSS) to track motion of points on the anterior rib cage and the spine, which were used to calculate skeletal deflection. In contrast, the THOR-50M tests used the internal IR-TRACC instrumentation, which measures deflection relative to the local spine segment, and the H3-50M tests used a string potentiometer array in the chest, which measured deflection relative to the spinebox. While these measurements are all intended to capture the same physical quantities, differences in instrumentation mounting locations, measurement error, and spine topology prevent an identical comparison.

BioRank Effectiveness

Overall, BioRank appears to be a useful tool in evaluating biofidelity, as it removes subjectivity from the assessment. However, it is not devoid of subjectivity, as there are still components of study design that can bias the assessment, such as the selection of test conditions, the selection of measurements in each test condition, and the association of BioRank values into defined classifications (excellent, good, marginal, and poor). This study erred on the side of inclusion; the evaluation included any test conditions, and measurements therein, for which BioRank-appropriate PMHS response corridors were available or could be created and for which THOR-50M test results were available. A limitation of this approach is that in test conditions or body regions where there are many available corridors for comparison, each individual measurement may have a negligible effect on the TCBR or BRBR. The alternative would be to select only measurements of interest, though such measurements of interest would depend on the application. The selection of BioRank classification nomenclature in this study was intended to simplify narrative ATD comparisons; perhaps a future study could compare the BioRank evaluation to expert opinions as was done for similar objective rating techniques (Davis et al. 2017).

There are some instances where the BioRank results are counterintuitive. One example occurs in the GS1 whole-body test condition in the evaluation of head Z-axis angular velocity (Figure 79). BioRank results for both the THOR-50M and H3-50M are both categorized as good, though neither accurately represents the rise and fall of the angular velocity between 50 and 100 milliseconds which occurs in the PMHS tests. If the BioRank calculation were carried out to 100 milliseconds instead of the full 200 milliseconds of the corridor, the THOR-50M would be classified as marginal (2.084) and the H3-50M as poor (3.409). Both responses are improved by the portion of the response after 100 milliseconds during the rebound phase. Such subdivisions were not made in this study as they would require numerous assumptions to be made throughout, which could in turn bias the results away from the intended application.

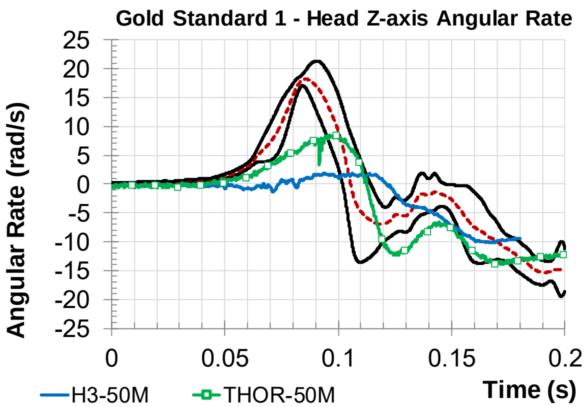

Figure 79. Head Z-axis angular velocity in the GS1 whole-body test condition.

In this study, the BioRank results were intentionally not weighted, as doing so would introduce subjective bias. In conditions such as the whole body sled test conditions, including a large number of test measurements can mask the importance of meaningful comparisons. For example, in the Gold Standard 3 condition, while the external biofidelity with regard to upper and lower shoulder belt loading is poor for the THOR-50M, the chest response the upper left chest (Figure 80), the point of peak deflection, demonstrates excellent biofidelity. As noted earlier, the poor external biofidelity could result from the exceedingly narrow nature of the belt load biofidelity corridors, despite the peak upper and lower shoulder belt loads measured by the THOR-50M being similar to those of the biofidelity corridor mean (Figure 70 and Figure 71). Since the proposed chest injury criterion for THOR used in the Oblique crash test mode (Saunders et al. 2015) considers the peak overall deflection measured at any quadrant, the excellent biofidelity of the THOR-50M at the location of peak overall deflection gives credence to its injury risk prediction ability in oblique thoracic belt loading conditions.

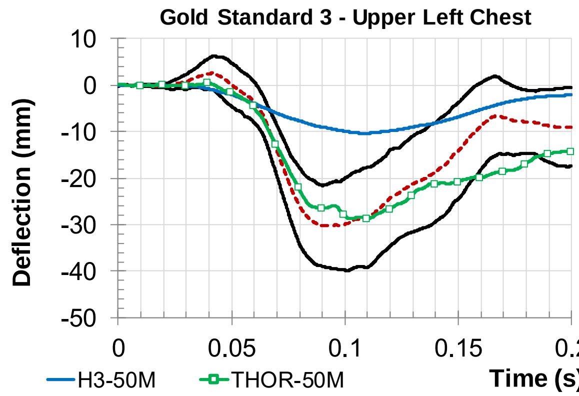

Figure 80. Upper left chest deflection in the GS3 whole-body test condition.

In this analysis, phase optimization was generally not implemented, aside from a few isolated conditions described above. There were two reasons for this. First, most of the biofidelity test conditions were well-controlled for time, either using contact triggers for impactor tests or applied acceleration time-histories for sled tests. Temporal shifting or scaling of the ATD response to align with the PMHS corridors would remove physically-meaningful information from the comparison. For application in restraint system development, an ATD design that does not accurately represent both the magnitude and timing of the biofidelity corridor could result in a sub-optimal restraint system design. Additionally, in several test conditions, phase optimization can result in unintended consequences. For example, in the face rigid bar impact condition, the corridor is defined by a rise time and a peak. Applying phase optimization would align the THOR-50M response in time nearly identical to that of the peak alignment strategy employed above. Phase optimization of the H3-50M response, on the other hand, shifts the peak beyond the corridor as to not be included in the calculation, thus artefactually improving the BioRank classification from marginal to good (Figure 81).

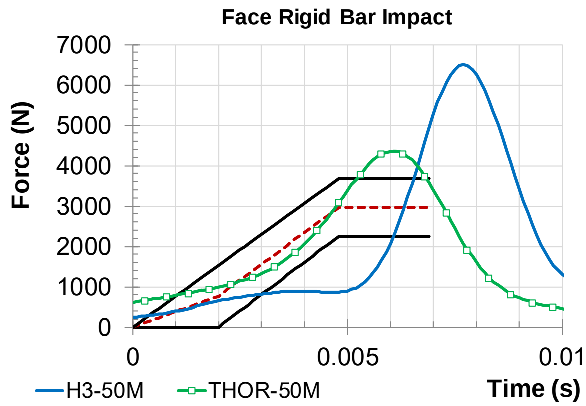

Figure 81. Force time-history in the face rigid bar impact condition, optimized to minimize BioRank.

As applied to compare the THOR-50M and H3-50M, there is an additional limitation to this worth noting. The selection of test conditions resulted in some instances where individual measurements or test conditions were not available for both the THOR-50M and H3-50M. As a result, the TCBR, BRBR, or overall BioRank values are not all based on the same number of measurements for both ATDs. In the present study, this occurred in the tibia axial compression and dorsiflexion test conditions, where H3-50M data were not available, and the FSO condition, where the head resultant acceleration data was not available for the H3-50M. An alternative approach to this analysis could be to eliminate any test conditions or measurements if the data were not available for both ATDs. If such an analysis were carried out, the THOR-50M BRBRs for the lower extremity and whole-body would be slightly higher and slightly lower, respectively, but the overall BioRank values would be identical.

One area where BioRank could be useful in the future is in the definition of design requirements. As an example, the THOR-50M knee slider was redesigned during the Mod Kit project to improve agreement with response force at 5 millimeters of deflection (Ridella and Parent, 2011). The design requirements provided to the manufacturer included two primary requirements, force at 5 and 17.8 millimeters, while the 10.2 millimeter requirement from the H3-50M was relegated to a secondary requirement. While the manufacturer successfully met the force requirement at 5 and 17.8 millimeters of deflection, this came at the expense of the 10.2 millimeter requirement. As a result, the redesigned knee slider does not dissipate enough energy early in the event, which causes the bottoming out effect evidenced by the high peak force late in the event (Figure 45). The BioRank classification of the THOR-50M knee response is marginal, compared to the good classification of the H3-50M. In hindsight, if BioRank were instead used as the design requirement, the manufacturer could have been required to achieve a specified BioRank (for instance, 1.0) to ensure that the biofidelity corridor was met for the entire force-deflection characteristic instead of just two points.

The BioRank biofidelity assessment method was selected for this study based on its previous use in the literature to quantitatively evaluate biofidelity (Rhule et al., 2009). There are other alternatives to quantify biofidelity, which were considered but not applied in this study. One alternative is the International Standards Organization (ISO) Biofidelity Classification System, though as noted by Rhule at al. (2005) contains many subjective features, including weighting of test conditions and body regions, which may introduce subjective bias. Another alternative is CORA – correlation and analysis (Gehre et al., 2009), which may be a useful tool to carry out quantitative analysis; however, the vast array of tunable parameters in the software can result in unintentional subjectivity and poor reproducibility. Further, there are no known and accepted relationships between CORA scores and biofidelity classifications.

Qualitative Biofidelity

Additional qualitative biofidelity findings can be drawn from this study. One such qualitative evaluation is the ability of the ATDs to represent the shoulder belt interaction with the torso of the PMHS in the oblique kinematics of the FSO condition. Shoulder belt slip, defined here as the inboard border of the shoulder belt moving outboard of the outboard border of the acromion, occurred in two out of the three PMHS tests. In tests b11500 and b11502, belt slip occurred at 144 milliseconds and 116 milliseconds after impact, respectively. In both cases, belt slip occurred after the time of peak head X-axis excursion. For the THOR-50M, all three postures and belt positions resulted in belt slip to varying degrees (Table 24). Belt slip also occurred in the THOR during the OMDB crash test (v09123) using the same vehicle represented by the sled test environment. For the H3-50M, belt slip did not occur. The shoulder belt interaction observed using the THOR-50M that was most visually similar to the PMHS occurred in the Position C configuration, where the belt slip occurred later in the event than in Position A or Position B.

Table 24. Belt slip characteristics in Far Side Oblique condition.

Subject	PMHS	PMHS	PMHS	THOR-50M
TSTNO	b11500	b11501	b11502	v09123
Image of Belt Slip	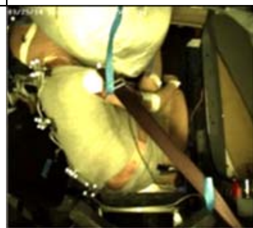	 No belt slip occurred. Peak head excursion @ 126ms	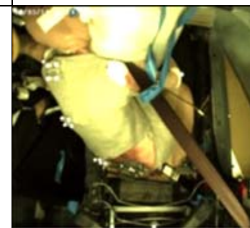	
Time of Belt Slip	144 ms	N/A	116 ms	80 ms
Subject	THOR-50M	THOR-50M	THOR-50M	H3-50M
Posture, Belt Postion	Position A	Position B	Position C	Position A
TSTNO	b11504	b11505	b11506	b11499
Image of Belt Slip			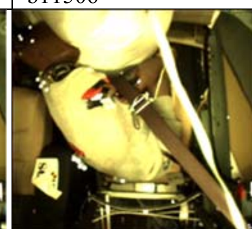	 No belt slip occurred. Peak head excursion @ 130ms
Time of Belt Slip	80 ms	120 ms	138 ms	N/A

CONCLUSION

The THOR-50M demonstrates overall internal and external BioRank scores of below 2.0, indicating good biofidelity. Both internal and external BioRank scores are lower than those of the H3-50M. The results highlight the excellent internal and external biofidelity of the THOR-50M thorax, compared to the good (internal) and marginal (external) biofidelity of the H3-50M. At the body region level, the internal and external BioRank scores for THOR-50M are all below 2.0 except for neck internal biofidelity and abdomen external biofidelity, which are marginal. For these body regions, the THOR-50M BioRank score indicates the quantitatively better biofidelity and the same or better categorical biofidelity compared to the H3-50M.

ACKNOWLEDGMENTS

Views expressed are those of the authors and do not represent the views of NHTSA. We gratefully acknowledge the Transportation Research Center staff at the Vehicle Research and Test Center for their support, and our many colleagues, referenced herein or not, for their contributions to the field of impact biomechanics.

REFERENCES

Balasubramanian, S., Beillas, P., Belwadi, A., Hardy, W., Yang, K., and King, A., Masuda, M. (2004) Below Knee Impact Responses using Cadaveric Specimens. Stapp Car Crash Journal, 48: 71-88.

Cavanaugh, J., Nyquist, G., Goldberg, S., and King, A. (1986) Lower Abdominal Tolerance and Response. Proc. 30th Stapp Car Crash Conference.

Davis, M.L., Koya, B., Schap, J.M., Hsu, F., Gayzik, F.S. (2017) Comparison of Objective Rating Techniques vs. Expert Opinion in the Validation of Human Body Surrogates. 25th ESV Conference, Paper No. 17-0141.

Eppinger, R., Marcus, J., and Morgan, R. (1984) Development of Dummy and Injury index for NHTSA's Thoracic Side Impact Protection Research Program. Society of Automotive Engineers Technical Paper 840885.

Funk, J.R., Tourret, L.J., Crandall, J.R. (2000) Experimentally Produced Tibial Plateau Fractures. Proc. 2000 IRCOBI Conference.

Funk, J.R., Crandall, J.R., Tourret, L.J., MacMahon, C.B., Bass, C.R., Patrie, J.T., Khaewpong, N., Eppinger, R.H. (2002) The Axial Injury Tolerance of the Human Foot/Ankle Complex and the Effect of Achilles Tension. Journal of Biomechanical Engineering, No. 124, pp 750-757.

Gehre, C., Gades, H., Wernicke, P. (2009) Objective Rating of Signals Using Test and Simulation

Responses, 21st ESV Conference, Paper No. 09-0407.

GESAC, Inc. (2001) Biomechanical Response Requirements of the THOR NHTSA Advanced Frontal Dummy, Revision 2001.02. Report No: GESAC-01-04, U.S. Department of Transportation, Washington, DC.

GESAC, Inc. (2005a) Biomechanical Response Requirements of the THOR NHTSA Advanced Frontal Dummy, Revision 2005.1. Report No: GESAC-05-03, U.S. Department of Transportation, Washington, DC.

GESAC, Inc. (2005b) THOR Certification Manual, Revision 2005.2. Report No: GESAC-05-04, U.S. Department of Transportation, Washington, DC.

Haffner, M., Rangarajan, N., Artis, M., Beach, D., Eppinger, R., Shams, T. (2001) Foundations and Elements of the NHTSA THOR Alpha ATD Design. 17th ESV Conference, Paper No. 458.

Hardy, W.N., Schneider, L.W., Rouhana, S.W. (2001) Abdominal Impact Response to Rigid-Bar, Seatbelt, and Airbag Loading. Stapp Car Crash Journal, Vol. 45.

Hodgson, V.R., Thomas, L.M. (1971) Comparison of Head Acceleration Injury Indices in Cadaver Skull Fracture. Proc. 15th Stapp Car Crash Conference, Society of Automotive Engineers 710854.

Hubbard, R.P., McLeod, D.G. (1974) Definition and Development of a Crash Dummy Head. Proc. 18th Stapp Car Crash Conference, Society of Automotive Engineers 741193.

Irwin, A. L., Mertz, H. J., Elhagediab, A. M., Moss, S. (2002) Guidelines for Assessing the Biofidelity of Side Impact Dummies of Various Sizes and Ages. Stapp Car Crash Journal, No. 46, pp. 297-319.Kent, R. W., Bass, C. R., Woods, W. A., Salzar, R. S., Lee, S. H., & Melvin, J. (2006) The role of muscle tensing on the force-deflection response of the thorax and a reassessment of frontal impact thoracic biofidelity corridors. Proceedings of the Institution of Mechanical Engineers, Part D: Journal of Automobile Engineering, 220(7), 853-868.

Kim, T., Funk, J.R., Bollapragada, V., Ye, X., Crandall, J. (2017) Evaluation of Biofidelity and Repeatability of THOR-Lx Metric under Axial Impact Loading. International Journal of Precision Engineering and Manufacturing,Vol. 18, No. 7. pp. 1027-1034.

Kuppa, S., Klopp, G.S., Crandall, J.R., Hall, G., Yoganandan, N., Pintar, F.A., Eppinger, R.H., Sun, E., Khaewpong, N., Kleinberger, M. (1998) Axial Impact Characteristics of Dummy and Cadaver Lower Limbs. Proc. 16th ESV Conference, Paper No. 98-S7-O-10.

Lebarbé, M., Petit, P. (2012) New Biofidelity Targets for the Thorax of a 50th Percentile Adult Male in Frontal Impact. Proc. 2012 IRCOBI Conference.

Lebarbé, M., Donnelly, B.R., Petit, P., Moorhouse, K. (2015a) A Frontal Response Specification for Assessing the Biofidelity of an Anthropometric Test Dummy: Part 1 - Upper Body. Proc. 2015 IRCOBI Conference.

Lebarbé, M., Donnelly, B.R., Petit, P., Moorhouse, K. (2015b) A Frontal Response Specification for Assessing the Biofidelity of an Anthropometric Test Dummy: Part 2 - Lower Body. Proc. 2015 IRCOBI Conference.

Lobdell, T.E., Kroell, C.K., Schneider, D.C., Hering, W.E., Nahum, A.M. (1973) Impact Response of the Human Thorax. Proc. Human Impact Response - Measurement and Simulation, pages 201–245.

Melvin, J. W., King, A. I., Alem, N. M. (1988) AATD System Technical Characteristics, Design Concepts, and Trauma Assessment Criteria; AATD Task EF Final Report, DOT HS 807 224, US Department of Transportation, Washington, DC.

Melvin, J., Shee, T. (1989) Facial Injury Assessment Techniques. In: Backaitis, S.H., Mertz, H.J., Hybrid III: The first human-like crash test dummy, pp. 453-62, Society of Automotive Engineers Paper No. 896072, Warrendale, PA.

Mertz, H.J., Patrick, L.M. (1971) Strength and Response of the Human Neck. 15th Stapp Car Crash Conference. SAE Paper # 710855.

Montesinos Acosta, S., Shaw, C.G., Ash, J., Lessley, D., Crandall, J. (2016) Comparison of Whole Body Response in Oblique and Full Frontal Sled Tests. Proc. 2016 IRCOBI Conference.

Moorhouse, K. (2013) An Improved Normalization Methodology for Developing Mean Human Response Curves. 23rd ESV Conference, Paper No. 13-0192.

Myers, B.S., McElhaney, J.H., Doherty, B.J., Paver, J.G., Nightingale, R.W., Ladd, T.P., Gray, L. (1989) Responses of the Human Cervical Spine to Torsion. 33rd Stapp Car Crash Conference, Paper No. 892437.

National Highway Traffic Safety Administration (2015a) THOR-50M Drawing Package, September 2015 Draft. U.S. Department of Transportation, Washington, DC.

National Highway Traffic Safety Administration (2015b) Laboratory Test Procedure for Oblique Offset Moving Deformable Barrier Impact Test. Docket ID NHTSA-2015-0119-0017.

National Highway Traffic Safety Administration (2016a) THOR-50M Drawing Package, August 2016 Draft. U.S. Department of Transportation, Washington, DC.

National Highway Traffic Safety Administration (2016b) THOR 50th Percentile Male Qualification Procedures Manual August 2016. U.S. Department of Transportation, Washington, DC.

National Highway Traffic Safety Administration (2017) Biomechanics Test Database (https://www-nrd.nhtsa.dot.gov/database/VSR/bio/QueryTest.aspx). U.S. Department of Transportation, Washington, DC.

Neathery, R.F. (1974) Analysis of Chest Impact Response Data and Scaled Performance Recommendations. Proc. 18th Stapp Car Crash Conference, Society of Automotive Engineers Paper No. 741188.

Nusholtz, G.S., Kaiker, P.S., Lehman, R.J. (1988) Steering System Abdominal Impact Trauma. University of Michigan Transportation Research Institute, UMTRI-88-19, Michigan, USA, 1988.

Nusholtz, G.S., and Kaiker, P. (1994) Abdominal Response to Steering Wheel Loading. Proc. ESV Conference, Paper No. 94-S1-O-05.

Nyquist, G.W., Cavanaugh, J.M., Goldberg, S.J., King, A.I. (1986) Facial Impact Tolerance and Response. Proc. 30th Stapp Car Crash Conference, pp. 379-400, Society of Automotive Engineers, Warrendale, PA.

Parent, D., Craig, M., Ridella, S., McFadden, J. (2013) Thoracic Biofidelity Assessment of the THOR Mod Kit ATD. 23rd ESV Conference, Paper No. 13-0327.

Patrick, L.M., Chou, C. (1976) Response of the Human Neck in Flexion, Extension, and Lateral Flexion," Society of Automotive Engineers Report VRI-7-3.

Ramachandra, R., Kang, Y., Bolte, J., Hagedorn, A., Herriott, R., Stammen. J., Moorhouse, K. (2016) Biomechanical Responses of PMHS Subjected to Abdominal Seatbelt Loading. Stapp Car Crash Journal, Vol. 60, pp. 59-87.

Rhule, D., Rhule, H., Donnelly, B. (2005) The Process of Evaluation and Documentation of Crash Test Dummies for Part 572 of the Code of Federal Regulations. 19th ESV Conference, Paper No. 05-0284.

Rhule, H., Maltese, M., Donnelly, B., Eppinger, R., Brunner, J., Bolte, J. (2002) Development of a New Biofidelity Ranking System for Anthropomorphic Test Devices. Stapp Car Crash Journal 46: 477-512.

Rhule, H., Moorhouse, K., Donnelly, B., Stricklin, J. (2009) Comparison of WorldSID and ES-2RE Biofidelity Using Updated Biofidelity Ranking System. 21st ESV Conference, Paper No.09-0563.

Rhule, H., Donnelly, B., Moorhouse, K., Kang, Y.S. (2013) A Methodology for Generating Objective Targets for Quantitatively Assessing the Biofidelity of Crash Test Dummies. 23rd ESV Conference, Paper No. 13-0138.

Ridella, S., Parent, D. (2011) Modifications to Improve the Durability, Usability, and Biofidelity of the THOR-NT Dummy. 22nd ESV Conference, Paper No. 11-0312.

Robbins, D.H. (1983) Development of Anthropometrically Based Design Specifications for an Advanced Adult Anthropomorphic Dummy Family; Volume 2-Anthropometric Specifications for mid-Sized Male Dummy, U.S. Department of Transportation, DOT HS 806 716, Washington, DC.

Rudd, R., Crandall, J.R., Millington, S., Hurwitz, S., Hoglund, N. (2004) Injury Tolerance and Response of the Ankle Joint in Dynamic Dorsiflexion. Stapp Car Crash Journal, Vol. 48, pp. 1-26.

Rupp, J., Reed, M., Madura, N., Schneider, L. (2003) Comparison of Knee/Femur Force-Deflection Response of the THOR, Hybrid III, and Human Cadaver to Dynamic Frontal Impact Knee Loading. Proc. 18th ESV Conference, Paper No. 160.

Saunders, J., Parent, D., Ames, E. (2015) NHTSA Oblique Crash Test Results: Vehicle Performance and Occupant Injury Risk Assessment in Vehicles with Small Overlap Countermeasures. Proc. 24th ESV Conference, Paper No. 15-0108.

Schneider, L., King, A., Beebe, M. (1989) Design Requirements and Specifications: Thorax-